PHTHALOCYANINE COMPOUNDS AS CORROSION INHIBITORS FOR METALS IN CORROSIVE ENVIRONMENT

By

THABO PESHA

███████████

DISSERTATION

Submitted in fulfilment of the requirements for the degree of

MASTER OF SCIENCE

In

CHEMISTRY

In the

FACULTY OF SCIENCE AND AGRICULTURE

(School of Physical and Mineral Sciences)

At the

UNIVERSITY OF LIMPOPO

SUPERVISOR: PROF M.J. HATO

CO-SUPERVISORS: DR K.D. MODIBANE

DR M.S. THOMAS

June 2018

DEDICATION

To my family

Success, David, Cathrine and Eric Pesha

DECLARATION BY CANDIDATE

I declare that PHTHALOCYANINE COMPOUNDS AS CORROSION INHIBITORS FOR METALS IN CORROSIVE ENVIRONMENT is my own work and that all the sources that I have used or quoted have been indicated and acknowledged by means of complete references and that this work has not been submitted before for any other degree at any other institution.

…………………………….. ………………………………

Full Names   Date

ACKNOWLEDGEMENTS

First and foremost, I would like to show my heartfelt and deep appreciation to my Lord and Saviour Jesus Christ. In particular, I deem it a rare privilege to pursue the research under the guidance of my beloved supervisor Prof. Mpitloane J. Hato for his meticulous guidance, congenial comprehensive and cloudness source of inspiration and constant support all through the course of the study. His benevoelent as well as humanitarian treatment in the up and down situations upgraded me a lot for the accomplishment of the target. I have learned a lot from you truly and for that am eternally grateful to have you as my supervisor and mentor. I also immensely appreciate the input and aid I received from my co-supervisors Dr K.D. Modibane and Dr M.S. Thomas (HOD), not only did you sharpen my vision in the field of research but you also pushed me to do my best.

To Mr K.E. Ramohlola, I would like to express my attitude of gratitude for your excellent leadership in our Nanotechnology Research Group at University of Limpopo (NanoRG@UL) for that I thank you. I thank Mr G.R. Monama for his assistance in helping me to prepare phthalocyanine inhibitors, I highly appreciate. Thank you to Dr M.E. Makhatha from University of Johannesburg (UJ, Doorfontein Campus) for offering me your laboratory to run electrochemistry studies. It's very much appreciated indeed. In addition, my great appreciation goes to Thabang Tshoenyane at UJ for assisting me with electrochemical characterisations. Furthermore, I appreciate Dr Kerileng Molapo for sharing more insights about electrochemical data analysis as well as her great support in writing the manuscripts in this study. Your presence during the tenure of my studies did not go unnoticed. A special thanks goes to NanoRG@UL group members for their continuous support throughout the journey.

Special gratitude to National Research Foundation of South Africa for funding my studies. My studies would have not been the same without your aid, thank you

ABSTRACT

The economy of nations depends highly on the industrial products which can be imported or exported. In addition, most industrial equipments such as engineering vehicles, reaction vessels and packaging machineries made from metallic products are prone to corrosion. One of the most efficient ways to mitigate corrosion process is through the use of chemical inhibition method. In this work, unsubstituted (CuPc, NiPc, ZnPc) and substituted phthalocyanines (TNCuPc, TNNiPc, TNZnPc) were synthesised and studied as corrosion inhibitors for aluminium (Al) metal in 1 mol. L^{-1} hydrochloric acid using gravimetric analysis, potentiodynamic polarisation (PDP) and electrochemical impedance spectroscopy (EIS) techniques. The synthesised inhibitors were characterised for their structure, spectroscopic and thermal properties using X-ray diffraction (XRD), ultraviolet visible (UV-vis), Fourier transform infrared spectroscopy (FTIR) and thermogravimetric analysis (TGA). Both XRD and FTIR indicated a successful synthesis of all inhibitors investigated in the study. Nevertheless, the crystallinity of both ZnPc and TNZnPc was higher as compared to other inhibitors. TGA results showed that NiPc and TNNiPc are most thermally stable amongst the inhbitors studied. The gravimetric data revealed that the inhibition efficiencies decreased with an increase in temperature. Nonetheless, NiPc exhibited the highest inhibition efficiency of 96.42% at 40 ppm as compared to other inhibitors. The PDP results indicated that NiPc, ZnPc, TNNiPc and TNZnPc are mixed-type inhibitors with the exceptions of both CuPc and TNCuPc showing a physisorption adsorption mechanism. The adsorption of the studied inhibitors on Al metal obeyed the Lanmuir adsorption isotherm. The Gibbs free energy indicated that the adsorption process was spontaneous, and that the corrosion inhibition took place by physical adsorption process.

RESEARCH OUTPUT

PUBLICATIONS

1. **Thabo Pesha,** Gobeng R. Monama, Mpitloane J. Hato, Mamookgo E. Makhatha, Kabelo E. Ramohlola, Kerileng M. Molapo, Kwena D. Modibane. Electrochemical and gravimetric studies of 4-tetranitro copper (II) phthalocyanine inhibitor as a corrosion inhibitor for aluminium metal in corrosive environment. Manuscript submitted for possible publication in International Journal of Electrochemical Sciences (**under review**) (APPENDIX 1).

2. **Thabo Pesha**, Gobeng Release Monama, Mpitloane Joseph Hato, Mamookgo E. Makhatha, Kabelo Edmond Ramohlola, Kerileng Mildred Molapo, Kwena Desmond Modibane. Improvement of corrosion resistance of aluminium metal in corrosive environment by 4-tetranitro zinc (II) phthalocyanine inhibitor as a corrosion inhibitor using electrochemical and gravimetric studies. Manuscript in preparation.

3. **Thabo Pesha**, Phuti Suzan Ramaripa, Kabelo Edmond Ramohlola, Gobeng Release Monama, Mpitloane Joseph Hato, Mamookgo Elizabeth Makhatha, Thabang George Tsouenyane, Kerileng Mildred Molapo, Kwena Desmond Modibane. Protection of corrosion rate on aluminium metal in acidic media by unsubstituted and 4-tetranitro substituted nickel (II) phthalocyanine inhibitors via electrochemical and gravimetric studies for hydrogen fuel cell. Manuscript submitted for possible publication in Results in Physics (**under review**) (APPENDIX 2).

PRESENTATIONS

Thabo Pesha, Mpitloane Joseph Hato, Kwena Desmond Modibane. Gravimetric and adsorption studies of some medicinally active compounds as corrosion inhibitors for

some metals in acidic medium. SACI Inorg2017 Conference Hermanus, Cape Town, Western Cape, South Africa on the 24-27th June 2017.

TABLE OF CONTENTS

LIST OF FIGURES

LIST OF TABLES

LIST OF ABBREVIATIONS

Al…………………………: Aluminium

[BF4]-……………………...: Tetrafluoroborate

KI…………………….…: Potassium iodide

[PF6]-……………………: Hexafluorophosphate

$N\ (SO_2CF_3)2$…….......…: N-Phenyl-bis (trifluoromethanesulfonimide)

CE……………………....: Counter electrode

CuPc………………..……: Copper (II) phthalocyanine

$CuPc\ (SO_3Na)_4$……...…: Copper phthalocyanine tetrasulfonic tetra sodium salt

CoPc…………………....: Cobalt phthalocyanine

CrPc…………….………..: Chromium phthalocyanine

DSC………………..…….: Differential scanning calorimetry

DNA………………….…...: Deoxyribonucleic acid

EIS………………………..: Electrochemical impedance spectroscopy

FePc……………………..: Iron phthalocyanine

FRA………………………: Frequency response analyser

FSH………………....…...: Follicle stimulating hormone

FTIR…………..............……: Fourier transform infrared spectroscopy

HCl………………………..: Hydrochloric acid

HOMO……………….....: Highest occupied molecular orbital

IE………………….………: Inhibition efficiency

LED………………….…...: Light emitting diodes

LH………………………...: Luteinising hormone

LUMO………………....…: Lowest unoccupied molecular orbital

MTNPcs……………………..:Metallotetranitro phthalocyanine

MIC……………..…...…...: Microbial influence corrosion

MO………………….………: Molecular orbital

MPc…………………….....: Metallophthalocyanine

MPcs………………….....: Metallophthalocyanines

NiPc…………………..……: Nickel (II) phthalocyanine

Pc……………………….....: Phthalocyanine

PDT……………………..…..: Photodynamic therapy

PFZ…………………………..: Precipitates free zone

RE……………………………...: Reference electrode

SCC…………….……..……: Stress corrosion cracking

SCE…………………..…..…: Saturated calomel electrode

SEM………………….……..…: Scanning electron microscopy

SnPc…………………..……: Tin phthalocyanine

TGA……………...………..…: Thermogravimetric analysis

TNCuPc………………..……: Tetranitro copper (II) phthalocyanine

TNNiPc………………..……: Tetranitro nickel (II) phthalocyanine

TNZnPc………………….…: Tetranitro zinc (II) phthalocyanine

UV-vis………………….…… Ultraviolet-visible spectroscopy

WE …………..……………....: Working electrode

XRD……………….…………: X-ray diffraction

ZnPc…………………….…...: Zinc (II) phthalocyanine

LIST OF SYMBOLS

Ag/AgCl…………………………: Silver/silver chloride

b_a……………………………...: Anodic Tafel slope

b_c……………………………: Cathodic Tafel slope

C_R……………………….......: Corrosion rate

C_{inh}…………………………: Inhibitor corrosion

C_{dl}…………………………: Double layer capacitance

E_a…………………………: Activation energy

E_r…………………………..…..: Reversible potential

E^o………………………….: Standard reversible potential

E_{corr}……………………….....: Corrosion potential

E_{pas}……………………….: Passivation potential

I_{corr}………………………....: Corrosion current density

I_{pas}…………………………: Passivation current density

K_{ads}…………………………..: Equilibrium adsorption constant

M…………………………....: Molar

M…………………………....: Metal surface atom

P_{H2}……………………….....…: Partial pressure of hydrogen gas

R……………………….….…: Gas constant

R_s………………………………: Resistor

R_{ct}………………………..: Resistance of charge transfer

S……………………....………: Surface area

T…………………………....……: Temperature

ΔS……………………………: Entropy

ΔH……………………………: Enthalpy

ΔG……………………………: Gibbs free energy

$ΔG^°_{ads}$…………………..……: Standard Gibbs energy of adsorption

CHAPTER ONE

INTRODUCTION

1.1. BACKGROUND

Metals are the preeminent essential materials used in structural and decorative applications. The corrosion, deterioration or destruction of metals is unavoidable but a controllable process. The corrosion of metals has a significant impact on the development of a country, which can be compared to any natural disasters like earthquake, flood, etc. For instance, the direct metallic corrosion cost in the US was estimated to be approximately $276 billion annually, which is several times greater than the normalised loss incurred owing to the natural disasters ($17 billion per annum). It was also suggested that about 25 to 30% of the annual corrosion costs could be saved by means of optimum corrosion management practices [1]. For example, aluminium (Al) is a light metal, which possesses good electric conductivity and has been used in variety of electronic applications [2]. One of the challenges in using Al metal, is the need to protect it from corrosion. Corrosion can be prevented by using various methods such as upgrading materials, blending of production fluids, process control and chemical inhibition [2-4]. Amongst these methods, the corrosion chemical inhibition is reported to be the best method to prevent destruction or degradation of metal surfaces in corrosive media due to its economic and practical usage [5-7]. Therefore, the search for an efficient corrosion inhibitor is paramount important and as a fundamental progressive step in this quest, it has been found that the use of organometallic compounds is one of the most practicable ways for providing protection of metals [8-10].

1.2. PROBLEM STATEMENT

Corrosion is a naturally occurring phenomenon which is defined as a process whereby a material decays or is destructed through chemical reactions with its surrounding environment. This phenomenon has tremendous negative economic and industrial effects due to the fact that some useful properties of materials and structures undergo degradation, including loss of strength and appearance [11]. For example, mild steel possesses different resistances to corrosion due to their various

properties. However, one of the challenges of mild steel is that it is more vulnerable to rusting due to its low amount of alloying elements [12]. Many techniques and methods such as plating and painting have been implemented to minimise the corrosion of mild steel. Nonetheless, plating technique usually suffers from adsorption efficiency of the coating component. However, if the plating is more noble than the substrate (for example, chromium on steel), a galvanic couple will cause any exposed area to corrode quickly than the unplated surface counterparts. For these reason, it is often wise to plate with active metal such as zinc or cadmium. In painting methods, the major problems are with drying times because they depend on both the temperature and humidity [13-15]. In order to circumvent these challenges, the use of corrosion inhibitors has found extensive usage in inhibiting corrosion of mild steel in various media such as acidic, alkaline, saline and other aggressive media. The main interest in using corrosion inhibitors are their availability, simplicity in mode of adsorption and affordability [16-18]. In the last few years, there has been an increasing interest in finding more environmentally friendly corrosion inhibitors. For instance, metallic phthalocyanines (MPcs) have been studied due to their high inhibition potential. Nonetheless, these materials possess low solubility in most organic solvents and they aggregate which will also result in their weakening performance as corrosion inhibitors. Consequently, the insolubility of the MPcs will impose a negative effect on their inhibition potential as corrosion inhibitors. In addition, it will be difficult to perform corrosion studies of MPcs due to their insolubility. Therefore, there is a need to prepare MPcs with effective functional groups in order to enhance its solubility.

1.3. RATIONALE

The solubility of the Pcs can be improved by introducing the nitro functional groups and this will generally enhance their inhibition potential in this study [19]. Many countries including South Africa spent a large financial expenditure to counteract the effects of corrosion. Intensive studies have been conducted regarding the prevention and the literature shows that prevention is the most cost effective method as opposed to repairing the damage caused thereafter. In order to enhance the range of application, a deeper knowledge of the corrosion inhibiting mechanism of these metals is necessary. Therefore, their behaviour in acid media is an important

property to be studied and explored. In recent years, there has been a high demand in using active compounds as corrosion inhibitors in acidic media. Among these compounds, Pcs, which exhibit several interesting properties and applications, have been studied [20,21]. This is due to their highly delocalised conjugated π-electron system, strong chemical adsorption on the metal surface, which is determined by planarity and lone pairs of electrons in heteroatoms and availability of multiple bonds that are unsaturated.

Aoki *et al.* [22] studied the corrosion inhibition efficiency of CuPc for mild steel in 16% HCl focusing on weight loss measurements fitted to Langmuir, Frumkin, Temkin and Flory-Huggins models to obtain adsorption isotherms. A better fit to the Langmuir isotherm was obtained. The polarisation curves showed that polarisation of both the anodic and cathodic reactions were verified for concentrations higher than 10^{-4} M, indicating a mixed type reaction. In addition, CuPc exhibited a high corrosion inhibition for all concentration studied. In another study [22], the effect of an addition of natural occurring Chenopodium Ambrosioides extract (CAE) on the behaviour of carbon steel corrosion in 0.5 M sulphuric acid (H_2SO_4) solution was investigated by the weight loss method, potentiodynamic polarisation (PDP) and impedance spectroscopy (EIS) measurements. The experimental results showed that extract has a good inhibiting effect on the metal tested in 0.5 M H_2SO_4 solution. The protection efficiency increases with increasing inhibitor concentration to attain 94% at 4 g/l. PDP studies clearly revealed that it acted essentially as a cathodic inhibitor. EIS results showed that the change in the impedance parameters (R_{ct} and C_{dl}) with concentration of extract of CAE is an indicative of the adsorption of molecules leading to the formation of a protective layer on the surface of carbon steel. The efficiency of the inhibitor decreased with the temperature. The adsorption of CAE extract was found to obey the Langmuir adsorption isotherm. Although tetranitro MPcs have been used in many applications such as chemical sensor, liquid crystals, nonlinear optics, optical data storage, various catalytic processes [23], and their use as corrosion inhibitors on Al metal in acidic environment have not been employed extensively.

1.4. RESEARCH AIM AND OBJECTIVES OF THE STUDY

1.4.1. AIM

The main aim of this work was to synthesise various metallophthalocyanine inhibitors and study their inhibition efficiency on aluminium metal in HCl as a corrosive environment.

1.4.2. OBJECTIVES

The objectives were to:

i.   synthesise unsubstituted and substituted MPcs inhibitors (M = Cu, Ni, and Zn) with nitro (NO_2) groups attached.
ii. characterise all the synthesised phthalocyanine inhibitors using FTIR, UV-vis, XRD, and TGA.
iii. investigate the effect of MPc concentration and temperature on the corrosion rate.
iv. apply thermodynamics, kinetics and adsorption principles in studying the inhibition potential of MPcs on aluminium metal.
v.   study electrochemical corrosion rate of the inhibitors using EIS and PDP.

1.5. DISSERTATION OUTLINE

This dissertation investigates the corrosion effect on Al metal using gravimetric method and electrochemical techniques. The dissertation comprises of six chapters and a brief description of each chapter and their layout are provided below.

Chapter one: This chapter provides a background of problems associated with corrosion of metals in industries, rational, aims and objectives of the study.
Chapter two: The chapter focuses on the literature review, it comprises of corrosion theory and forms of corrosion, rate of corrosion, factors affecting corrosion, consequences of corrosion, corrosion on metals, prevention of corrosion and types

of inhibitors, properties and synthesis of various inhibitors, electrochemistry, adsorption studies, gravimetric analysis, and analytical techniques.

Chapter three: The electrochemical and gravimetric studies of 4-tetranitro copper (II) phthalocyanine inhibitor as a corrosion inhibitor for aluminium metal in corrosive environment are presented in this chapter.

Chapter four: This chapter deals with the improvement of corrosion resistance of aluminium metal in corrosive environment by tetranitro zinc (II) phthalocyanine inhibitor as a corrosion inhibitor using electrochemical and gravimetric studies.

Chapter five: Protection of corrosion rate on aluminium metal in acidic media by unsubstituted and 4-tetranitro substituted nickel (II) phthalocyanine inhibitors via electrochemical and gravimetric studies for hydrogen fuel cell.

Chapter six: The chapter provides overall conclusions drawn from the study and recommendations for future research.

1.6. REFERENCES

1. L. E. Smart, E. A. Moore, 4th Ed, Solid state chemistry: an introduction. *CRC press* (2012).

2. E. A. Starke, Aluminium alloys of the 70's: Scientific solutions to engineering problems. An invited review, *Adv. Mater. Sci. Eng.* 29(1997) 99-115.

3. J. T. Staley, Aluminum alloys and composites, *Encyclopedia of Physical Science.* (1992) 591.

4. P. Arellanes-Lozada, O. Olivares-Xometl, D. Guzmán-Lucero, N. V. Likhanova, M. A. Domínguez-Aguilar, I. V. Li janova, E. Arce-Estrada, the inhibition of aluminium corrosion in sulphuric acid by poly (1-vinyl-3-alkyl-imidazolium hexafluorophosphate), *materials.* 7 (2014) 5711-5734.

5. U. Trdan, J. Grum, Evaluation of corrosion resistance of AA6082-T651 aluminium alloy after laser shock peening by means of cyclic polarisation and EIS methods, *Corros. Sci.* 59(2012) 324-333.

6. M. T. Muniandy, A. A. Rahim, H. Osman, A. M. Shah, S. Yahya, P. B. Raja, Investigation of some schiff bases as corrosion inhibitors for aluminium alloy in 0.5 M hydrochloric acid solutions, *Surf. Rev. Lett.* 18 (2011) 127-133.

7. M. Tourabi, K. Nohair, M. Traisnel, C. Jama, F. Bentiss, Electrochemical and XPS studies of the corrosion inhibition of carbon steel in hydrochloric acid

pickling solutions by 3, 5-bis (2-thienylmethyl)-4-amino-1, 2, 4-triazole, *Corros. Sci.* 75(2013)123-133.

8. S. Şafak, B. Duran, A. Yurt, G. Türkoğlu, Schiff bases as corrosion inhibitor for aluminium in HCl solution*, Corros. Sci.* 54(2012) 251-259.

9. B. Sanyal, Organic compounds as corrosion inhibitors in different environments— a review, *Prog. Org. Coat.* 9(1981) 165-236.

10. A. Singh, Y. Lin, M. A. Quraishi, L. O. Olasunkanmi, O. E. Fayemi, Y. Sasikumar, B. Ramaganthan, I. Bahadur, I. B. Obot, I.B., Adekunle, M. M. Kabanda, Porphyrins as corrosion inhibitors for N80 Steel in 3.5% NaCl solution: Electrochemical, quantum chemical, QSAR and Monte Carlo simulations studies, *Molecules.* 20(2015) 15122-15146.

11. K. M. Usher, A. H. Kaksonen, I. Cole, D. Marney, Critical review: microbially influenced corrosion of buried carbon steel pipes, *Int. Biodeterior. Biodegrad.* 93(2014) 84-106.

12. T. Sheppard, 2013, Extrusion of aluminium alloys. Springer Science & Business Media.

13. S. Pommiers-Belin, J. Frayret, A. Uhart, J. Ledeuil, J. C. Dupin, A. Castetbon, M. Potin-Gautier, Determination of the chemical mechanism of chromate conversion coating on magnesium alloys EV31A, *Appl. Surf. Sci.* 298(2014) 199-207.

14. G. Lopez, H. Tiznado, G. Soto Herrera, W. De la Cruz, B. Valdez, M. Schorr, Z. Roumen, Use of AES in corrosion of copper connectors of electronic devices and equipments in arid and marine environments, Anti-Corros, *Methods. Mater.* 58 (2011) 331-336

15. G. Hu, S. Zhang, J. F. Bu, C. J. Lin, G. L. Song, Recent progress in corrosion protection of magnesium alloys by organic coating, *Prog. Polym. Sci.* 73 (2012) 129-141.

16. U. Trdan, J. Grum, Evaluation of corrosion resistance of AA6082-T651 aluminium alloy after laser shock peening by means of cyclic polarisation and EIS methods, *Corros. Sci.* 59(2012) 324-333.

17. M. T. Muniandy, A. A. Rahim, H. Osman, A. M. Shah, S. Yahya, P. B. Raja, Investigation of some schiff bases as corrosion inhibitors for aluminium alloy in 0.5 M hydrochloric acid solutions, *Surf. Rev. Lett.* 18 (2011) 127-133.

18. M. Tourabi, K. Nohair, M. Traisnel, C. Jama, F. Bentiss, Electrochemical and XPS studies of the corrosion inhibition of carbon steel in hydrochloric acid

pickling solutions by 3, 5-bis (2-thienylmethyl)-4-amino-1, 2, 4-triazole, *Corros. Sci.* 75(2013)123-133.

19. K. M. Kadish, S. A. Smith, R. Guilard, The Porphyrin Handbook: Phthalocyanines: Properties and Materials; Elsevier Science: San Diego, California, CA, USA, 2003; Volume 17.

20. A. M. El-Shamy, M. F. Shehata, A. I. M. Ismail, Effect of moisture contents of bentonitic clay on the corrosion behaviour of steel pipelines, *Appl. Clay. Sci.* 114 (2015) 461-466.

21. M. S. Ağırtaş, M.S. Izgi, Synthesis and characterization of new metallophthalocyanines with four phenoxyacetamide units, *J. Mol. Struct.* 927 (2009) 126-128.

22. I. V. Aoki, I. C. Guedes, S. L. A. Maranhao, Copper phthalocyanine as corrosion inhibitor for ASTM A606-4 steel in 16% hydrochloric acid, *J. Appl. Electrochem.* 32(2002) 915-919.

23. L. Bammou, M. Belkhaouda, R. Salghi, O. Benali, A. Zarrouk, H. Zarrok, B. Hammouti, Corrosion inhibition of steel in sulfuric acidic solution by the Chenopodium Ambrosioides extracts, *J. Assn. Arab Univ Basic Appl. Sci.* 16 (2014) 83-90.

CHAPTER TWO

LITERATURE REVIEW

2.1. CORROSION

2.1.1. CORROSION AND ITS CLASSIFICATIONS

Corrosion is the degradation of material's properties because of interaction (chemical reaction) with its surrounding environment. Generally, the term corrosion is applied to metals, but sometimes can also be referred to the degradation of plastics, ceramics, concrete and woods. Corrosion of metals depends on the environment to which it is exposed and temperature of the surrounding [1]. When metals corrode they form oxides, this is shown mostly by the brownish color on its surface, commonly known as rust. Rust is usually formed by the reaction of metal with oxygen in the presence of water. There are various forms of corrosion which can degrade the properties of the metal [2].

2.1.1.1. Pitting corrosion

Pitting corrosion is a form of localised corrosion and is characterised by attacks at small discrete spots on the metal surface. It is distinguished in four stages [3-6]: (i) the occurrence of processes on the passive film, at both the passive film boundary and the solution; (ii) the occurrence of the processes inside the passive film, when there is an absence of changes of visible microscopic in a film; (iii) this is the intermediate in pitting process which comprises of the metastable pits formation which initiate and grow for short time period under the critical pitting potential and then the passivation of the film; and (iv) the last step is called the stable pit growth which is above a specific potential termed the critical pitting potential.

2.1.1.2. Crevice corrosion

Crevice corrosion refers to attack on metal surface adjacent, the gap or crevice between two joining surface which refers to is one of the most often experienced localised corrosion forms and it occurs in the alloys that usually show an ideal resistance of corrosion such as stainless steel [7]. In addition, crevice accelerates corrosion because it makes a chemical surrounding which differs from that of a freely vulnerable surface and this surrounding store moisture, it traps pollutants and concentrates the products of corrosion meanwhile excluding oxygen [8]. Most crevice corrosion cases take place in the near-neutral solutions where the cathode reactant it's a dissolved oxygen. There are three factors which contribute to the occurrence of crevice corrosion [9], i.e.

✓ The geometry of the structure, e.g. riveted plates, threaded joints and welded fabrications.
✓ The contact of the metal with non-metallic solids, e.g. plastics, glass and rubber.
✓ Sand deposits, products of permeable corrosion on the metal surface and this is crevice corrosion type referred to as deposit attack.

2.1.1.3. Microbiological corrosion

Microbiological corrosion occurs when micro-organisms like bacteria attract and adhere to the metal surface. Some waste products produced by bacteria are aggressive and stimulate this form of corrosion [10, 11]. It is a microbial influenced corrosion (MIC) which refers to the microorganism's influence on the kinetics of a metal's corrosion process' which is caused by microorganisms cohering to the interfaces normally called biofilms [10]. The existence of microorganisms is the prerequisite for the MIC and if corrosion is affected by their activity, will result in additional requirements which are [11]:

✓ Source of energy
✓ Source of carbon
✓ Electron donator
✓ Electron acceptor

✓ The presence of water

2.1.1.4. Intergranular corrosion

Intergranular corrosion occurs at the grain frontier thus resulting in lower corrosion resistance around the grain. It occurs mainly along the boundaries of the grain as the results of the micro galvanic coupling between the precipitates free zone (PFZ) and the precipitates of grain boundary [12-15]. The PFZ is adjacent to the grain boundary as a solute-depleted layer. It is required that the corrosion potential between the PFZ and the grain boundary be more than 100mV for the propagation of the intergranular corrosion, and it also required that there be a continuity of the grain boundary precipitates which contributes to the intergranular corrosion along the boundary [15].

2.1.1.5. Erosion corrosion

Erosion corrosion is due to the combination of both stress and the corrosive environment attacking on the metal surface. It is also called abrasion corrosion since abrasive particles uncover new and fresh surface of a metal resulting in high corrosion rate. During production systems of both oil and gas, this corrosion is primarily generated by particle impingement on tubing materials [16]. Generally, CO_2, salt water and hydrogen sulphide are the regarded corrosive reagents [17-22].

2.1.1.6. Galvanic corrosion

Galvanic corrosion occurs when two different metals are in contact with each other in the same corrosive medium under electrochemical action. It may be located at the water main junction, where a copper pipe and a steel pipe join, or in microelectronic device where various metals and semiconductors are placed together, or in a matrix composite material of a metal in which fortifying substances such as graphite are diffused in a metal, or in a ship where the different water immersed components are made of various metal alloys [23]. Galvanic corrosion may lead to a fast metal's degradation in many cases, however in other cases it can serve as a protective layer of metal which the method known as the cathodic protection by sacrificial anodes basis [24]. The subject of galvanic corrosion is firmly investigated, and it is well

understood qualitatively, but it has been difficult to work with in a quantitative way due to its highly complex nature [24].

2.1.1.7. Dealloying corrosion

Dealloying corrosion results when the corrosion resistance metal in an alloy loses its atomic components (characteristics), thus deactivating its corrosion resistant potential. Various metals and alloys possess various electrochemical potentials in similar electrolyte. Contemporary alloys have many various elements used for alloying which show distinct corrosion potentials. The driving force for the desired attack on the more active element in the alloy, is the potential difference between the alloying elements [25]. Zinc is desirably leached out of the copper-zinc alloy in the case of dezincification process of brass, as a result it leaves porous and brittle copper-rich surface layer [26].

2.1.1.8. Stress corrosion cracking

Stress corrosion cracking (SCC) is a form of corrosion that results in the formation of cracks on the metal surface under tensile stress and in acidic environment. It occurs at the temperature above 60 ^{o}C [27]. It's a phenomenon which is a slow crack growth (typically less than 10^{-6}m/s) that takes place when a material is exposed to a certain corrosive environment and when a material is loaded in tension [27]. At relatively low applied stresses, SCC generally results in brittle failure of a material which is nominally ductile and this is the main engineering concern. The failure of SCC frequently happens at tensile loads below the bulk material's yield strength [28]. From the manufacturing process, tensile stresses can be applied externally. SCC growth is normally divided into three definite regimes [29, 30]:

✓ Crack initiation
✓ Steady state crack growth
✓ Catastrophic failure

2.1.1.9. Filiform corrosion

Filiform corrosion takes place on a surface with organic coatings. This type of corrosion has taken place on other metals which are coated such as zinc, iron, and steel and it occurs mainly at high humidity greater than 75% and at a room temperature [31]. The appearance of this corrosion is like thread-like filaments under coating. The corrosion products thereof influence the coating to cause the appearance of the surface to be like the lawn riddle with mole tunnels [32]. Where the coating is no longer continuous, the filaments proceed. Plenteous coating systems are susceptible. The halides, sulphates, carbonates, nitrates containing condensates have been associated with filiform corrosion [33]. Although the damage encountered on a metal tends to be limited, its appearance effect tends to be harmful.

2.1.1.10. Uniform corrosion

Uniform corrosion is also known as the general corrosion. The whole surface of metal is attacked by corrosion media and it is the least dangerous form of corrosion. It's a metal uniform thinning without any localized attack, as a result, corrosion process does not penetrate deeply and the common example is the rusting of steel in air [34].

2.1.1.11. Corrosion Fatigue

Corrosion fatigue is the result of combined action of an alternating or cyclic stresses and a corrosive environment [35]. The fatigue process is thought to cause rupture of the protective passive film upon which corrosion is accelerated. If the metal is simultaneously exposed to a corrosive environment, the failure can occur at even loads and after shorter period. In a corrosive environment, the stress level at which it could be assumed a material has infinite life is lowered or removed completely [36-38].

2.1.2. RATE OF CORROSION

Corrosion rate is how fast the metal degradation occurs. The rate is dependent on the surroundings in which the material is residing, the kind of material and the time of vulnerability [39, 40]. The corrosion rate C_R is calculated as given in Equation 2.1 [41]:

$$C_R = \frac{\Delta W}{St}$$
(2. 1)

where, ΔW is the weight loss of the metal in immersion time (t), and S is the surface area of the metal exposed.

2.1.2.1. Factors affecting the rate of corrosion

Corrosion is influenced by two-fold concepts, namely: nature of metal and nature of corrosive environment [42].

2.1.2.1.1. Nature of metal:

✓ **Purity of a metal:** The more impure the metal is, the more the corrosion rate.
✓ **Physical state of metal:** Corrosion rate is affected by the physical state of metal and the stress. Stressed areas experiences corrosion more greatly.
✓ **Nature of oxide layer:** Rate of corrosion depend on the essence of the oxide layer whether it is stable, unstable, porous etc.
✓ **Nature of corrosive products:** The corrosion increases if corrosion products are soluble in occurrence.

2.1.2.1.2. Nature of corrosive environment:

✓ **Temperature:** Corrosion rate increases with an increase in temperature.
✓ **Moisture:** The more moisture present, the higher the corrosion rate
✓ **pH value:** corrosion rate is more in lesser pH values (e.g. acidic conditions)
✓ **Nature of electrolyte:** The corrosion rate is increased by the presence of salts in the electrolyte.

2.1.2.2. Corrosion of metals

2.1.2.2.1. Mild steel

Mild steel is an alloy containing large amount of iron with some elements such as carbon, manganese, copper and silicon in small amount. In this case, it is also called low carbon steel since it has small amount of carbon element. Its Strength depends on the amount of carbon present. Moreover, mild steel is cheap and the most common type of steel which is mainly used for construction and due to its high accessibility [43].

When metals or alloys are exposed to the corrosive environment such as saline environment or acidic media during manufacture, they become degraded i.e. rate of corrosion increases on their surface. When mild steel undergoes corrosion process, iron is the first constituent to be corroded, resulting in formation of iron oxide commonly known as rust. For iron to be corroded, the relative humidity must be high, more than 60% or otherwise corrosion won't take place [44]. The rate of corrosion process may be accelerated by rain, dew, radiation, wind, and others. Since metals are economically of great value, there is a need to protect them. Corrosion rate can be prevented in various ways depending on the environmental conditions as well as ecosystem. Various prevention methods such as painting, water-absorption products (silica gel) and dehumidification are commonly used. However, these methods are not favoured because they high operational labour, cost of application and some are not eco-friendly [45].

Corrosion of mild steel is an electrochemical process involving redox reaction as depicted in Figure 2.1. This process requires oxygen and moisture to take place. When mild steel is placed in a solution, iron is oxidised to form a rust shown by the overall redox reaction below.
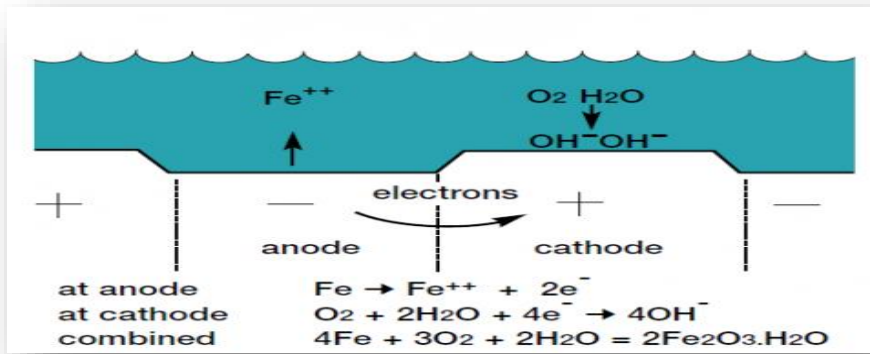
Figure 2. 1: Illustration of chemical process in mild steel [44].

2.1.2.2.2. Zinc metal

Zinc is reckoned to be corrosion resistant in majority of natural atmospheres, the anomaly being aerated indoor atmospheres where there is extremely low corrosion of zinc [47]. Zinc metallic coatings are normally considered as the most economical way of protection against corrosion. Zinc is gradually attacked by the atmospheric oxygen in dry air resulting in the formation of an oxide layer. Even though the outer layer breaks away occasionally, there is a protection to the metal denying its interaction with oxygen by the interior layer which remains from coating [48].

The zinc oxides are very gradual under conditions which occur in some tropical climates [49]. Corrosion occurrence has been explained to be due to air at temperatures ranging between -18 to 70 °C in an open and encircled miscellaneous spaces. Since corrosion is substantially an electrochemical phenomenon, it comprises the transfer of electrons between a metal surface and an aqueous electrolyte solution as shown in Figure 2.2 [50]. It is the result of the metal's tendency to interact with water, oxygen and other substances in an aqueous medium. The corroding metal area where there is metallic dissolution is anode, whereas the corroding area where hydrogen and oxygen reduction occurs is cathode [51].
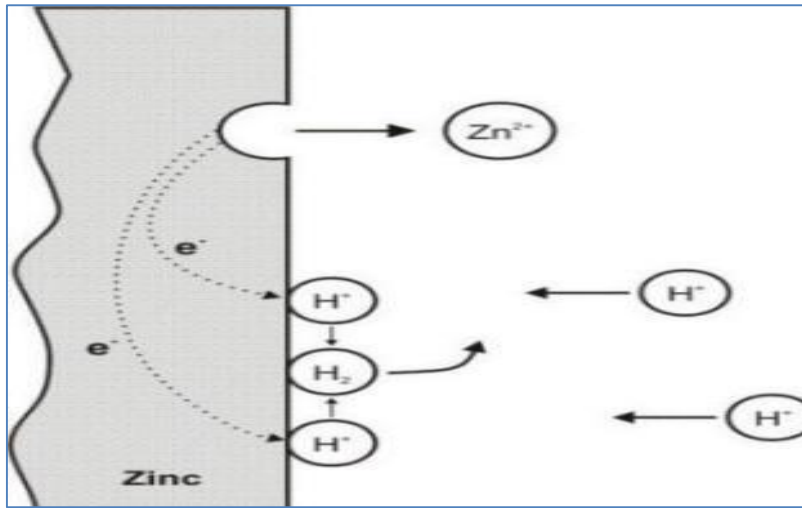
Figure 2. 2: Corrosion mechanism taking place on zinc metal.

During corrosion process, zinc loses its electrons forming zinc ions, hence the metal degradation occurs. The following reactions show how zinc ions are formed during corrosion process.

Anodic reaction: $Zn_{(s)} \rightarrow Zn^{2+} + 2e^-$ (2.2)

Cathodic reaction: $2H^+ + 2e^- \rightarrow H_{2\ (g)}$ (2.3)

Overall corrosion reaction: $Zn + 2H^+ \rightarrow Zn^{2+} + H_{2\ (g)}$ (2.4)
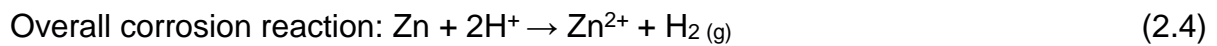
2.1.2.2.3. Aluminium metal

Aluminium is a very light metal which is widely used by many industrial companies to make pipes, batteries, machine etc. [52, 53]. Aluminium is a light material, therefore, it is easy to transport and one of the most produced types of metal around the world [52]. In addition, aluminium possesses other advantages such as electrical conductivity, thermal conductivity, ease of use, resistance to corrosion, suitability of surface treatment, and diversity of aluminium alloys [53].

It has been reported that corrosion rate on aluminium is slow as compared to other metals such as mild steel and zinc. Corrosion resistivity of this metal is because of the presence of thin, adherent and protective surface oxide film on the surface (Figure 2.3) [54]. The thin film of aluminium oxide is non-labile, and it acts as a protective blockade between the metal and corrosive environment. However, corrosion of aluminium takes place when the pH of the surrounding environment is

below and above 4-9 range, since the solubility of aluminium oxide film increase in both sides of metal surface [55-57]. Hence the investigation of corrosion inhibitors for aluminium metal is paramount important in both conditions.
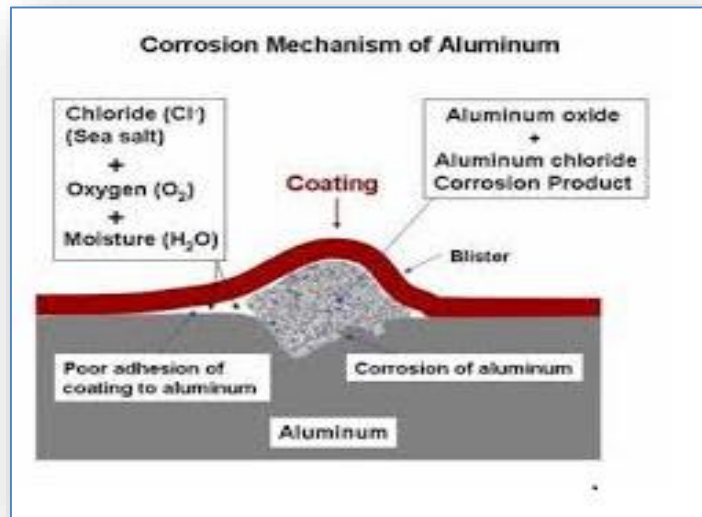
Figure 2. 3: Corrosion mechanism taking place on aluminium.

2.1.3. CORROSION THEORY

2.1.3.1. Kinetics

The corrosion process on a metal can be further explained by using kinetic model. The temperatures of the surrounding influence this process in various manners. High temperature speeds up this process while low temperature slows down the process [58, 59]. Like any other chemical reactions, corrosion process also passes through the activated complex through which reactants are broken up into intermediates before the formation of corrosion products. The energy required for the corrosion reactants to get to activated complex is called activation energy. In this study, Arrhenius equation was used to determine the activation energy (E_a) of the reaction. Arrhenius Equation is shown in Equation 2.5:

$$\log C_R = \log A - \frac{E_A}{2.303RT}$$

(2.5)

where C_R is the corrosion rate, A is the Arrhenius pre-exponential factor, E_a is the corrosion activation energy, R is the gas constant and T is the absolute temperature.

Corrosion kinetics enlighten about the rate of corrosion at a given time and environment. Corrosion reactions are both producing and consuming electrons and as the result these electrons can be quantified further as current. The electrochemical behaviour of materials made of metals in media which is aggressive can be examined through the temperature influence on the kinetic process of corrosion. The following equation (Equation 2.1) displays the dependence of chemical rate constant on temperature [60, 61].
According to Equation 2.1, the rate of corrosion should increase as the temperature increases and E_a and A can vary with temperature. Corrosion rate is differently being measured depending on the analysis method practiced.

2.1. 3.2. Adsorption isotherms and thermodynamic parameters

Adsorption studies elucidate on how the corrosion inhibitor compound adsorbs on a metal surface. In this case, adsorption process is the primary step for the interaction of the corrosion inhibitor compound with the metal surface and it depends on the type of metal, chemical structure of the inhibitor and on the type of the electrolyte [62]. Various adsorption isotherms mainly tested in corrosion studies are Langmuir, Temkin, Frumkin, and Freundlichh adsorption isotherms [63]. The degree of surface coverage obtained from the weight loss at different concentration of the inhibitor and different temperature is mainly used to determine the type of adsorption isotherm which correlates with the experimental results [64]. Best relationship between the results and isotherm functions is acquired by using Langmuir adsorption isotherm with large regression coefficient of approximately 0.99. The equation of Langmuir adsorption isotherm is given Equation 2.6, from which the adsorption/desorption equilibrium constant is obtained:

$$\frac{C_{inh}}{\theta} = \frac{1}{K_{ads}} + C_{inh}$$

(2.6)

where C_{inh} is the concentration of the inhibitor, Ɵ is the degree of the surface coverage, and K_{ads} is the adsorption equilibrium constant.

Furthermore, corrosion can best be defined in terms of the chemical stability of the species and reactions involved in it. With the help of thermodynamic control concept, corrosion is understood much better although corrosion rates cannot be predicted by the thermodynamic calculations. When the composition of the surrounding is known then thermodynamics can be used in calculating the theoretical activity of the given metal. The adsorption equilibrium constant is related to change in Gibbs free energy of adsorption (ΔG_{ads}) by Equation 2.7:

$$K_{ads} = \frac{1}{55.55} \exp(-\frac{\Delta G}{RT})$$

(2.7)

where ΔG is the Gibbs free energy of adsorption, R and T are gas constant and temperature respectively and 55.5 is the water concentration of solution. From this equation, it is easy to determine the values of change in Gibbs free energy of adsorption (ΔG_{ads}). Change in Gibbs free energy values mainly obtained are negative and this indicates that spontaneous process took place. It is also reported that negative values of change in free Gibbs energy (ΔG_{ads}) imply the spontaneity of the process and a good stability of inhibitor compound on the metal surface [65]. Moreover, there are two ways to explain how change in free Gibbs energy (ΔG_{ads}) varies with temperature:

✓ When ΔG_{ads} increase with an increase in temperature, the process is exothermic.
✓ When ΔG_{ads} decrease with an increase in temperature, the process is endothermic.

The values of ΔG_{ads} play a major role in determining the type of adsorption process taking place on the metal surface, this is whether the adsorption process will be physisorption (physical adsorption) or chemisorption (chemical adsorption). The ΔG_{ads} values ranging from -40 kJ.mol^{-1} and above symbolises chemisorption process, wherein adsorption of the inhibitor possesses chemical bonding. Furthermore, values of ΔG_{ads} ranging from -20 kJ.mol^{-1} and lower symbolize physisorption process, this process possesses weak van der Waals interaction

rather than chemical bonding [66]. Other thermodynamic parameters such as adsorptive enthalpy, ΔH^o and the standard entropy, ΔS^o can be derived. The adsorptive enthalpy can be deduced from Van't Hoff equation:

$$\frac{dInK_{eq}}{dt} = \frac{\Delta H^\theta}{RT^2}$$

(2.8)

where K is the adsorptive constant.

The standard entropy, ΔS^o can be calculated using the equation below:

$$\Delta G^o{}_{ads} = \Delta H^o{}_{ads} - T\Delta S^o{}_{ads}$$

(2.9)

The equilibrium constant (K_{eq}) for the reaction is calculated using the Equation 2.10 were F is the Faraday's constant:

$$RTInK_{eq} = -\Delta G^o = nF\Delta E^o$$

(2.10)

2.1.4. ELECTROCHEMISTRY

In electrochemistry, the positively charged metal ions tend to proceed from the metal into the solution and as a result electrons are left behind on the metal; this process occurs when the oxide-free metal surface becomes exposed to the solution according to the following equation [67, 68]

$$M \rightarrow M^{n+} + ne^-$$

(2.11)

where M is the atom in metal surface, M^{n+} is ion in solution and ne^- are electrons in a metal.

The potential difference between the metal and the solution increases due to the negative charge on the metal by the residual electrons and this potential is the electrode or metal potential. The potential change retards the metal ions dissolution but support the deposition of metal ions dissolved from the solution onto the metal and this is basically the reverse of Equation 2.11. The continuance of both the dissolution and deposition of metal ions would tend to enhance the metal reaching its potential stability such that the dissolution and deposition rate will be equal [69]. As

the result, this potential is named the reversible potential (E_r) and its value is concentration dependent of both dissolved metal ions and the standard reversible potential ($E°$) for unit activity of dissolved metal ions, $a_M{}^{n+}$:

$$M^{n+} + ne^- \leftrightarrow M \qquad (2.12)$$

$$E_{r,M^{n+}/M} = E^o{}_{M^{n+}/M} + \frac{RT}{nF} \ln a_{M^{n+}} \qquad (2.13)$$

where R is the gas constant, T the absolute temperature, F the Faraday and n the number of electrons transferred per ion. No further net dissolution of metal occurs once the potential reaches the reversible potential. The metal net amount dissolving in this process is generally very small.

The metal potential in a solution normally does not reach the reversible potential, however, the metal potential remains extra positive because electrons can be eradicated from the metal by different reactions [69]. Furthermore, electrons can both react with hydrogen ions and adsorb on the metal surface from the acidic solution to produce hydrogen gas (Equation 2.14).

$$2H^+ + 2e^- \rightarrow H_2 \qquad (2.14)$$
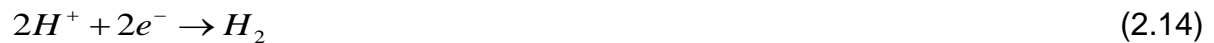
The reaction above allows the continued passage of the same quantity of metal ions into solution which leads to the corrosion of metal as the result and its reversible potential is given in Equation 2.14.

$$E_{r,H^+/H_2} = E^o{}_{H^+/H_2} - \frac{RT}{F} \frac{In P_{H_2}^{0.5}}{a_H^+} \qquad (20.15)$$

where P_{H2} is the partial pressure of hydrogen gas. The reversible potential of reaction (Equation 2.14) could be attained if the partial pressure of hydrogen is permitted to build up. The net dissolution of metal ions would effectively cease since there will no longer be any further net reaction of hydrogen ions.

The hydrogen ions concentration in neutral solutions is small to permit reaction (Equation 2.14) to continue at a significant rate. However, the electron in the metal can effectively react with oxygen molecules which are adsorbed on the metal surface

dissolved in the solution from air to produce hydroxyl ions as demonstrated in Equation 2.16.

$$O_2 + 2H_2O + 4e^- \rightarrow 4OH^-$$
(2.16)
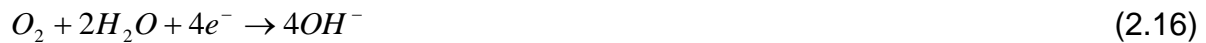
The potential of the metal remains more than the reversible potential for reaction (Equation 2.17):

$$E_{r,O_2/OH^-} = E^o{}_{O_2/OH^-} - \frac{RT}{4F} \ln \frac{a_{OH^-}{}^4}{P_{O_2}}$$
(2.17)

Equation 2.11 and 2.16 can couple and thus corrosion can proceed. The electrode in which oxidation reaction take place is called anode in electrochemical terminology. Oxidation process involves a loss of electrons by the reacting species as taking place in the dissolution reaction (Equation 2.11) of the metal. In this way, the corroding metal area where the metal dissolution take place is an anode and hence metal dissolution is the anodic reaction of corrosion. Reduction reaction occurs at the electrode called cathode. There is a gaining of electrons in reduction reaction as shown in Equation 2.14 and 2.16. The reduction of both hydrogen ions and oxygen are in this way the cathodic reactions of corrosion and the corroding metal area where these reactions occur is a cathode [70, 71].

2.1.5. CORROSION INHIBITORS

Corrosion inhibitors are chemical compounds that reduce corrosion rate when applied to the metal surface in a minute concentration. Inhibitors are widely used in water treatment facilities, chemical production companies, oil and gas exploration etc. Corrosion inhibitor method is the most widely used corrosion prevention presently. Corrosion inhibitors are broad and slow the rate of corrosion in various ways. Inhibitors can be classified as mixed and adsorption inhibitors. Mixed inhibitors slow down both cathodic and anodic reactions, while in adsorption, the inhibitor adsorb to the metal surface forming a thin film to protect metal from corrosion [72]. Different inhibitors are used for different metals in different environments. Corrosion inhibitors are effective, and most of them are eco-friendly, especially organic

compounds such as ionic liquids. Ionic liquids can reduce corrosion rate on metals such as mild steel, zinc and aluminium. For example, Table 2.1 shows some corrosion inhibitors which are being discussed in the next section.

Table 2. 1: Different types of corrosion inhibitors [73].

Inhibitors	Examples
Ionic liquid	1-butyl,3-methylimidazolium tetrafluroborate
Roots extracts or plant leaves	*Rauwolfia serpentine*
Sulphonamides	Sulphamethazine
Polymers	Polydiphenylamine
Dyes	Thiazine
Aromatic derivatives	Quinolone

2. 2. CORROSION INHIBITORS

2.2.1. SOME ORGANIC COMPOUNDS AS CORROSION INHIBITORS

2.2.1.1. Sulphonamides

The comprehension of how inhibitor molecules act on a metal surface can greatly increase the capacity to manage the crucial interfacial properties in a broad variation corrosion problem. The adsorption of the inhibitor molecules on surfaces has previously become the field of rigorous propped in the subject of corrosion research. Commonly, molecules of organic inhibitor might chemically or physically adsorb on a metal which is corroding [74].

Adsorption is commonly upon the surface of a metal and the resulting adsorption work as a barrier, separating the metal from the corrosion. Elements which influence the adsorption of these molecules, such as steric factor, functional group, molecular

size, electron density at the donor atoms and orbital nature of electron donation had been regarded and examined in terms of their abilities of inhibition. The inhibition efficiency has been associated to the inhibitor adsorption potentials [75] and molecular properties for various kinds of organic compounds.

The inhibition power depends on the molecular structure of the inhibitor. Organic compounds, comprising functional electronegative entities and $\pi -$ electron in triple or conjugated double bonds, are normally good inhibitors. The major adsorption centers are the heteroatoms such as phosphorus, sulphur, nitrogen, and oxygen, together with aromatic rings in their structure. The more significant features that dictate the adsorption of molecules on the metallic surface are the planarity and the lone electron pairs in the heteroatoms [76].

The mechanism of corrosion inhibition has been explained by theoretical chemistry such as quantum chemical calculations, which have been proven to be a very substantial tool for investigating the mechanism [77]. The reactive potential of the inhibitor is nearly connected to their frontier molecular orbitals (MO), comprising highest filled molecular orbital, HOMO, and lowest unoccupied molecular orbital, LUMO, and the other frameworks such as hardness and softness [78]. Quantum chemical studies have been performed successfully to connect the corrosion inhibition efficiency with molecular orbitals (MO) energy levels for certain various types of organic compounds, e.g., amides, amino acids and hydroxyl carboxylic acids, pyridine-pyrazole compound, sulphonamides to mention but a few [75].
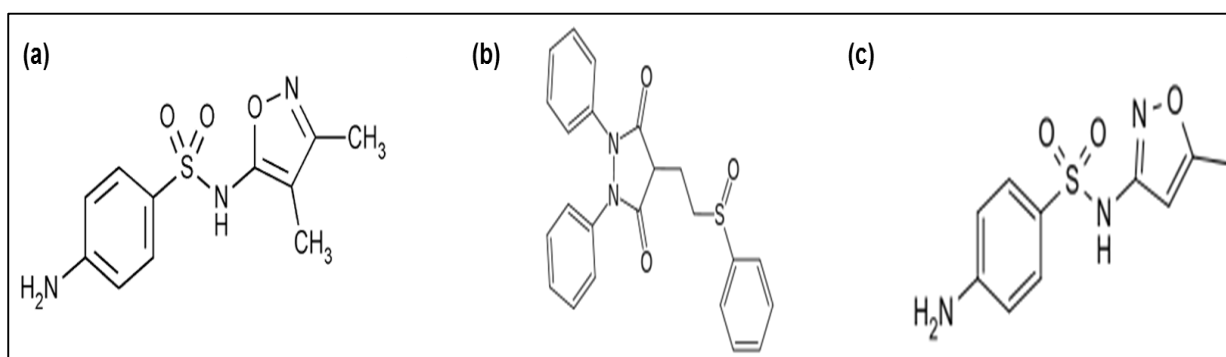
Figure 2. 4: (a) Sulphixazole, (b) Sulphinpyrazone and (d) Sulphamethoxazole.

Figure 2.4 presents some of medicinally active compounds [79]. Sulphisoxazole (Figure 2.4(a)) is a sulphonamide antibiotic. It works by inhibiting the growth and replication of bacteria [79]. Sulphinpyrazone (Figure 2.4(b)) is a uricosuric medication used to treat gout. Uricosuric medications are substances that increase the excretion of uric acid in the urine, thus reducing the concentration of uric acid in blood plasma [80]. Excellent characteristics of good corrosion inhibitors include the presence of heteroatoms (S, N, and O) that have lone pair of electrons, the presence of multiple bonds and the presence of aromatic rings that are electron rich [75].

The effect of inhibition of four sulfa drugs compounds such as sulfaguanidine, sulfamethazine, sulfamethoxazole (Figure 2.4(b)) and sulfadiazine on mild steel corrosion in 1.0M HCl solutions were assessed making use of both galvanostatic polarisation and weight loss technique [75]. The inhibition efficiency continuously increases with concentration to impel with sulfamethoxazole and sulfamethazine respectively because the inhibition efficiency propagates through a maximum for sulfaguanidine. The measurements of galvanostatic polarisation show that all the compounds that are examined are of assorted inhibitor kind with cathodic effectiveness that is predominant [81]. In addition, the outcomes exposed a performance that is better for these compounds as inhibitors of corrosion in a medium HCl than in a medium sulphuric acid solutions [82].

Owing to the toxicity of broadly utilised corrosion inhibitors and their ever-tenacious environment controls, there is a need to substitute those harmful inhibitors with non-hazardous choices that are effective. The substantial research and formation have led to the inventory of brand new corrosion inhibitor classes, and the significant growth on the utilisation of many drugs as inhibitors of corrosion. This review gives most of the inputs designed to the literature on the utilisation of drugs as corrosion inhibitors of diverse types of metals in previous years [83].
.
Chemical inhibitors influence a major part in the strategies of protection and mitigation for stagnation of corrosion. The organic compounds that comprises $\pi -$ bonds, heteroatoms such as P, S, N, and O are the most effective and efficient inhibitors together with the inorganic compounds, such as chromate, dichromate, nitrite, and so on [75]. Nevertheless, the utilisation of these compounds has been

lately interrogated, by the reason of many effects that are negative which they have caused in the surrounding. However, the formation of the interestingly new and unusual corrosion inhibitors of a source that is natural and a type that is not toxic has been regarded to be more significant and admirable. Because of their origin that is natural and also their properties that are not toxic and the impacts of negligible negative effects on the aquatic surrounding, drugs (chemical medicines) seem to be ideal candidates to substitute traditional toxic corrosion inhibitors [83].

The proclivity towards eco-friendly development of corrosion inhibitors intersects across several goals of pharmaceutical research, one of which is to develop molecules with desired biological activity. Endeavours to accomplish this goal are vigorously influenced by the idea of similarity of a molecule because common molecules tend to undergo a certain similar behaviour [84].

Virtual screening is known to be a phenomenon which is define as the assignment of a molecule that is unknown to the group of molecules that are active or inactive utilising an inter-molecular similarity, and has been reported to be prominent as a procedure to induce the inventory process of corrosion inhibitor's potential. More enlightenment of virtual screening computational techniques which lies exterior of the scope of a present review can be discovered elsewhere [85].

The sharing of so many similarities by the substructures of drugs and corrosion inhibitors is what is noteworthy in the outcomes of screening procedure. Both the carboxylic and heterocyclic systems are found everywhere in a structure of a drug. Five and six membered rings are the most common, but minute ring systems take place with logical frequency, for example, the cyclopropane ring in ciprofloxacin and the aziridine ring in mitomycin of the five and six membered systems, the majority are aromatic. In this manner, replaced benzene rings are more frequent, and the compounds that are heterocyclic such as pyridines, furans, thiophenes, imidazoles, isoxazoles [83] and some happen generally in a structure of a drug. Due to the structural nearness mentioned above, properties of the corrosion protection of several drugs have fascinated more attention in previous years. This review shows a general description of the extent research on many drugs utilised as corrosion

inhibitors [83] for miscellaneous metals, supplying a background for arrangement into groups on the basis of their uses that are clinical.

2.2.1.2. Ionic liquids

Many compounds have been developed and applied as corrosion inhibitors. Some organic compounds such as pyridines, imidazole's, 1, 3-azole, and fatty amides have been employed. Many inhibitors have been developed, but the challenge arises from the cost, environmental protection standards, toxicity and their availability. Recent studies are concerned about developing new compounds which are eco-friendly, and inexpensive.

Studies of ionic liquids have been carried out for the last two decades due to their good physical and chemical properties. They have low vapour pressure, high thermal and chemical stability, low or non-flammable and can work as catalyst. Ionic liquids have been reported as corrosion inhibitors by various authors. Ionic liquids can adsorb easily to the active site of material in order to reduce corrosion rate. Most commonly used ionic liquids are the ones that constitute heteroatoms such as nitrogen, oxygen, sulphur and phosphorus which serve as adsorption center due to the presence of lone pair of electrons. In addition, more electronegative heteroatom will tend to pull electrons towards itself and not efficient in inhibiting corrosion. Factors such as type and structure of ionic liquid, metal surface, corrosive environment all affect the mode of adsorption of liquid to metal surface.

Zhang and Hua [86, 87] studied different ionic liquid containing alkyl methylimidazolium as cation and either chloride or hydrogen sulphate as anion, which have shown good properties as corrosion inhibitors for carbon steel in aqueous 1 M HCl. Es'haghi studied 1-butyl-3-methylimidazolium bromide as corrosion inhibitor for carbon steel corrosion in aqueous hydrochloric acid, which showed good inhibitor properties.

There is a limited knowledge about physical, chemical and biological properties of ionic liquids as compared to organic solvent. Determination of properties and their trends is the most important or crucial step in designing ionic liquids for specific application [88], for example, the substitution of alkyls on the imidazolium ring and

the selection of large anion species have been the main trend to control the properties of imidazolium ionic liquids. Investigation of ionic liquids as ion conductive matrix and reaction solvent has been conducted due to their different physical properties such as, high liquidus range, high ionic conductivity, large voltage window, negligible vapour pressure and non-volatility. The major or representative cations of ionic liquids are imidazolium, pyridinium, and quaternary ammonium with major anions being $[BF_4]^-$, $[PF_6]^-$ and $N(SO_2CF_3)^-_2$.

Imidazolium ionic liquids have higher ionic conductivities and lower viscosity [66]. Investigations on imidazolium-based ionic liquids for capacitors, corrosion inhibitor and batteries have been conducted [67]. Tetrafluoroborate anion is mostly used due to its competitive properties and inexpensive. Some properties of ionic liquids are described below:

2.2.1.3. Liquidus range and thermal stability

Liquidus range is the temperature range between melting point and boiling point. Ionic liquids have high liquidus range compared to organic and any other molecular solvents. Ionic liquids do not evaporate at very high temperature, since they have negligible vapour pressure. They form glasses at a very low temperature. The maximum of liquid temperature is determined by the boiling point temperature. Many imidazolium salts have quite large liquidus range of over 300 ^{o}C, compared to that of water which is 100 ^{o}C. Ions or molecule with high boiling point have high thermal stabilities. Ionic liquids have high boiling point, so they are thermally stable, and the experiment can be conducted on these solvents at high temperature without degrading them [87].

2.3. PHTHALOCYANINES (Pcs)

2.3.1. HISTORY AND DISCOVERY OF METALLOPHTHALOCYANINES

Phthalocyanine (Pc), very similar to porphyrin compounds (see Figure 2.5) is a conjugated, aromatic and symmetrical macro molecules with 18π electron system

and four isoindole groups linked by four nitrogen atoms [88, 89]. Pcs possess similar structural features to naturally occurring porphynrins, though they have extended conjugation engendered by benzene rings. For this reason, Pcs exhibit improved chemical and thermal [90].
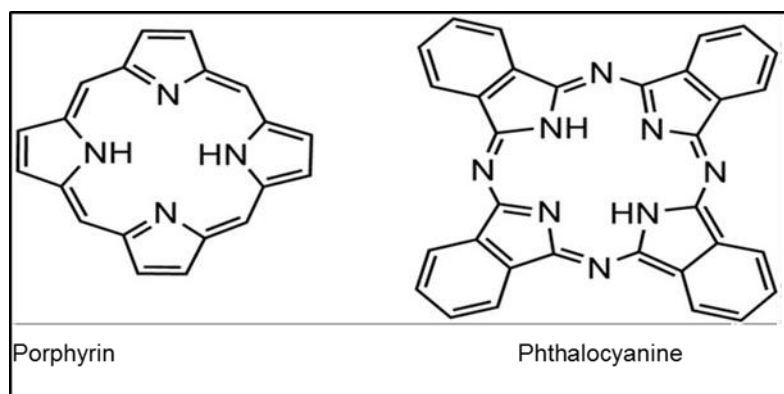
Figure 2. 5: Metal free phthalocyanine [89].

The useful properties of Pcs are due to their $\pi - \pi^*$ bands in association with the planar aromatic π-conjugation system. Phthalocyanine possess very fascinating photophysical and photochemical properties which show their importance in molecular functional materials [91]. The typical absorption spectrum of metallophthalocyanine (MPcs) (i.e. blue-green color) and unsubstituted Pc (red color) is presented in Figure 2.6 [92]. MPcs normally exhibit an intense absorption peak in the near infrared region (650-1050 nm) that plays a major role in many applications [93]. The intense peaks of the substituted and substituted Pcs in both UV regions are Q and B-bands [92]. The blue-green colored derivatives are used are often used as inhibitors and pigments [91]. It is through 18π electron macrocyclic conjugation systems that these blue-green compounds which possesses high stability against light and air have considerably attracted a great deal of interest in various application areas [92]. Pcs are used as inhibitors and pigments and also utilised in several industry branches and in medical field at incremental speed since are completely synthetic compounds. They are mainly used in liquid applications [93, 94], chemical sensors [95-96], solar cells [97-99], corrosion inhibitors [100, 101], gas sensors [102], optical data storage devices [103, 104], light emitting diodes (LED) [105], semiconductors [106, 107]. For the health of human beings, the usage of Pcs

as light-sensitive material for the treatment of cancer cells with photodynamic therapy (PDT) attracted great attention and this has been investigated by many scientists as a vital issue [108].
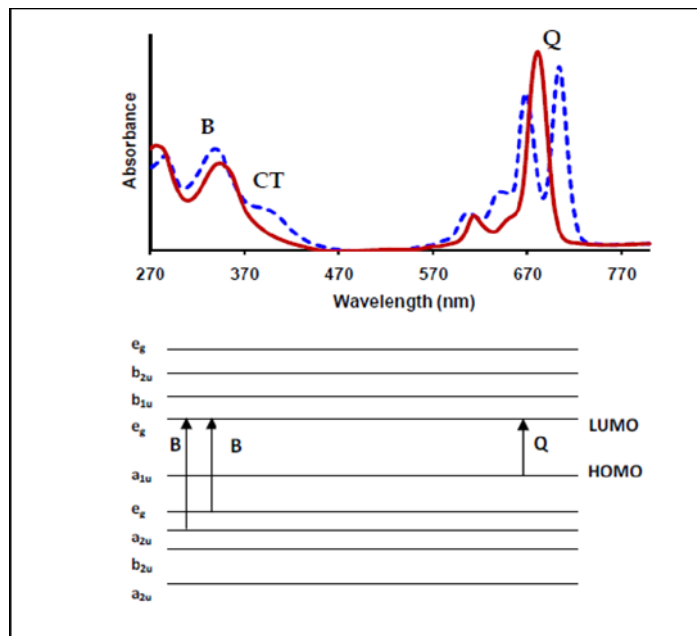
Figure 2. 6: Absorption spectrum of phthalocyanine with Q and B electronic transition bands [92].
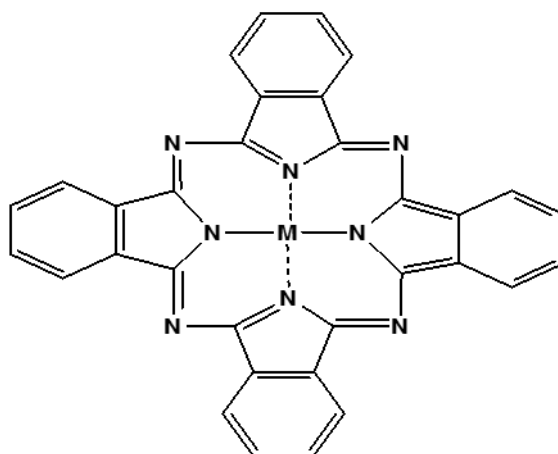
Figure 2. 7: The structure of metallophthalocyanine.

2.3.2. THE STRUCTURE OF PHTHALOCYANINE

The general feature of this macrocyclic compound is the normal structure consisting of four pyrrole units which are arranged in a circular form by the methane or azamethine bridges. Pcs share the same structure as porphyrins. Their essential

properties are accredited to their effective electron transfer abilities. About 63 various elemental ions including hydrogen [109], where the central atom connects with the pyrrole nitrogens are accommodated in the central cavity of Pcs which is one of its capability as a synthetic material (see Figure 2.7). From the bridges connecting the pyrrole units, the size of the hole can be determined.

MPcs have been used in several fields such as molecular electronics, optoelectronics, photonics, etc. MPcs functionalities are mainly based on reactions comprising electron transfer due to the 18π electron conjugated ring system located in their molecular structures [110, 111]. Pcs having some transition metals for an example, Cr, Mn, Fe and Co contains more complex electronic structures due to the open (n-1) d shell showing many energetically close-lying electronics states as the result [112]. Therefore, the chemical and physical properties of Pc can vigoriously be influenced by the choice of the central metal cation used [90].

2.3.3. SYNTHESIS OF PHTHALOCYANINE

There are three widely used methods for the synthesis of phthalocyanines, (1) the dry baking process, (2) the solvent and (3) microwave method. In the above mentioned methods, phthalocyanine can be prepared in non-substituted and substituted forms [113, 114]. The synthesis process of substituted and unsubstituted will be discussed below. Most known Pc precursors are ortho-disubstituted benzene derivatives and, these include phthalonitrile, phthalic acid, phthalic anhydride, phthalimide, diiminoisoindoline, o-cyanobenzamide, o-dibromobenzene and other derivatives shown in Figure 2.8. Phthalonitrile is the most prominent choice for laboratory synthesis as it gives high Pc product yields, for mass production of Pc, the phthalic anhydride is used as it is relatively cheap [115].

2.3.3.1. The reaction of phthalonitrile with metal or metal salts

Metallophthalocyanine such as Cobalt phthalocyanine (CoPc), Nickel phthalocyanine (NiPc), Chromium phthalocyanine (CrPc) and Iron phthalocyanine (FePc) are prepared by this method. Products of quinoline or urea decomposition behave as

absorbing materials of halogen in the absence of which the halogen atom settles in the Pc molecules.

2.3.3.2. The reaction of phthalic anhydride, phthalic acid or phthalimide, urea, metal salt and catalyst.

This synthetic method makes use of the phthalic anhydride or phthalic imide, a metal salt, urea and a catalyst. The reaction completion is about 4hrs upon heating from 170-200 ^{o}C. Generally, trichlorobenzene, nitrobenzene or chloronaphthalene are used as reaction mediums and about 85% yields are obtained in this reaction. Ammonium molybdate, boric acid and ferric chloride are mainly used as catalysts. Metallophthalocyanines such as CuPc, CoPc, NiPc, FePc and SnPC are generally prepared using this synthetic method. Below is the schematic synthetic procedure of metallophthalocyanines [116]:
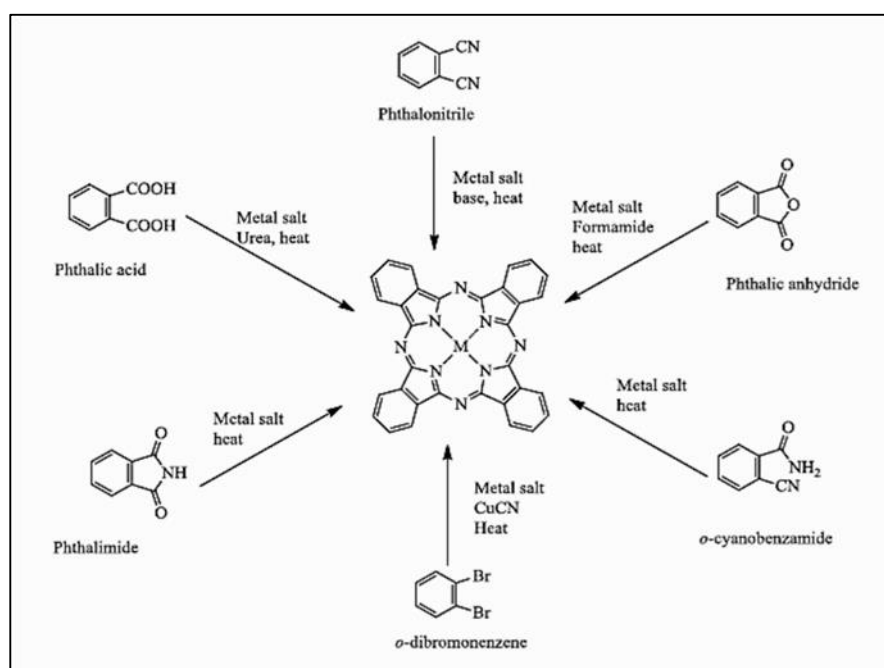
Figure 2. 6: Various precursors that are mainly used for the preparation of metallophthalocyanines [116].

2.3.4. SOLUBILITY OF PHTHALOCYANINE

There are different origins in the solubility of phthalocyanine that are found in the substituent groups or the coordinated ligands. For the Pcs chromophore to be manipulated, peripheral groups are primarily designed to promote the solubility in certain solvents [117]. In the Pc chromophore resides aggregation which is the results of the attractive interactions between two or more of them. In this case, the preferred solvents will be those containing maximum effects on reducing aggregation. However, the aggregated interaction is enhanced by the nature of a complexed ion in the cavity and by electronic and steric effects of peripheral groups [118]. Pcs compounds without ionic peripheral groups in organic solutions shows dependence on solvents and correlates with the solvent polarity influenced by the peripheral group [119].

The partial solubility of unsubstituted metallophthalocyanine is also a major problem, and this can be solved by introducing suitable substituents onto the ring system. For example, pyridine nitrogen quaternization of metallophthalocyanine analogous having a pyridine ring instead of one or more of the benzoic rings is considered to give solubility in aqueous media [120]. The solubility of targeted Pcs can dramatically increase in water or common organic solvents by introducing peripheral substituents. Unsubstituted Pc complexes are known to possess low solubility in solvents which are mostly known such as containing some solvents as 1-chloro- or 1-bromonaphthalene and quinoline, with sulfuric acid was examined to be the best solvent for Pcs [121].

2.3.5. UNSUBSTITUTED PHTHALOCYANINE

Pc can be synthesised from a number of ortho-disubstituted benzene derivatives that are cyclotetramerisation based like phthalic acids, phthalic anhydrides, or phthalonitriles in the presence of a metal salt, functioning as a template during the macrocyclic formation [122, 123]. Most recently, phthalocyanine complexes were unsubstituted on the periphery and had a low solubility in most known solvents even in such high-boiling aromatic solvents such as 1-chloro- or 1-bromonaphthalene and

quinoline, however, sulfuric acid was found to be the convenient solvent to dissolve them [124, 125].

2.3.6. SUBSTITUTED PHTHALOCYANINE

In corrosion studies both the functionality and solubility of the inhibitor compound are taken into consideration, thus this suggest that substituted phthalocyanine are the most preferred compounds due to their solubility in organic solvents unlike unsubstituted phthalocyanines [126]. The introduction of nitro groups into aromatic and heteroaromatic compounds clearly adjust the spectral characteristics of the compounds. The nitro group is in the exterior of the plane of the macro heterocyclic ring in nitro-substituted phthalocyanine [127].

This functional is responsible for the splitting of the Q band in the absorption spectra and the shift of peaks [128, 33] as well as the reduction in the luminescence intensity of the Pc [129] (Figure 2.9). Metallic tetranitrophthalocyanines are suitably synthesised from a compound of the metal of interest, together with the proper nitro-phthalic anhydride, in conjunction with urea [119]. Figure 2.9 shows the typical molecular structure of the metallic tetranitro phthalocyanine.
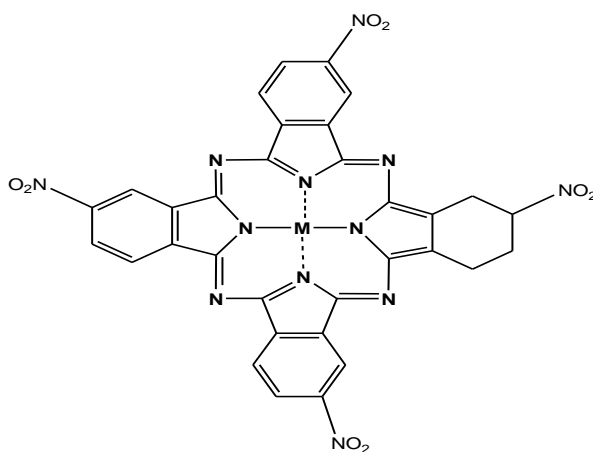
Figure 2. 7: Substituted metallophthalocyanine [119].

2.3.7. PROPERTIES AND APPLICATIONS OF PHTHALOCYANINE

Pc and their derivatives have been used in essential functional materials in numerous fields [130]. Their useful properties are accredited to their effective electron transfer abilities, accessibility in terms of the cost and straight forward synthesis on a big scale [131-133]. The functions of Pcs are electron transfer reactions universally based because of the 18π electron conjugated ring system located in their molecular structure [134, 135]. In the last 10 years, their high electron transfer capabilities have been used in numerous fields such as molecular electronics, optoelectronics and photonics [136, 137]. Furthermore, to traditional applications as inhibitors and pigments, peripherally substituted phthalocyanines are currently broadly utilised as industrial catalytic systems; photosensitizers for photodynamic therapy of cancer and as semiconductors [138, 139]. For several applications, the absorption maxima of Pc's are suitable if shifted to near infrared region. Heterocyclic compounds that contain nitrogen are an essential class of chemical compounds with a notable potential for industrial, pharmaceutical, and agrochemical applications [140, 141].

2.3.8. PHTHALOCYANINES AS CORROSION INHIBITORS

The study of corrosion is very active in research field due to its processes and their inhibition by organic inhibitors [142]. The dependability of the inhibition effect is mainly on physicochemical and electronic properties of the inhibitor compound due to its functional groups, steric effect, electronic density of the donor atoms, and orbital character of donating electrons [143, 144]. The mechanism of inhibition is mainly explained by adsorption film studies where the inhibitor compound adsorbs on the metal surface either physically or chemically [145, 146].

The reason Copper phthalocyanine (CuPc), Zinc phthalocyanine (ZnPc) and Nickel phthalocyanine (NiPc) are preferred as corrosion inhibitors in this project is because they display diverse interesting properties due to their extremely delocalized conjugated π electron system. The high inhibition of CuPc, ZnPc, and NiPc is accredited to the strong chemical adsorption the metallic phthalocyanine exhibit on a metal surface [147, 148].

Novel phthalocyanines in hydrochloric acid solution have been employed by Ozdemir et al [149] in studying the corrosion inhibition and electrochemical techniques such as potentiodynamic polarisation (PDP) and electrochemical impedance spectroscopy (EIS) were used to carry this experiment. Their experimental data fitted well with Langmuir adsorption isotherm. And the inhibition efficiency increased with the phthalocyanine concentration and decreased with increasing temperature.

The inhibition of corrosion of mild steel by other macrocyclic inhibitor compounds in the temperature range of 25 to 70 ^oC and conc. HCl by gravimetric analysis (weight loss) and Potentiodynamic polarisation studies was investigated by Quraish and Rawat [150]. From temperature range of 25 to 70 ^oC, both the inhibition efficiency (IE) and corrosion rate (C_R) of these compounds were evaluated and upon addition of potassium iodide (KI), IE values were enhanced due to synergism. It is shown by adsorption studies that the compounds of interest perform well in inhibiting corrosion of mild steel in 5N HCl by adsorption mechanism.

Hettiachchi *et al* [151] trust that it is expected of a planar molecule to give a high degree of coverage thus a higher inhibition efficiency. Phthalocyanine have become the object of intensive world-wide investigation due to their range of good properties. Zhao *et al.* [152] in 2005 studied the effect of inhibition for a metal-free phthalocyanine (H_2Pc), Copper phthalocyanine (CuPc) and Copper phthalocyanine tetra sulfuric tetra sodium ($CuPc(SO_4Na)_4$) on mild steel in $1mol.L^{-1}$ HCl in 1.0×10^{-5} to 1.0×10^{-3} $mol.L^{-1}$ concentration range. In addition, electrochemical test, scanning electroscope with energy disperse spectrometer (SEM/EDS) and quantum chemical method were imployed. The mild steel PDP curves in HCl containing this compound displayed that both cathodic and anodic processes of steel were suppressed, and the impedance Nyquist plots were mainly expressed as a capacitive loop with various compounds and concentrations. According to the electrochemical measurement results, the EI values for these three phthalocyanines with the same concentration decreased in the order of $CuPc(SO_4Na)_4$ > CuPc > H_2Pc. It is also shown from the SEM/EDS analysis that there is the presence of lightly corroded and oxidative steel surface for the metals after immersion in acidic solution containing 1.0×10^{-3} $mol.L^{-1}$ phthalocyanines than that in blank. The IE results of these Pcs increased with decrease in molecule's LUMO energy according to the quantum chemical calculation results which was different from the macrocyclic compounds.

2.4. CORROSION TESTING

2.4.1. GRAVIMETRIC ANALYSIS

Gravimetric method also known as a weight loss is a widely used method of inhibition. In many corrosion monitoring programs, the technique offers simplicity and reliability such that it generates the baseline method of measurement. During the corrosion process, the corroded metal loses its molecular mass, this is known as weight loss. In addition, when the weight loss is measured per unit time is considered as the rate of corrosion.

2.4.2. ADSORPTION STUDIES

The adsorption films forming on a metal surface during corrosion process of a metal in the presence of the inhibitor, are normally scratched off from the metal surface and the powder is analysed using the FTIR technique as a useful in studying the adsorption film resulting during the adsorption process [72]. Both liquid and solid samples spectra can be obtained and analysed using this technique. The technique is very accurate for measuring infrared absorption spectrum and it is very fast. It is mainly used for qualitative analysis in which the functional groups of the samples are determined.

2.5. ANALYTICAL TECHNIQUES

2.5.1. ULTRAVIOLET-VISIBLE SPECTROSCOPY (UV-vis)

Ultraviolet-visible (UV-vis) spectroscopy denotes the absorption spectroscopy which make use of incident light around the ultraviolet-visible region, meaning it uses light in the visible and adjacent (near-UV and near-infrared) ranges. Fundamentally, it is used for the study of electronic transitions which molecules undergo when light is irradiated on a molecule. The π electrons or non-bonding electrons absorb the energy in the form of ultraviolet or visible light and excited from ground state to higher energy state [153-155]. UV-vis is mainly used in analytical chemistry for quantitative and qualitative analysis for characterisation of the solute under study. It

can also be employed to determine the amount of impurities in organic solvents. In this study, inhibitors (i.e. metallophthalocyanine compounds) will be synthesised and confirmed using UV-vis spectroscopy. It has been seen that MPcs are blue-green coloured compounds with a characteristic intense absorption peak around the Q-band appearing between 600-735 nm where the blue-green colour absorbs [156].

2.5.2. FOURIER TRANSFORM INFRARED SPECTROSCOPY (FTIR)

FTIR is an analytical technique used to determine functional groups present in materials and it uses infrared light to interact with the sample of interest to provide spectrum of absorption or emission. This absorption corresponds specifically to the functional groups present in the molecule. The FTIR frequency range are measured as wave numbers typically over the range 4000–400 cm^{-1}. The background emission spectrum of the IR source is first recorded which will be used to correct the spectra reading of analyte, followed by the emission spectrum of the IR source with the sample in place. The ratio of the sample spectrum to the background spectrum is directly related to the sample's absorption spectrum. The resultant absorption spectrum from the bond natural vibration frequencies indicates the presence of various chemical bonds and functional groups present in the sample. In this work, FTIR was used to confirm the formation of phthalocyanine and introduction of NO_2 groups on the Pc at peripheral position.

2.5.3. X-RAY DIFFRACTION (XRD)

X-ray diffraction (XRD) is an analytical technique primarily utilised for phase identification of a crystalline material and can help in providing the information on unit cell dimensions. The material for analysis is finely grounded, homogenised and the mean bulk composition is determined. When conditions satisfy Bragg's law ($n\lambda=2d\sin\theta$), the interaction of the incident rays with the sample produces constructive interference (and a diffracted ray). The technique contains several advantages for the identification of unknown materials such as being powerful and rapid (<20 min) and the interpretation of data is relatively straight forward. However, a disadvantage about is that peak overlay may take place and worsens for high

angle reflections and that for fixed materials, detection limit is ~2% of sample. In this study, XRD was used to for the phase identification in the phthalocyanine structure.

2.5.4. THERMOGRAVIMETRIC ANALYSIS (TGA)

TGA is a method of thermal analysis in which changes in physical and chemical properties of materials are determined as a function of increasing temperature or as a function of time isothermally in inert atmosphere such nitrogen, helium, vacuum or air. They analyse materials such as inorganic materials, polymers, plastics, ceramics, glasses and composite materials can also be analysed [157]. TGA and DSC are mostly utilised to determine selected material's characteristics that show either mass loss or gain due to decomposition, oxidation, or loss of volatiles like moisture and providing the melting and recrystallization transitions. Their common applications are (i) determination of organic content in a sample, and (ii) studies of degradation mechanisms and reaction kinetics. Furthermore, TGA can be used to examine the material's thermal stability. If TGA is coupled with differential scanning calorimeter (DSC), it is normally referred to as a simultaneous thermal analysis (STA). This powerful technique can be employed to obtain a handful of information such as melting and crystallization with the same sample can be measured. In this work, the TGA they will be used to determine the thermal stability of the as-synthesised inhibitors [158].

2.5.5. ELECTROCHEMICAL TECHNIQUES

Electrochemical methods are a class of techniques in analytical chemistry which examines an analyte by measuring the potential (volts) and/or current (amperes) in an analyte containing electrochemical cell. These methods can be divided into several categories depending on which aspects of the cell are controlled and which are measured. The three main categories are potentiometry (the difference in electrode potentials is measured), coulometry (the cell's current is measured over time), and voltammetry (the cell's current is measured while actively altering the

cell's potential) [159]. In electrochemical techniques, redox reactions take place during operations and uses the principles of the electrochemical cell. This means that there is an electron loss and gain between the species of interest. The easiest electrochemical cell will contain two electrodes immersed in an electrolyte solution separated by a salt bridge. Chemical reactions mainly take place on the surface of the electrodes exhibiting several half reactions. Mostly three compartment electrodes are used which are places in an electrolytic solution in a glass [160]. The reactions take place on the working electrode of the surface. During operations, there must be a standardisation process which take place in reference electrode. The potential in reference electrode is fixed and the potential change is monitored on working electrode such as metals. The commonly used reference electrode are saturated calomel electrode (SCE) and silver/silver chloride (Ag/AgCl) electrode. Then ultimately there is an auxiliary electrode known as a counter electrode which serves as a sink for electrons for the current flow from the external circuit. The electro analytical technique was used in this work to determine electrochemical corrosion rates in corrosive environment.

2.5.5.1. Potentiodynamic polarisation (PDP)

The PDP method is normally utilised to obtain the relevant electrochemical parameters such as the E_{corr}, i_{corr}, anodic Tafel slope, b_a and cathodic Tafel slope, b_c. The measured corrosion current densities are used to calculate the inhibition efficiency according to the following equation [161, 162]:

$$\% IE_{PDP} = \left(\frac{i^0_{corr} - i^i_{corr}}{i^0_{corr}} \right) \text{X} 100 \qquad (2.18)$$

where i^0_{corr} and i^i_{corr} are values of corrosion current density in absence and in presence of inhibitor, respectively.

2.5.5.2. Electrochemical impedance spectroscopy (EIS)

EIS is used to study the corrosion of metals in corrosive environments. This technique can also be employed to investigate electrochemical parameters including the resistance of charge transfer, capacity of double layer, the constant phase element and exponents. These parameters are used to calculate the inhibition efficiency from the Equation 2.19 [162]:

$$\% IE_{EIS} = \left(1 - \frac{R^0{}_{ct}}{R_{ct}}\right) X100$$

(2.19)

where $R^0{}_{ct}$ and the charge is transfer resistance in the absence of the inhibitor and R_{ct} is the charge transfer resistance in the presence of the inhibitor.

2.6. CONCLUSIONS

In summary, this chapter presented a review of the literature related to the study of corrosion. The chapter introduced corrosion classifications, forms, and rate together with its mitigation method. Corrosion is a phenomenon that occurs when a material is exposed to air and moisture and this reaction involves water molecules and oxygen resulting in hydrogen evolution. Furthermore, this chapter elucidates the corrosion behavior of mild steel, aluminium and zinc. In this literature, inhibitors which are substances used in minute concentrations have been studied to prevent corrosion. There are several techniques used in the study of corrosion, however, this chapter outlines two of them: namely gravimetric analysis and electrochemical techniques. Under gravimetric analysis (weight loss), three crucial parameters such as corrosion rate, surface coverage and inhibition efficiency are outlined. The only one parameter determined in weight loss and electrochemical techniques is the percentage inhibition efficiency. Phthalocyanine was selected as inhibitor compound of interest and the literature review was outlined in this chapter. Three metals such as copper, zinc, and nickel were identified to be used as central metals in the synthesis of MPcs to improve the Pc thermal stability property. Variations concerning both substituted and unsubstituted MPcs were taken into considerations based on their theoretical

findings, as the result, unsubstituted MPcs were found to be insoluble in most solvents as opposed to the substituted MPcs. The literature review also presented that electrochemical and structural properties of the MPcs can be evaluated using analytical techniques such as grametric method, UV-vis, FTIR, XRD, TGA, PDP and EIS.

2.7. REFERENCES

1. K. M. Manamela, L. C. Murulana, M. M. Kabanda, E. E. Ebenso, Adsorptive and DFT studies of some imidazolium based ionic liquids as corrosion inhibitors for zinc in acidic medium, *Int. J. Electrochem. Sci.* 9 (2014) 3029-3046.

2. K. Myle. Corrosion Control (principles and practice). K. Myle and associates cc. ISBN 0 9583947 1 7.

3. G. Acosta, L. Veleva, J. L. López, Power Spectral Density Analysis of the Corrosion Potential Fluctuation of Aluminium in Early Stages of Exposure to Caribbean Sea Water. *Int. J. Electrochem. Sc*i, 9(2014) 6464-6474.

4. N. Ebrahimi, M. Momeni, A. Kosari, M. Zakeri, M. H. Moayed, A comparative study of critical pitting temperature (CPT) of stainless steels by electrochemical impedance spectroscopy (EIS), potentiodynamic and potentiostatic techniques, *Corros. Sci.* 59(2012) 96-102.

5. J. Soltis, Passivity breakdown, pit initiation and propagation of pits in metallic materials–review, *Corros. Sci.* 90(2015) 5-22.

6. N. Murer, R. G. Buchheit, Stochastic modeling of pitting corrosion in aluminum alloys*, Corros. Sci.* 69(2013) 139-148.

7. C. Bitondo, A. Bossio, T. Monetta, M. Curioni, F. Bellucci, The effect of annealing on the corrosion behaviour of 444 stainless steel for drinking water applications, *Corros. Sci.* 87(2014) 6-10.

8. P. Venugopal, V. Gopalan, Crevice Corrosion of Aluminium and its Prevention in Automobile Coolant Circuit (No. 2017-26-0170), SAE Technical Paper, 2017.

9. Marcus, P. 3rd Ed, Corrosion mechanisms in theory and practice. Crc Press (2011).

10. R. Javaherdashti, Microbiologically influenced corrosion: an engineering insight. *Springer* (2016).

11. T. Hvitved-Jacobsen, J. Vollertsen, A. H. Nielsen, 2nd Ed, Sewer processes: microbial and chemical process engineering of sewer networks. *CRC press* (2013).

12. K. Oldham, J. Myland, Fundamentals of electrochemical science. *Elsevier* (2012).

13. L. Bertolini, B. Elsener, P. Pedeferri, E. Redaelli, R. B. Polder, 2nd Ed, Corrosion of steel in concrete: prevention, diagnosis, repair*, John Wiley & Sons* (2013).

14. J. Xiao, S. Chaudhuri, Predictive modeling of localized corrosion: an application to aluminum alloys*, Electrochim. Acta*. 56(2011) 5630-5641.

15. E. S. M. Sherif, Corrosion and corrosion inhibition of aluminum in Arabian Gulf seawater and sodium chloride solutions by 3-amino-5-mercapto-1, 2, 4-triazole. *Int. J. Electrochem. Sci*, 6(2011) 1479-1492.

16. V. S. Sastri, Challenges in Corrosion: Costs, Causes, Consequences, and Control, *John Wiley & Sons* (2015).

17. X. Hu, R. Barker, A. Neville, A. Gnanavelu, Case study on erosion–corrosion degradation of pipework located on an offshore oil and gas facility, *Wear*. 271(2011) 1295-1301.

18. F. M. AlAbbas, C. Williamson, S. M. Bhola, J. R. Spear, D. L. Olson, B. Mishra, A. E. Kakpovbia, Microbial corrosion in linepipe steel under the influence of a sulfate-reducing consortium isolated from an oil field, *J. Mater. Eng. Perform*. 22(2013) 3517-3529.

19. F. Lees, 4th Ed, Lees' Loss prevention in the process industries: Hazard identification, assessment and control. Butterworth-Heinemann (2012).

20. J. Han, J. Zhang, J. W. Carey, Effect of bicarbonate on corrosion of carbon steel in CO_2 saturated brines, *Int. J. Greenhouse Gas Control*. 5(2011) 1680-1683.

21. A. M. Nor, The Effect of Turbulent Flow on Corrosion of Mild Steel in High Partial CO 2 Environments. Ohio University (2013).

22. H. A. El-Lateef, H.A., Abbasov, V.M., Aliyeva, L.I. and Ismayilov, T.A., Corrosion protection of steel pipelines against CO_2 corrosion-A review, *Chem. J.* 2(2012) 52-63.

23. K. B. Deshpande, Numerical modeling of micro-galvanic corrosion, *Electrochim. Acta*. 56(2011) 1737-1745.

24. P. Gilbert, 1st Ed, Depression: The evolution of powerlessness. *Routledge* (2016).

25. P. K. Wong, C. T. Kwok, H. C. Man, F. T. Cheng, Corrosion behavior of laser-alloyed copper with titanium fabricated by high power diode laser, *Corros. Sci.* 57(2012) 228-240.

26. A. Bahadori, Glossary of Terms. Corrosion and Materials Selection: A Guide for the Chemical and Petroleum Industries (2014) 461-521.

27. S. Bauer, P. Schmuki, K. von der Mark, J. Park, Engineering biocompatible implant surfaces: Part I: Materials and surfaces*, Prog. Mater Sci.* 58(2013) 261-326.

28. F. Ellyin, Fatigue damage, crack growth and life prediction. *Springer Science & Business Media (*2012).

29. D. W. Hoeppner, C. A. Arriscorreta, Exfoliation corrosion and pitting corrosion and their role in fatigue predictive modeling: state-of-the-art review, *Int. J. Aerospace Engineering*, (2012) 1-29.

30. T. J. Eggum, Hydrogen in Low Carbon Steel: Diffusion, Effect on Tensile Properties, and an Examination of Hydrogen's Role in the Initiation of Stress Corrosion Cracking in a Failed Pipeline (Doctoral dissertation) University of Calgary (2013).

31. X. G. Zhang, Corrosion and electrochemistry of zinc. *Springer Science & Business Media* (2013).

32. G. Williams, R. Grace, Chloride-induced filiform corrosion of organic-coated magnesium, *Electrochim. Acta.* 56(2011) 1894-1903.

33. V. S. Sastri, 1ˢᵗ Ed, Green corrosion inhibitors: theory and practice, *John Wiley & Sons* (2012).

34. M. G. Alexander, C. Fourie, Performance of sewer pipe concrete mixtures with portland and calcium aluminate cements subject to mineral and biogenic acid attack*, Mater. Struct.* 44(2011) 313-330.

35. F. Ellyin, Fatigue damage, crack growth and life prediction. *Springer Science & Business Media* (2012).

36. M. A. Maleque, M. S. Salit, Materials selection and design. *Springer Singapore* (2013).

37. R. A. Antunes, M. C. L. de Oliveira, Corrosion fatigue of biomedical metallic alloys: mechanisms and mitigation, *Acta Biomater.* 8(2012) 937-962.

38. F. Zarone, M. Ferrari, F. G. Mangano, R. Leone, R. Sorrentino, Digitally Oriented Materials: Focus on Lithium Disilicate Ceramics, *Int. J.dentistry*. (2016) 1-10.

39. K. O. Oparaodu, and G.C. Okpokwasili, Comparison of Percentage Weight Loss and Corrosion Rate Trends in Different Metal Coupons from two Soil Environments, *Int. J. Environ. Bioremediat. Biodegrad.* 2 (2014) 243-249.

40. F. Aouiniti, H. Elmsellem, A. Bachiri, M. L. Faunconnier, A. Chetouani, B. Chaouki, A. Aouniti, B. Hammout, Plants as a source of green corrosion inhibitors on mild steel in hydrochloric acid: The case of oil extract of leaves of Pistacia lentiscus from Saidia Morocco, *J. Chem. Pharm. Res.* 6 (2014) 10-23.

41. E. E. Ebenso, I.B. Obot, L.C. Murulana, Quinoline and its derivatives as effective corrosion inhibitors for mild steel in acidic medium, *Int. J. Electrochem. Sci.* 5 (2010) 1574-1586.

42. M. Otieno, H. Beushausen, M. Alexander, Prediction of corrosion rate in reinforced concrete structures–a critical review and preliminary results, *Mater. Corros.* 63(2012) 777-790.

43. Kumar, H., Saini, V., & Yadav, V. Study of Vapour Phase Corrosion Inhibitors for Mild Steel under different Atmospheric Conditions, *Int. J. Eng. & Innovative Tech.* 3(2013) 206-211.

44. G. G. Scatigno, M. P. Ryan, F. Giuliani, M. R. Wenman, The effect of prior cold work on the chloride stress corrosion cracking of 304L austenitic stainless steel under atmospheric conditions, *Mat. Sci. Eng.i: A.* 668(2016) 20-29.

45. G. Subramanian, S. Palraj, S. Palanichamy, Galvanic corrosion behaviour of aluminium 3004 and copper in tropical marine atmosphere, *J. Mar. Sci. Appl.* 13(2014) 230-236.

46. B. R. DuBay, Urban soil genesis, weathering of waste building materials, and bioavailability of lead in a chronosequence at former demolition sites, Detroit, Michigan (Doctoral dissertation), Wayne State University (2012).

47. C. Leygraf, I. O. Wallinder, J. Tidblad, T. Graedel, Atmospheric corrosion. *John Wiley & Sons (*2016).

48. A. C. Rady, S. Giddey, S. P. Badwal, B. P. Ladewig, S. Bhattacharya, Review of fuels for direct carbon fuel cells, *Sust. Energy Fuels.* 26(2012) 1471-1488.

49. M. P. Taylor, J. J. Chen, B. R. Young, 3rd Ed, Control for aluminum production and other processing industries. *CRC Press,* 2013.

50. V. E. Carter, 1st Ed, Metallic Coatings for Corrosion Control: Corrosion Control Series. Newnes (2013).

51. E. Husain, T. N. Narayanan, J. J. Taha-Tijerina, S. Vinod, R. Vajtai, P. M. Ajayan, 2013, Marine corrosion protective coatings of hexagonal boron nitride thin films on stainless steel, *ACS Appl. Mater. Interfaces.* 5(2013) 4129-4135.

52. A. Chilukuri, Corrosion inhibition by inorganic cationic inhibitors on the high strength alumunium alloy, 2024-T3, The Ohio State University (2012).

53. K. R. Ansari, M. A. Quraishi, A. Singh, Schiff's base of pyridyl substituted triazoles as new and effective corrosion inhibitors for mild steel in hydrochloric acid solution, *Corros. Sci.* 79(2014) 5-15.

54. P. M. Krishnegowda, V. T. Venkatesha, P. K. M. Krishnegowda, S. B. Shivayogiraju, Acalypha torta leaf extract as green corrosion inhibitor for mild steel in hydrochloric acid solution, *Ind. Eng. Chem. Res.* 52(2013) 722-728.

55. M. Salahshoor, Y. Guo, iodegradable orthopedic magnesium-calcium (MgCa) alloys, processing, and corrosion performance, *Materials.* 5(2012) 135-155.

56. N. O. Eddy, S. R. Stoyanov, E. E. Ebenso, Fluoroquinolones as corrosion inhibitors for Mild steel in acidic medium; experimental and theoretical studies, *Int. J. Electrochem. Sci.* 5(2010) 1127-1150.

57. A. Döner, R. Solmaz, M. Özcan, G. Kardaş, Experimental and theoretical studies of thiazoles as corrosion inhibitors for mild steel in sulphuric acid solution, *Corros. Sci.* 53(2011) 2902-2913.

58. A. Latnikova, D. Grigoriev M. Schenderlein, H. Möhwald, D. Shchukin, A new approach towards "active" self-healing coatings: exploitation of microgels, *Soft Matter.* 8(2012) 10837-10844.

59. A. N. Ababneh, M. A. Sheban, M. A. Abu-Dalo, Effectiveness of benzotriazole as corrosion protection material for steel reinforcement in concrete, *J. Mater. Civ. Eng. 24*(2011) 141-151.

60. S. I. Durowaye, G. I. Lawal, I. A. Raheem, V. O. Durowaye, Corrosion Response of Cast Aluminium Alloy for Extension Clamp Fabrication, *American Journal of Mat. Sci. 4*(2014) 159-164.

61. M. Pourbaix, Lectures on electrochemical corrosion. *Springer Science & Business Media* (2012).

62. A. Ghazoui, N. Bencaht, S. S. Al-Deyab, A. Zarrouk, B. Hammouti, M. Ramdani, M. Guenbour, An Investigation of Two Novel Pyridazine Derivatives as Corrosion Inhibitor for C38 Steel in 1.0 M HCl, *Int. J. Electrochem. Sci.* 8(2013) 2272-2292.

63. A. K. Singh, M. A. Quraishi, Effect of Cefazolin on the corrosion of mild steel in HCl solution, *Corros. Sci.* 52(2010) 152-160.

64. L. Herrag, B. Hammouti, S. Elkadiri, A. Aouniti, C. Jama, H. Vezin, F. Bentiss, Adsorption properties and inhibition of mild steel corrosion in hydrochloric solution by some newly synthesized diamine derivatives: experimental and theoretical investigations, *Corros. Sci.*52(2010) 3042-3051.

65. A. A. M. Beigi, M. Abdouss, M. Yousefi, S. M. Pourmortazavi, A. Vahid, Investigation on physical and electrochemical properties of three imidazolium based ionic liquids (1-hexyl-3-methylimidazolium tetrafluoroborate, 1-ethyl-3-methylimidazolium bis (trifluoromethylsulfonyl) imide and 1-butyl-3-methylimidazolium methylsulfate), *J. Mol. Liq.*177(2013) 361-368.

66. L. Suo, Y. S. Hu, H. Li, M. Armand, L. Chen, A new class of solvent-in-salt electrolyte for high-energy rechargeable metallic lithium batteries,*Nat. Commun.* 4(2013) 1481-1489.

67. I. Acar, Z. Bıyıklıoğlu, A. H. Kantekin, Synthesis, electrochemical, in situ spectroelectrochemical and in situ electrocolorimetric characterization of new metal-free and metallophthalocyanines substituted with 4-{2-[2-(1-naphthyloxy) ethoxy] ethoxy} groups, *Polyhedron.* 29(2010) 1475-1484.

68. A. Zarrouk, B. Hammouti, T. Lakhlifi, M. Traisnel, H. Vezin, F. Bentiss, New 1H-pyrrole-2, 5-dione derivatives as efficient organic inhibitors of carbon steel corrosion in hydrochloric acid medium: Electrochemical, XPS and DFT studies, *J. Corros. Sci.* 90 (2015) 572-584.

69. X. Li, S. Deng, X. Xie, Experimental and theoretical study on corrosion inhibition of o-phenanthroline for aluminum in HCl solution, *J. Taiwan Inst. Chem. Eng.* 45(2014) 1865-1875.

70. N. Soltani, H. Salavati, M. Paziresh, A. Moghadasi, Electrochemical and Quantum Chemical Calculations of Two Schiff Bases as Inhibitor for Mild Steel Corrosion in Hydrochloric Acid Solution, *IRAN J ANAL CHEM*. *2*(2015) 22-35.

71. H. Gerengi, M. Mielniczek, G. Gece, M. M. Solomon, Experimental and quantum chemical evaluation of 8-hydroxyquinoline as a corrosion inhibitor for copper in 0.1 M HCl, *Ind. Eng. Chem. Res.* 55(2016) 9614-9624.

72. M. A. Hegazy, A. M. Badawi, S. A. El Rehim, W. M. Kamel, Corrosion inhibition of carbon steel using novel N-(2-(2-mercaptoacetoxy) ethyl)-N, N-dimethyl dodecan-1-aminium bromide during acid pickling, *Corros. Sci.* 69(2013) 110-122.

73. I. B. Obot, D. D. Macdonald, Z. M. Gasem, Density functional theory (DFT) as a powerful tool for designing new organic corrosion inhibitors Part 1: an overview, *Corros. Sci.* 99*(2015)* 1-30.

74. P. B. Raja, A. K. Qureshi, A. A. Rahim, H. Osman, K. AwangNeolamarckia cadamba alkaloids as eco-friendly corrosion inhibitors for mild steel in 1M HCl media, *Corros. Sci.* 69(2013) 292-301.

75. E. E. Ebenso,T. Arslan, F. Kandemirli, N. Caner, I. Love, Theoretical studies of some sulphonamides as corrosion inhibitors for mild steel in acidic medium, *Int. J. Quantum Chem.* 110(2010) 2614-2636.

76. P. Niu, G. Liu, H. M. Cheng, Nitrogen vacancy-promoted photocatalytic activity of graphitic carbon nitride, *Phys. Chem C.* 116(2012) 11013-11018.

77. I. Danaee, O. Ghasemi, G. R. Rashed, M. R. Avei, M. H. Maddahy, Effect of hydroxyl group position on adsorption behavior and corrosion inhibition of hydroxybenzaldehyde Schiff bases: Electrochemical and quantum calculations, *J. Mol. Struct.*1035(2013) 247-259.

78. M. Rizzotto, Metal complexes as antimicrobial agents. In *A Search for Antibacterial Agents. InTech* (2012).

79. E. P. de Oliveira, R. C. Burini, High plasma uric acid concentration: causes and consequences, *Diabetol Metab Syndr.* 4(2012) 12.

80. P. B. Matad, P. B. Mokshanatha, N. Hebbar, V. T. Venkatesha, H. C. Tandon, Ketosulfone drug as a green corrosion inhibitor for mild steel in acidic medium, *In. Eng. Chem. Res.* 53(2014) 8436-8444.

81. O. Olivares-Xometl, C. López-Aguilar, P. Herrastí-González, N. V. Likhanova, I. Lijanova, R. Martínez-Palou, J. A. Rivera-Márquez, Adsorption and corrosion inhibition performance by three new ionic liquids on API 5L X52 steel surface in acid media, *In. Eng. Chem. Res.* 53(2014) 9534-9543.

82. G. Gece, Drugs: A review of promising novel corrosion inhibitors, *Corros. Sci.* 53 (2011) 3873-3898.

83. S. D. Patel, *Design and Evaluation of Different Gastroretentive Drug Delivery Systems of Some HMG Co-A Reductase Inhibitors* (Doctoral dissertation) Saurashtra University (2012).

84. F. Feixas, S. Lindert, W. Sinko, J. A. McCammon, Exploring the role of receptor flexibility in structure-based drug discovery, *Biophys. Chem.* 186(2014) 31-45.

85. M. J. Walker, Safeguarding food: advances in forensic measurement science and the regulation of allergens, additives and authenticity (Doctoral dissertation) Kingston University (2016).

86. Q. Zha*ng*, Y. *H*ua, Corrosion inhibition of aluminum in hydrochloric acid solution by alkylimidazolium ionic liquids, *Mat. Chem. Phys.* 1(2010), 57-64.

87. M. Freemantle, An introduction to ionic liquids. *RCS Advance* (2010).

88. A. A. M. Beigi, M. Abdouss, M. Yousefi, S. M. Pourmortazavi, A. Vahid, Investigation on physical and electrochemical properties of three imidazolium based ionic liquids (1-hexyl-3-methylimidazolium tetrafluoroborate, 1-ethyl-3-methylimidazolium bis (trifluoromethylsulfonyl) imide and 1-butyl-3-methylimidazolium methylsulfate), *J. Mol. Liq.* 177(2013) 361-368.

89. J. W. Colson, W. R. Dichtel, Rationally synthesized two-dimensional polymers, *Nat. Chem. 5*(2013) 453-465.

90. X. S. Wang, M. Chrzanowski, C. Kim, W. Y. Gao, L. Wojtas, Y. S. Chen, X. P. Zhang, S. Ma, SQuest for highly porous metal–metalloporphyrin framework based upon a custom-designed octatopic porphyrin ligand, *Chem. Commun.* 48(2012) 7173-7175.

91. C. Jagadish, S. J. Pearton, 1st Ed, Zinc oxide bulk, thin films and nanostructures: processing, properties, and applications. *Elsevier* (2011).

92. F. Yuksel, M. Durmuş, V. Ahsen, Photophysical, photochemical and liquid-crystalline properties of novel gallium (III) phthalocyanines, *Dyes Pigm.* 90(2011) 191-200.

93. W. Lee, S. B. Yuk, J. Choi, D. H. Jung, S. H. Choi, J. Park, J. P. Kim, Synthesis and characterization of solubility enhanced metal-free phthalocyanines for liquid crystal display black matrix of low dielectric constant, *Dyes Pigm.* 92(2012) 942-948.

94. C. Wang, H. Dong, W. Hu, Y. Liu, D. Zhu, Semiconducting π-conjugated systems in field-effect transistors: a material odyssey of organic electronics, *Chem. Rev.* 112(2011) 2208-2267.

95. A. A. Esenpınar, E. Durmaz, F. Karaca, M. Bulut, Synthesis and characterization of metallo phthalocyanines bearing 7-oxy-3-(4-pyridyl) coumarin substituents and their supramolecular structures with vanadyl bis (acetylacetonate), *Polyhedron.* 38(2012) 267-274.

96. B. Valeur, J. C. Brochon, New trends in fluorescence spectroscopy: applications to chemical and life sciences. *Springer Science & Business Media* (2012).

97. M. E. Ragoussi, M. Ince, T. Torres, Recent Advances in Phthalocyanine-Based Sensitizers for Dye-Sensitized Solar Cells, *Eur. J. Org. Chem.* 2013(2013) 6475-6489.

98. Z. Yao, M. Zhang, H. Wu, L. Yang, R. Li, P. Wang, Donor/acceptor indenoperylene dye for highly efficient organic dye-sensitized solar cells, *J. Am. Chem.* 137(2015) 3799-3802.

99. A. K. Sarker, M. G. Kang, J. D. Hong, A near-infrared dye for dye-sensitized solar cell: catecholate-functionalized zinc phthalocyanine, Dyes Pigm. 92(2012) 1160-1165.

100. L. Bammou, M. Belkhaouda, R. Salghi, O. Benali, A. Zarrouk, H. Zarrok, B. Hammouti, Corrosion inhibition of steel in sulfuric acidic solution by the Chenopodium Ambrosioides Extracts, *J. Assn. Arab. Univ. Basic. Appl. Sci.* 16(2014) 83-90.

101. L. Li, X. Zhang, J. Lei, J. He, S. Zhang, F. Pan, Adsorption and corrosion inhibition of Osmanthus fragran leaves extract on carbon steel, *Corros. Sci.* 63(2012) 82-90.

102. T. Sizun, M. Bouvet, Y. Chen, J. M. Suisse, G. Barochi, J. Rossignol, Differential study of substituted and unsubstituted cobalt phthalocyanines for gas sensor applications, *Sens. Actuators, B: Chemical.* 59(2011) 163-170.

103. T. Henning, D. Semenov, Chemistry in protoplanetary disks, *Chem. Rev.* 113(2013) 9016-9042.

104. A. Baba, N. Aoki, K. Shinbo, K. Kato, F. Kaneko, Grating-coupled surface plasmon enhanced short-circuit current in organic thin-film photovoltaic cells, *ACS Appl. Mater. Interfaces.* 3(2011) 2080-2084.

105. X. Yang, S. Zhuang, X. Qiao, G. Mu, L. Wang, J. Chen, D. Ma, High efficiency blue phosphorescent organic light-emitting diodes with a multiple quantum well structure for reduced efficiency roll-off, *Opt. Express.* 20(2012) 24411-24417.

106. Z. Li, Y. Li, W. Qin, X. Wu, Methylene blue photocatalytic degradation under visible irradiation of Al doped ZnO powders by hydrothermal synthesis sensitized with octa-iso-pentyloxyphthalocyanine lead, *J. Mater. Sci. Mater. Electron.* 27(2016) 6673-6680.

107. A. Nas, S. Fandaklı, H. Kantekin, A. Demirbaş, M. Durmuş, Novel organosoluble metal-free and metallophthalocyanines bearing triazole moieties: Microwave assisted synthesis and determination of photophysical and photochemical properties, *Dyes Pigm.* 95(212)8-17.

108. Z. Bıyıklıoğlu, M. Durmuş, H. Kantekin, Tetra-2-[2-(dimethylamino) ethoxy] ethoxy substituted zinc phthalocyanines and their quaternized analoques: synthesis, characterization, photophysical and photochemical properties, *J. Photochem. Photobiol. A.* 222(2011) 87-96.

109. Y. Tang, F. Zhang, S. Hu, Z. Cao, Z. Wu, W. Jing, Novel benzimidazole derivatives as corrosion inhibitors of mild steel in the acidic media. Part I: gravimetric, electrochemical, SEM and XPS studies, *Corros. Sci.* 74(2013) 271-282.

110. H. Jing, H. Song, Z. Liang, G. Fuxing, H. Yuh-Shan, Equilibrium andThermodynamic parameters of adsorption of Methylene blue onto Rectorite, *FRESEN. ENVIRON. BULL.* 19(2010) 2651-2656.

111. X. Li, S. Deng, H. Fu, Triazolyl blue tetrazolium bromide as a novel corrosion inhibitor for steel in HCl and H 2 SO 4 solutions, *Corros. Sci.* 53(2011) 302-309.

112. J. Sleven, C. Gorller-Walrand, K. Binnemans, Synthesis, spectral and mesomorphic properties of octa-alkoxy substituted phthalocyanine ligands and lanthanide complexes, *Mater. Sci. Eng. C.* 18(2001) 229–238.

113. S. A. R. A, J. Keshavayya, S. Prasanna, K. K. C. T, Synthesis and Characterisation of novel derivatives of oxadiazole substituted metal(II)phthalocyanines, *Arch. Appl. Sci. Res.* 5(2013) 189–196.

114. M. Camur, M. Durmus, A. R. Ozkaya, M. Bulut, Synthesis, photophysical, photochemical and electrochemical properties of crown ether bearing coumarin substituted phthalocyanines, *Inorganica Chim. Acta.* 383(2012) 287–299.

115. I. Acar, Z. Bıyıklıoğlu, A. H. Kantekin, Synthesis, electrochemical, in situ spectroelectrochemical and in situ electrocolorimetric characterization of new metal-free and metallophthalocyanines substituted with 4-{2-[2-(1-naphthyloxy) ethoxy] ethoxy} groups, *Polyhedron.* 29(2010) 1475-1484.

116. S. Carlo, A. W. Snow, R. S. Pong, J. S. Shirk, S. R. Flom, The United States Of America As Represented By The Secretary Of The Navy, Fabricating polymers for optical devices. U.S. Patent 8,003,713 (2011).

117. X. Y. Shen, Y. J. Wang, E. Zhao, W. Z. Yuan, Y. Liu, P. Lu, A. Qin, Y. Ma, J. Z. Sun, B. Z. Tang, Effects of substitution with donor–acceptor groups on the properties of tetraphenylethene trimer: aggregation-induced emission, solvatochromism, and mechanochromism, *J. Phys. Chem C.* 117(2013) 7334-7347.

118. T. Tanaka, A. Osuka, Conjugated porphyrin arrays: synthesis, properties and applications for functional materials, *Chem. Soc. Rev.* 44(2015) 943-969.

119. S. Tuncel, F. Dumoulin, J. Gailer, M. Sooriyaarachchi, D. Atilla, M. Durmuş, D. Bouchu, H. Savoie, R. W. Boyle, V. Ahsen, A set of highly water-soluble tetraethyleneglycol-substituted Zn (II) phthalocyanines: synthesis, photochemical and photophysical properties, interaction with plasma proteins and in vitro phototoxicity, *Dalton Trans.* 40(2011) 4067-4079.

120. S. Banerjee, V. Srivastava, M. M. Singh, Chemically modified natural polysaccharide as green corrosion inhibitor for mild steel in acidic medium, *Corros. Sci.* 59(2012) 35-41.

121. P. Ma, L. Lv, M. Zhang, Q. Yuan, J. Cao, C. Zhu, Synthesis of catalytically active porous organic polymer from iron phthalocyanine and diimide building blocks, *J. Porous Mater.* 22(2015) 1567–1571.

122. R. Seoudi, Z. A. El Sayed, FTIR , TGA and DC electrical conductivity studies of phthalocyanine and its complexes, *J. Molecu. Struct.* 753(2005) 119–126.

123. B. Köksoy, M. Durmuş, M. Bulut, Tetra- and octa-[4-(2-hydroxyethyl)phenoxy bearing novel metal-free and zinc(II) phthalocyanines: Synthesis, Characterisation and investigation of photophysicochemical properties, *J. Lumin.* 161(2015) 95–102.

124. M. A. Zolfigol, A. R. Pourali, S. Sajjadifar, S. Farahmand, Preparative method of novel phthalocyanines from 3- nitro phthalic anhydride, cobalt salt and urea

with chloromethylpolyestyrene as a heterogenous, reusable and efficient catalyst, *Der Pharma Chem.* 4(2012) 1397–1403.

125. Y. Wang, N. Hu, Z. Zhou, D. Xu, Z. Wang, Z. Yang, H. Wei, E. S. W. Kong, Y. Zhang, Single-walled carbon nanotube/cobalt phthalocyanine derivative hybrid material: preparation, characterization and its gas sensing properties, *J. Mater. Chem.* 21(2011) 3779-3787

126. R. Bayrak, H. T. Akçay, M. Durmuş, I. Değirmencioğlu, Synthesis, photophysical and photochemical properties of highly soluble phthalocyanines substituted with four 3, 5-dimethylpyrazole-1-methoxy groups, *J. Chem. Organomet.* 696(2011) 3807-3815.

127. J. Zhu, Y. Li, Y. Chen, J. Wang, B. Zhang, J. Zhang, W. J. Blau, Graphene oxide covalently functionalized with zinc phthalocyanine for broadband optical limiting, *Carbon.* 49(2011) 1900-1905

128. P. Pavaskar, J. Theiss, S. B. Cronin, S.B., 2012. Plasmonic hot spots: nanogap enhancement vs. focusing effects from surrounding nanoparticles, *Opt. Express* 20(2012) 4656-14662.

129. D. Wöhrle, G. Schnurpfeil, S. G. Makarov, A. Kazarin, O. N. Suvorova, Practical applications of phthalocyanines - from dyes and pigments to materials for optical, electronic and photo-electronic devices, *Macroheterocycles.*5(2012) 191–202, 2012.

130. S. Loera-Serna, E. Ortiz, H. I. Beltrán, First trial and physicochemical studies on the loading of basic fuchsin, crystal violet and Black Eriochrome T on HKUST-1, *New J. Chem.* 3097–3105.

131. A. Armağanı, S. Arslan, Phthalocyanines: Structure, Synthesis, Purification and Applications, *J. Life Sci.* 6(2016) 88–197.

132. N. Torabi, A. Rahnamanic, H. Amrollahi, F. Mirjalili, M. A. Sadeghzade, and A. Behjat, Performance enhancement of perovskite solar cell by controlling deposition temperature of copper phthalocyanine as a dopant-free hole transporting layer, *Org. Electron, physics, Mater. Appl.* 48(2017) 211–216.

133. A. A. M. Farag, Optical absorption studies of copper phthalocyanine thin films, *Opt. Laser Technol.* 39(2007) 728–732.

134. K. Sakamoto, E. Ohno-Okumura, Syntheses and functional properties of phthalocyanines, *Materials (Basel).* 2(2009) 1127–1179.

135.   C.-H. Lee, R. Filler, J. Lee, J. Li, B. K. Mandal, Synthesis and hydrogen adsorption properties of a new phthalocyanine-based metal–organic framework, *Renew. Energy.*35 (2010) 1592–1595.

136.   J. Li, S. Wang, S. Li, Water-phase synthesis of ordered hierarchical copper tetranitrophthalocyanine bundles with desirable superhydrophobicity, *J. Nanopart Res.* 14(2012) 1273-1280.

137.   D. Akyüz, H. Dinçer, A. R. Özkaya, and A. Koca, Electrocatalytic hydrogen evolution reaction with metallophthalocyanines modified with click electrochemistry, *Int. J. Hydrogen Energy.* 40(2015) 12973–12984.

138.   N. Touka, H. Benelmadjat, B. Boudine, O. Halimi, M. Sebais, Copper phthalocyanine nanocrystals embedded into polymer host: Preparation and structural Characterisation, *J. Assoc. Arab Univ. Basic Appl. Sci.* 13(2013) 52–56.

139.   E. D. P. Almeida, A. A. Costa, M. R. Serafini, F. C. Rossetti, J. M. Marchetti, V. H. V. Sarmento, R. d.. Nunes, M. E. G. Valerio, A. A.S. Arauˊjo, A. A. M. Lira, Preparation and Characterisation of chloroaluminum phthalocyanine-loaded solid lipid nanoparticles by thermal analysis and powder X-ray diffraction techniques, *J. Therm. Anal. Calorim.* 108(2012) 191–196.

140.   B. N. Achar, K. S. Lokesh, Studies on tetra-amine phthalocyanines, *J. Organomet. Chem.* 689(2004) 3357–3361.

141.   A. Zarrouk, B. Hammouti, T. Lakhlifi, M. Traisnel, H. Vezin, F. Bentiss, New 1H-pyrrole-2, 5-dione derivatives as efficient organic inhibitors of carbon steel corrosion in hydrochloric acid medium: Electrochemical, XPS and DFT studies, *J. Corros. Sci.* 90 (2015) 572-584.

142.   X. Li, S. Deng, X. Xie, Experimental and theoretical study on corrosion inhibition of o-phenanthroline for aluminum in HCl solution, *J. Taiwan Inst. Chem. Eng.* 45(2014) 1865-1875.

143.   N. Soltani, H. Salavati, M. Paziresh, A. Moghadasi, Electrochemical and Quantum Chemical Calculations of Two Schiff Bases as Inhibitor for Mild Steel Corrosion in Hydrochloric Acid Solution, *IRAN J ANAL CHEM*. *2*(2015) 22-35.

144.   H. Gerengi, M. Mielniczek, G. Gece, M. M. Solomon, Experimental and quantum chemical evaluation of 8-hydroxyquinoline as a corrosion inhibitor for copper in 0.1 M HCl, *In. Eng. Chem. Res.* 55(2016) 9614-9624.

145.   H. Elmsellem, N. Basbas, A. Chetouani, A. Aouniti, S. Radi, M. Messali, B. Hammouti, Quantum chemical studies and corrosion inhibitive properties of mild

steel by some pyridine derivatives in 1 N HCl solution,.*Electrochim. Acta.* 32(2014) 77-108.

146.   A. Staicu, A. Pascu, A. Nuta, A. Sorescu, V. Raditoiu, M. Pascu, Studies about phthalocyanine photosensitizers to be used in photodynamic therapy, *Rom. Rep. Phys.* 65(2014) 1032-1051.

147.   S. Pochekailov, J. Nožár, S. Nešpůrek, J. Rakušan, M. Karásková, Interaction of nitrogen dioxide with sulfonamide-substituted phthalocyanines: towards NO_2 gas sensor, *Sens. Actuator B-Chem.*169 (2012*)* 1-9.

148.   A. Kosari, M. Momeni, R. Parvizi, M. Zakeri, M. H. Moayed, A. Davoodi, H. Eshghi, Theoretical and electrochemical assessment of inhibitive behavior of some thiophenol derivatives on mild steel in HCl, *Corros. Sci.* 53(2011) 3058-3067.

149.   O. K. Ozdemir, A Aytac, D Atilla, M. Durmus, Corrosion inhibition of aluminium by novel phthalocyanines in hydrochloric acid solution, *J. Mater. Sci.* 46(20 1 1) 752-758.

150.   M. A. Quraishi, J. Rawat, Inhibition of mild steel corrosion by some macrocyclic compounds in hot and concentrated hydrochloric acid, *Mater. Chem. Phys.* 73(2002) 118-122.

151.   S. Hettiarachchi, Y. W. Chan, R. B. Wilson V. S. Agarwala, Macrocyclic corrosion inhibitors for mild steel in acid chloride environments, *Corros.* 45(1989) 30 -33.

152.   P. Zhao, Q. Liang, Y. Li, Electrochemical, SEM/EDS and quantum chemical study of phthalocyanines as corrosion inhibitors for mild steel in I mol/l HCl, *Appl. Surf. Sci.* 252(2005) 1596-1607.

153.   Q. B. Zhang, X. Y. Hua, Corrosion inhibition of mild steel by alkylimidazolium ionic liquids in hydrochloric acid, *Electrochim. Acta.* 54(2009) 1881 - 1887.

154.   H. A. Reece, Structural analysis and co-crystallization of neurotransmitter analogues (Doctoral dissertation), University of the Witwatersrand (2009).

155.   J. Bennett, T. Forster, IR cards: inquiry-based introduction to infrared spectroscopy, *J. Chem. Educ.* 87(2009) 73-77.

156.   S. S. Pingale, Study of microbial potential of Tridax procumbens I, *Int. J. Bioassays.* 2(2013) 866-869.

157. A. Chunder, T. Pal, S. I. Khondaker, L. Zhai, Reduced graphene oxide/copper phthalocyanine composite and its optoelectrical properties, *J.Phys. Chem*. 114 (2010) 15129-15135.

158. J. B. Houseknecht, Topic sequence and emphasis variability of selected organic chemistry textbooks, *J. Chem. Educ*. 87(2010) 592-597.

159. L. L. Faulkner, A. J. Bard, Electrochemical Methods and Applications. *Wiley* (2001).

160. B. D. Fahlman, What is Materials Chemistry? In *Materials chemistry*, Springer Netherlands. (2011)1-12.

161. P. Bollini, S. A. Didas, C. W. Jones, Amine-oxide hybrid materials for acid gas separations, *J. Mater. Chem.* 21(2011) 15100-15120.

162. A.Espinoza-Vázquez, G. E. Negrón-Silva, R. González-Olvera, D. Angeles-Beltran, M. Romero-Romo, M. Palomar-Pardavé, Effect of hydrodynamic conditions, temperature and immersion times on the corrosion inhibition efficiency of API 5L X52 steel in 1M HCl containing 1H-1, 2, 4 or 1H-1, 2, 3-triazoles, *Arabian J. Chem.* 1(2017)163-174.

CHAPTER THREE

ELECTROCHEMICAL AND GRAVIMETRIC STUDIES OF 4-TETRANITRO COPPER (II) PHTHALOCYANINE AS A CORROSION INHIBITOR FOR ALUMINIUM METAL IN CORROSIVE ENVIRONMENT

Thabo Pesha[1], *Gobeng R. Monama*[1], *Mpitloane J. Hato*[1,*], *Mamookgo E. Makhatha*[2], *Kabelo E. Ramohlola*[1], *Kerileng M. Molapo*[3], *Kwena D. Modibane*[1,**]. Electrochemical and Gravimetric Studies of 4-Tetranitro Copper (II) Phthalocyanine Inhibitor as a Corrosion Inhibitor for Aluminium Metal in Corrosive Environment. International Journal of Electrochemical Sciences.

[1]Department of Chemistry, School of Physical and Mineral Sciences, Faculty of Science and Agriculture, University of Limpopo (Turfloop Campus), Polokwane, Sovenga 0727, South Africa
[2]Department of Metallurgy, School of Mining, Metallurgy and Chemical Engineering, Faculty of Engineering and Built Environment, University of Johannesburg (Doorfontein Campus), Johannesburg 2001, South Africa
[3]Department of Chemistry, Faculty of Natural Science, University of the Western Cape (Bellville Campus), Cape Town 7535, South Africa

[*]E-mails: kwena.modibane@ul.ac.za (KD Modibane); mpitloane.hato@ul.ac.za (MJ Hato)

ABSTRACT

The inhibition effect of copper phthalocyanine (CuPc) and 4-tetranitro copper phthalocyanine (TNCuPc) on aluminium metal in 1mol.L^{-1} HCl was investigated by gravimetric and electrochemical techniques. The CuPc and TNCuPc inhibitors were synthesised and confirmed by using X-ray diffraction (XRD), Fourier transform infrared (FTIR), simultaneous thermal analysis (STA, thermal gravimetric analysis (TGA)/differential scanning calorimetry (DSC)), and ultraviolet-visible spectroscopy (UV-vis). XRD, UV-vis and FTIR analyses showed a successful formation of CuPc and TNCuPc inhibitors. The thermal stability of CuPc increased upon introduction of NO$_2$ group in the peripheral position. The corrosion inhibitor concentrations included 0, 40, 60, and 80 ppm, whereas testing temperatures were 303, 313, and 323 K. The results indicated that metallophthalocyanines (MPcs) is a good corrosion inhibitor with its efficiency increasing with the concentration. Both CuPc and TNCuPc inhibitors followed Langmuir's adsorption isotherm. The gravimetric measurements aided in the classical prediction of a first order kinetics for the corrosion inhibition process. The electrochemical results obtained show that the inhibitors significantly increased the polarisation resistance of Al-metal by reducing corrosion current densities. The inhibition efficiency increased with corresponding increase in the concentrations of the test inhibitor.

Keywords: Phthalocyanine, 4-tetranitro copper (II) phthalocyanine, corrosion inhibitor; aluminium metal, gravimetric analysis, PDP, EIS.

3.1. INTRODUCTION

Metals and their alloys find extensive use in our daily life and form part of human body system [1, 2]. For example, aluminium (Al) is a light metal, which is a good electric conductor and it has been used in variety of electronic applications [3]. However, one of the challenging problem for the usage of aluminium metal is the need to protect it from corrosion attack. It has shown that corrosion can be prevented by using various methods such as upgrading materials, blending of production fluids, process control and corrosion chemical inhibition [3-5]. Amongst these methods, the corrosion chemical inhibition is reported to be the best method to prevent destruction or degradation of metal surfaces in corrosive media due to economic and practical usage [6-8]. The search for an efficient corrosion inhibitor is paramount important and as a fundamental progressive step in this quest, it has been found that the use of organometallic compounds is one of the most practicable ways for providing protection of metals [9-11]. This is due to $\pi-$electron systems and presence of highly electronegative atoms such as O, N, S and P [12, 13].

Metallophthalocyanines (MPcs) are organometallic complexes with planar molecules with 8 N- atoms in a macrocyclic nucleus entailing an extended conjugated 18$\pi-$ electron systems and aromatic rings [14-19]. Recently, there has been a lot of attention paid to the use of phthalocyanines as potential corrosion inhibitors for different metals environments [17-19]. This is due to their planarity and the size of their molecular volume adsorption onto metal surface and the surface coverage have been enhanced thus efficient corrosion inhibition potentials [14]. In addition, MPcs have efficient corrosion inhibition properties because they are cost effective, synthesised easily, thermally stable and chemically noble [14, 18, and 19], and this emphasises the preference of chemical corrosion inhibition method. For example, CuPc has shown to possess good inhibition characteristics for high strength low alloy (HSLA) steel in 16% HCl [20]. Valle-Quitana *et al.* [19] carried out corrosion inhibition for 1018 carbon steel in 0.5 mol.L^{-1} H_2SO_4 using copper phthalocyanine and found CuPc acts as a good corrosion inhibitor with its efficiency increasing with the inhibitor concentration. However, solubility and aggregation are other important properties of MPcs which in turn can affect the adsorption and corrosion inhibition properties [14, 19, and 20]. MPcs solubility in different solvents mainly depends on the substituent

groups or coordinated ligand [21]. It has been reported that inhibitors which are completely soluble in the medium of interest exhibit higher inhibition efficiency [14, 21]. Hence, the aim of this work is to evaluate the corrosion inhibitory properties of phthalocyanine inhibitors for Al metal in acidic environment, organic inhibitors with good solubility in H_2SO_4, whose chemical structure is given in Figure 3.1 and possesses N and Cu atoms. To our knowledge, the use of CuPc and TNCuPc as corrosion inhibitors for aluminium metal sheet in HCl environment was not reported to date. In the present paper, CuPc and TNCuPc as simple phthalocyanines that could be easily synthesised were selected as materials of interest for corrosion studies. Furthermore, TNCuPc has nitro (NO_2) group at the peripherally to enhance adsorption of the inhibitor on the aluminium metal. The corrosion inhibition behaviour of CuPc and TNCuPc inhibitors for aluminium in corrosive environment of 1 mol. L^{-1} HCl solution was investigated by gravimetric and electrochemical analyses as part of our contribution to the quest for a substance which do not only possess good inhibitive effect but is eco-friendly and can be accessed with ease.
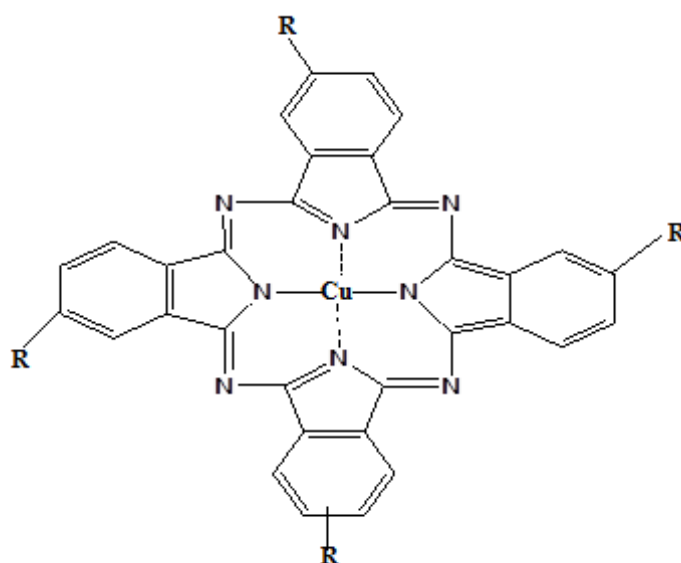
Figure 3. 1: Molecular structure of copper phthalocyanine (R=H) and 4-tetranitro phthalocyanine (R=NO_2) [22].

3.2. EXPERIMENTAL SECTION

3.2.1. MATERIALS

Copper nitrate trihydrate (Cu $(NO_3)_2.3H_2O$), trimesic acid, 1.3.5-benzenetricarboxylic acid (H_3BTC) and tetrabutylammonium percholate (TBAP) were purchased from Sigma Aldrich, South Africa. Phthalimide, 32% hydrochloric acid (HCl), methanol, nitrobenzene, ethanol, nitric acid (HNO_3) and sulphuric acid (H_2SO_4) were purchased from Rochelle chemicals. Ammonium heptamolybdate (($NH_4)_6Mo_7O_{24}$), and urea (CH_4N_2O) were purchased from uniLAB.

3.2.2. SYNTHESIS OF COPPER (II) PHTHALOCYANINES

Copper (II) phthalocyanine (CuPc) was synthesised from phthalimide according to previous method reported elsewhere [22]. Typically, a mixture of phthalimide (3.00 g, 0.0200 mol) in the presence of excess urea (3.00 g, 0.0500 mol), ammonium heptamolybdate (0.0800g, 0.0600 mmol) and copper nitrate (1.40 g, 0.0058 mol) in nitrobenzene (15.00 mL) was refluxed for 5 hours at 180 °C with a constant stirring. The product was washed with ethanol and dried at 110 °C giving a yield of 1.3 g, 51 %.

Synthesis and purification of 4-tetranitro copper (II) phthalocyanine (TNCuPc) was done as outlined for CuPc above. In this case, 4-nitrophthalimide was used instead of phthalimide following the reported literature for preparation of phthalocyanine inhibitor [23]. Briefly, a mixture of 4-nitrophthalimide (3.00 g, 0.0156 mol) in the presence of excess urea (3.00 g, 0.0500 mol), ammonium heptamolybdate (0.0800g, 0.0687 mmol) and copper nitrate (1.40 g, 0.0058 mol) in nitrobenzene (15.00 mL) was refluxed for 5 hours at 180 °C to give a target compound. The product was washed with ethanol and dried at 110 °C giving a yield of 2.64g (70 %) and melting point >300 °C.

3.2.3. CHARACTERISATION TECHNIQUES

Absorbance spectra were recorded at room temperature in the wavelength region 200 nm – 900 nm and 1 cm optical path length quartz cuvette using a Varian Cary

300 UV-vis-NIR spectrophotometer using H_2SO_4 as a solvent. FTIR spectra were recorded on Spectrum II spectrometer (Perkin Elmer). The spectra were obtained in the wavenumber range between 400 and 4500 cm^{-1} at room temperature. A minimum of 32 scans were collected at a resolution of 4 cm^{-1}. The crystal structure of the inhibitors was investigated using X-ray diffraction (XRD Phillips PW 1830, CuK_α radiation, λ = 1.5406 A). The thermal stability of the samples was performed using a PerkinElmer STA 6000 instrument connected to a PolyScience digital temperature controller under N_2 gas purged at a flow rate of 20 ml/min. The calibration of the instrument was performed using indium (melting point =156.6 °C) and aluminium (melting point = 660 $^{\circ}$C). The weight of the samples ranging between 1−4 mg were heated from 30-500 °C under N_2 environment at a constant heating rate of 20 °C /min. The data was collected and analyzed using Pyris software®.

3.2.4. GRAVIMETRIC METHOD

Corrosion measurements were performed on 98% Al sheets with dimensions 3 cm × 4 cm. The surface of the Al specimens were grounded using silicon carbide papers of various grades (600–1000), washed with distilled water, degreased in acetone, wiped with a clean towel paper and finally air-dried. Aggressive solution of 1 $mol.L^{-1}$ HCl was prepared by diluting 32% analytical grade HCl with distilled water. Metallophthalocyanines were first dissolved in minimum amount (10 mL equivalent to 4% by vol.) of H_2SO_4 and then diluted to various concentrations (40, 60, and 80 ppm) in 250 mL volumetric flask.

The samples were weighed (w_1) and then suspended freely in glass reaction vessels with the aid of glass hooks and rods. The suspended samples were completely immersed in 100 mL of the aggressive solutions of 1 $mol.L^{-1}$ HCl without and with various concentrations of the studied inhibitors at 303–323 K in thermo stated water baths. The samples were retrieved after 15 hours, gently brushed, washed with distilled water, rinsed with acetone, dried with warm air and finally re-weighed (w2). The experiment was conducted in triplicates for each concentration and the average weight loss (W = (w1 + w2+ w3)/3 in grams) was recorded. The corrosion rate (C_R in

gcm^{-2}·h^{-1}), percentage inhibition efficiency (%IE) and surface coverage (θ) were calculated from the weight loss using the equations [14, 24] (Eq. 2.1, 3.1,3.2):

$$\theta = \left(1 - \frac{\rho_1}{\rho_2}\right) \tag{3.1}$$

$$\%IE = \left(1 - \frac{\rho_1}{\rho_2}\right) \times 100\% \tag{3.2}$$

where W is the average weight loss of the Al sheets, S is the total surface area of the Al specimen (cm^2), t is the immersion time (h), while ρ_1 and ρ_2 are the corrosion rates with and without inhibitors respectively.

3.2.5. ELECTROCHEMICAL MEASUREMENTS

Electrochemical measurements were performed using Bio-Logic SP150 Potentiostat electrochemical workstation. The data was collected using a conventional three-electrode set-up with Al metal (1 cm^2 area) as a working electrode, Pt wire as a counter electrode and Ag/AgCl wire as a reference electrode. The electrolyte solution, 1.0 mol. L^{-1} HCl, was prepared from the reagent grade HCl and double distilled water at 298 K. Repetitive scanning of the solutions of CuPc and TNCuPc (1.0 mol.L^{-1}) was measured from -0.250 to +0.250 mV at the constant sweep rate of 1 mV/s. Electrochemical experiments were performed in 10 ml of 0.1 M TBAP/DMSO electrolytic system. Before each experiment, the working electrode was immersed in the test cell until it reached steady state condition. Electrochemical impedance spectroscopy (EIS) measurements were carried out in frequency range of 100 kHz to 10 MHz with amplitude of 10 mV peak-to-peak using ac signals at open circuit potential. Double layer capacitance (C_{dl}) and charge transfer resistance (R_{ct}) values were obtained from impedance measurements [14, 24]. Cathodic and anodic Tafel slopes (b_c and b_a) and corrosion current density (icorr) were extracted by Tafel extrapolating the anodic and cathodic plots. The percentage inhibition efficiency values were calculated using the following Equations 2.18 and 2.19 [14, 24, 25]:

3.3. RESULTS AND DISCUSSION

3.3.1. STRUCTURAL PROPERTIES

The XRD patterns of CuPc and TNCuPc inhibitors are presented in Figure 3.2(a). The patterns of CuPc are similar to the one reported by by Zongo et al [22], suggesting a cubic structure of phthalocyanine. Moreover, a numerous number of sharp diffraction peaks appearing at 2Θ = 5.7, 6.9 and 9.1° corresponding to miler indices (100), (110) and (111), respectively, are observed. These sharp peaks indicate highly crystalline structure [22, 27]. However, the diffraction peaks of TNCuPc possessed a decrease and broadening patterns at 2Θ = 13.0, 14.5 and 27.2°. This behaviour suggests a large crystal size of the CuPc upon introduction of the nitro groups at the periphery with amorphous character [28-30].
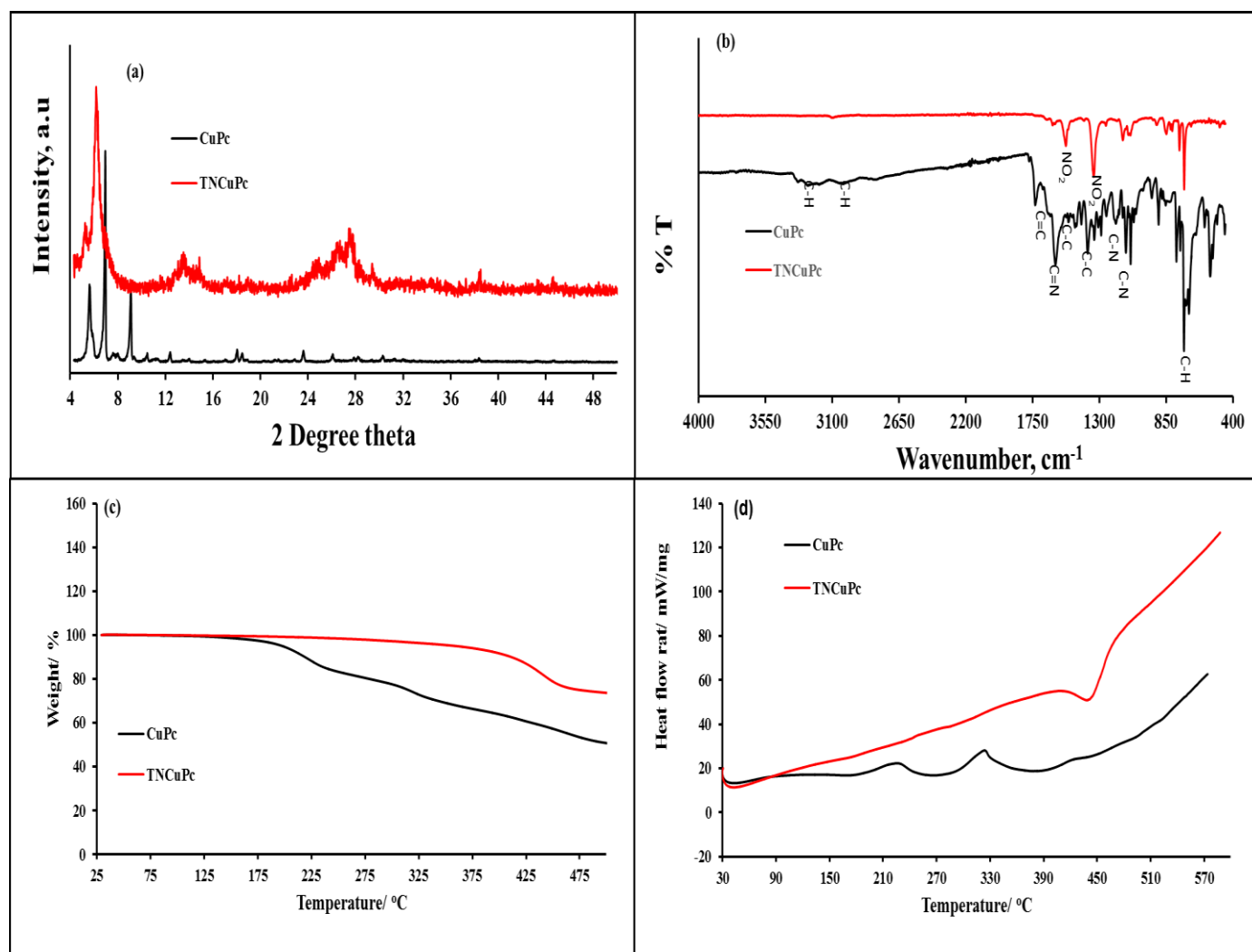
Figure 3. 2: (a) XRD, (b) FTIR, (c) TGA, and (d) DSC of CuPc and TNCuPc inhibitors.

The successful synthesis of CuPc and TNCuPc was further confirmed by FTIR and the results are demonstrated in Figure 3.2(b). The assignment of CuPc vibrational modes is an essential step towards determining structural properties of the compounds. The peaks at 3283 and 1720 cm-1 correspond to the N-H and C=O vibrations of the phthalimide, respectively [30]. Interestingly, these vibrations disappeared after conversion into both CuPc and TNCuPc, indicating successful synthesis of metallophthalocyanine [31]. The vibrational peaks between 700 and 1000 cm^{-1} are typically due to phthalocyanines skeletal vibrations [32]. The characteristic of NO_2 stretch was observed at around 1350 and 1450 cm^{-1}, which is a substituent in the prepared TNCuPc. The two observable peaks at 3049 and 2910 cm^{-1} for CuPc are attributed to the symmetric C-H stretching in the ring and in the alkyl group, respectively [22]. The peak around 1609 cm^{-1} is due to C=C deformation of macro cycle ring in pyrrole and at around 1506 cm^{-1} is due to the C=N stretching. For isoindole, C-C stretching appeared at 1428 and 1332 cm^{-1}. At around 909, 882, and 728 cm^{-1} is the appearance of the C-H bending. However, the peaks at around 1284, 1162 and 1070 cm^{-1} are accredited to C-N stretching in isoindole, C-N in plane bending, and C-H in plane bending respectively [22, 28-32]. TNCuPc also showed strongest peaks of NO_2 group at 1334 and 1525 cm^{-1} on the phthalocyanine ring [28].

Parts (c) and (d) of Figure 3.2 show thermogravimetric and differential scanning calorimetry (DSC) curves of CuPc and TNCuPc inhibitors. The weight loss in TGA corresponds to the change in transition phase in the DSC curve. At the initial period, weight loss is observed which is due to the evaporation of water [33]. TNCuPc shows the most thermal stability as compared to CuPc inhibitor. The high thermal stability may be the stabilising effect of NO_2 associated to the electron density acting as stabilising effect to the structure and blocking of Cu diffusion typically for Pcs [34]. In addition, another degradation step is observed around 400 °C, corresponding to the oxidative degradation of TNCuPc [22, 34]. In Figure 3.2(d), the DSC curves of both CuPc and TNCuPc are presented. In these results, both recrystallisation and melting transitions were observed. These observable peaks correspond to exothermic and endothermic processes, respectively. Melting transition peaks were observed at 217 and 321 °C for CuPc which associated to endothermic process while for TNCuPc recrystallisation was observed at 450 °C. In TGA curves, CuPc

decomposes from 200-217 °C and from 300-321 °C while the TNCuPc decomposes in a single step at 400-450 °C.

Figure 3.3(a) shows the UV-vis spectroscopic data of the CuPc and TNCuPc in H_2SO_4. The spectra for the CuPc and TNCuPc displayed an intense Q absorption band in the 720-780 nm region of the visible range and a B band between 300-400 nm in the UV region. Both Q and B bands are known to arise from π-π* transitions originating from the phthalocyanine ligand, and are assigned to the $6e_g \rightarrow 2a_{1u}$ transition for the Q-band and the $6eg \rightarrow 4a2u$ for the B-band [23, 31, 35]. The maximum wavelength values of the Q bands for all the TNCuPc and TNCuPc/MOF composite are consistent with the data presented by Cong *et al*. [35] and also as an indicative of presence of phthalocyanine in the composite. The metallotetranitro phthalocyanine (MTNPcs) have shown a broader and a slightly blue-shifted Q-band [35] relative to the MPcs. The unusual Q-band broadening and split may be due to the effect of the nature of solvent used [35] In addition, the stronger intermolecular interactions lead to a higher degree of aggregation causing the replacement of the typical monomer Q-band structure by two broader bands and a blue shifted absorption band [27]. The nitro functionalized phthalocyanine inhibitor comprises of both B- and Q-bands. The B-band of these phthalocyanines appears between 315-352 nm, and the Q-band was observed between 600-750 nm where the blue colour actually absorbs [22]. These bands arise from $\pi - \pi^*$ transitions and this can be inferred from the four frontier orbitals (HOMO and LUMO orbitals) [31]. Furthermore, two splitting absorption bands are observed around 630 and 710 nm, which is likely due to the vibronic coupling in the excited state [31]. For example, Beer-Lambert's law was obeyed for the compound ranging from 0 to 5 ppm in Figure 3.3(b). The absorptivity coefficient of CuPc from Beer's law was found to be logε of 5.11 at 790 nm corresponding to the reported one [22]. On the other side, the TNCuPc possessed the split absorbance with logε of 4.67 and 4.65 at 763 and 739 nm respectively. These log ε values also show that there are lot of molecules interacting with light which will enhance the inhibition efficiency of the inhibitor on Al metal [36].
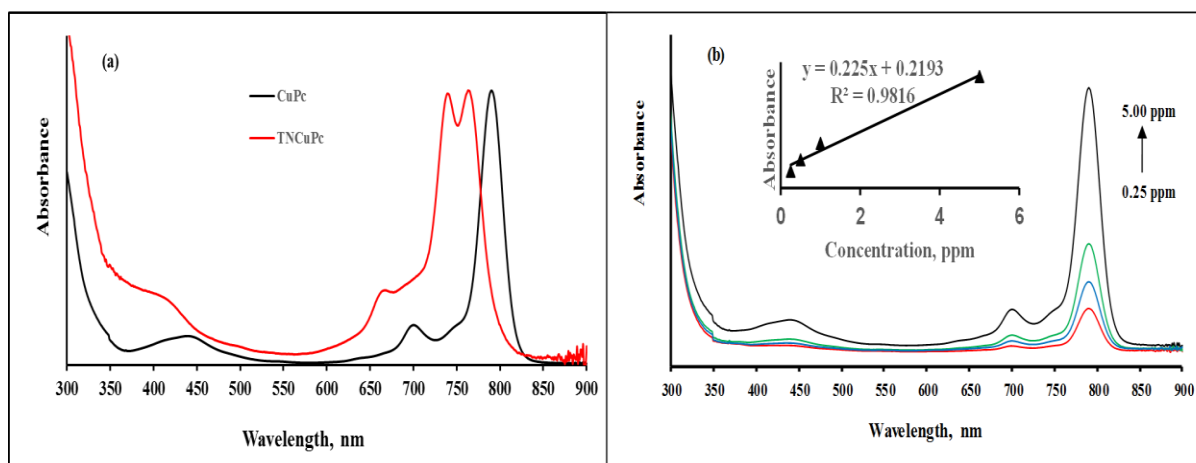
Figure 3. 3: (a) UV-vis spectra of CuPc and TNCuPc in H_2SO_4 (~10 ppm), and (b) UV-vis spectrum of CuPc at different concentration from 0 to 5 ppm. Inset: concentration dependence of CuPc.

3.3.2 GRAVIMETRIC MEASUREMENTS

3.3.2.1. EFFECT OF INHIBITOR CONCENTRATION AND TEMPERATURE

Table 3.1 and parts (a) and (b) of Figure 3.4 show the corrosion rate results, in terms of percentage inhibition efficiency (%IE) obtained from weight loss measurements for Al metal sheet in $1\,mol.L^{-1}$ HCl at different inhibitor concentrations from 0-80 ppm and at 303–323 K. It can be seen in Table 3.1 that when 40 ppm of inhibitor is added the corrosion rate decreases compared to that for uninhibited solution, at the three different temperatures, but with a further increase in the inhibitor concentration the corrosion rate decreases. Furthermore, corrosion rate decreases as the inhibitor concentration increases due to the fact that the inhibitor adsorption surface coverage, Ө on the Al metal surface starts to increase [37]. It can also be observed that the corrosion rate, C_R increases with an increase in the temperature for both CuPc and TNCuPc.
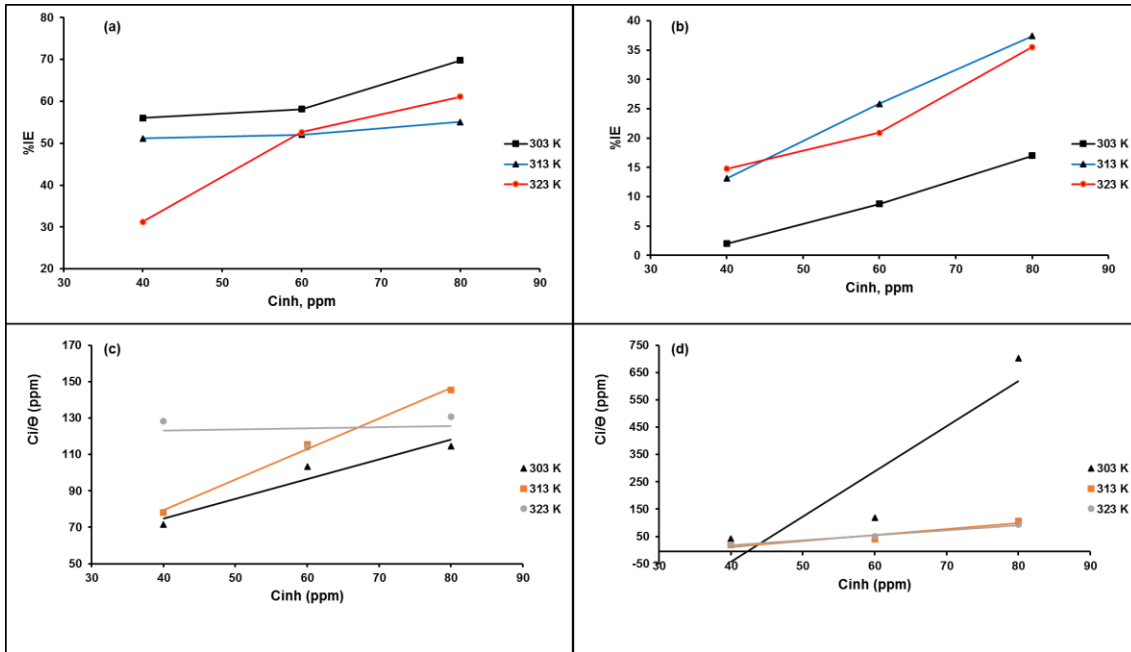
Figure 3. 4: Plot of inhibition efficiency (%IE) against inhibitor concentration (ppm) for (a) CuPc and (b) TNCuPc; and Langmuir adsorption isotherms using (c) CuPc and (d) TNCuPc inhibitors on Al metal sheet at 303, 313 and 323 K.

Inhibitor efficiency at the different concentrations and temperatures is given in Figure 3.4(a) and (b) for CuPc and TNCuPc, respectively. From these results, its can be seen that the highest efficiency values are obtained at 80 ppm. It should be noted that the %IE of CuPc decreases with increasing the temperature. This observation is related to inhibitor molecules that are physically adsorbed on the Al metal surface [38]. Whereas TNCuPc shows a chemical adsorption from 303 to 313 K that implies an increase in the inhibitor efficiency with an increase in the temperature [38]. Furthermore, it has been described that inhibitor can form coordination bonds between the unshared electron pair of N atom and the empty d iron electron of the phthalocyanine rings [39]. The coordinate bond could be formed by donating the lone electron pairs of N atoms to the unfilled orbits of Cu. It has been reported that phthalocyanine molecules are subjected to protonation in acidic solution [40]. Cl$^-$ ions could accumulate gradually close to the metal/solution interface, being specifically adsorbed [41]. They create an excess negative charge towards the solution and favour more adsorption of the cations; then the protonated inhibitor may adsorb through electrostatic interactions between the positively charged molecules and the negatively charged metal surface [42]. It has been reported that protonated

phthalocyanine adsorbed on metal surface, coordinate bond may be formed by partial transference of electrons from the N polar atom to the metal surface [43].

Table 3. 1: The values of corrosion rate (C_R), percentage inhibition efficiency (%IE) and surface coverage (θ) of CuPc and TNCuPc at 303, 313 and 323 K for aluminium metal sheet.

Sample	Temp. (K)	Conc. (ppm)	Δw (g)	C_R (X10^{-3} g.cm^{-2}.hr^{-1})	%IE	θ	C/θ (ppm)
CuPc	303	0	0.559	3.106	_	_	_
		40	0.246	1.367	55.99	0.56	71.4
		60	0.234	1.300	58.14	0.58	103.2
		80	0.169	0.939	69.77	0.70	114.7
	313	0	0.692	3.844	_	_	_
		40	0.339	1.883	51.01	0.51	78.4
		60	0.301	1.672	56.50	0.57	106.2
		80	0.263	1.461	61.99	0.62	129.0
	323	0	0.718	3.989	_	_	_
		40	0.494	2.744	31.20	0.31	128.2
		60	0.34	1.889	52.65	0.53	114.0
		80	0.279	1.550	61.14	0.61	130.8
TNCuPc	303	0	0.559	3.106			
		40	0.548	3.044	1.97	0.02	2032.7
		60	0.51	2.833	8.77	0.09	684.5
		80	0.464	2.578	16.99	0.17	470.7
	313	0	0.692	3.844	_	_	_
		40	0.601	3.339	13.15	0.13	304.2
		60	0.513	2.850	25.87	0.26	232.0
		80	0.433	2.406	37.43	0.37	213.7
	323	0	0.718	3.989	_	_	_
		40	0.611	3.394	14.90	0.15	268.4
		60	0.568	3.156	20.89	0.21	287.2
		80	0.463	2.572	35.52	0.36	225.3

The inhibition efficiency increases with an increasing concentration of the inhibitor, but decreases as temperature increases despise the discrepancy observed at 60 and 40 ppm for both CuPc and TNCuPc respectively. At 80ppm and at all temperatures the inhibition efficiency of CuPc and TNCuPc ranges between 61-70% and 17-37% respectively. At 60 ppm and all temperatures the inhibition efficiency is between 53-58% and 9-26% for CuPc and TNCuPc respectively. Ultimately at 40 ppm and all temperatures in their close proximity the inhibition efficiency of CuPc and TNCuPc ranges from 31-60% and 2-15% respectively. Despite the fact that both the inhibitors inhibited corrosion on the aluminium metal surface, it is observed that the unsubstituted inhibitor (CuPc) performs very well as compared to the nitro substituted inhibitor (TNCuPc). The non-uniform of %IE values for both CuPc and TNCuPc at 60 and 40 ppm respectively may be due to the inhibitor's varying aggregative interactions [14, 44], which have been reported to depend on solubility in the solvent of interest, and this can be affected by both concentrations and temperatures [44]. Furthermore, the lower %IE of TNCuPc with electro-withdrawal NO_2 substituents compared to unsubstituted CuPc is attributed to the competitive effects of steric hindrance [14] and electron-withdrawal features of the NO_2 groups.

The adsorption isotherm results are shown in Figure 3.4(c) and (d) for CuPc and TNCuPc, respectively. Adsorption isotherms provide the information on how the inhibitor adsorb on the metal surface. Langmuir adsorption isotherm, the surface coverage (θ) of the inhibitor on the aluminium surface is related to the concentration (C_{inh}) of the inhibitor in the bulk of the solution according to:

$$\theta = \frac{K_{ads}C_{inh}}{1 + K_{ads}C_{inh}}$$
(3.3)

and its linear form is given by:

$$\frac{C_{inh}}{\theta} = \frac{1}{K_{ads}} + C_{inh}$$
(3.4)

where C_{inh} is the concentration of the inhibitor, θ is the degree of surface coverage and K_{ads} is the equilibrium constant of the adsorption process. Figure 3.4 (c) and (d), the plots of C_{inh}/θ against C_{inh} will give a straight line with the intercept being the inverse of K_{ads}. The K_{ads} values are presented in Table 3.2, there is no regular pattern in the values of K_{ads} obtained at various temperatures. The similar behaviour

of no regular pattern on the values of K_{ads} was observed by the previous researchers using phthalocyanine and naphthalocyanine derivatives as corrosion inhibitor for aluminium metal [14]. In this study, the large magnitude of K_{ads} for both inhibitors is an indication of of the adsorption process which is reported to be favoured by large K_{ads} values [14]. From the data in this figure, it can be seen that the adsorption of the studied inhibitiors followed Langmuir adsorption isotherm. Furthermore, the values of the slope obtained indicate a monolayer and also multiple bonds formation of the inhibitor adsorbed on the metal surface [14, 44, 45]. The values of K_{ads} obtained can be used to determine the free energy of adsorption (ΔG°_{ads}) using the Equation 3.5:

$$\Delta G^o = -2.303RT \log(55.5K_{ads})$$

(3.5)

where, ΔG°_{ads} is the Gibbs free energy of adsorption, the value 55.5 is the molar concentration of water in solution, T is the absolute temperature and K_{ads} is the equilibrium constant for the adsorption process and the results of ΔG°_{ads} are given in Table 3.2. From this table, it is noticeable that ΔG°_{ads} values for CuPc and TNCuPc inhibitors are above -20 kJ.mol^{-1}, which indicate a physisorption adsorption mechanism [14, 44-48].

Table 3. 2: Adsorption parameters derived from the Langmuir adsorption isotherm for CuPc and TNCuPc for aluminium.

Inhibitor	T (K)	Kads (x 10^3 L.mol^{-1})	-ΔG^o_{ads} (kJ.mol^{-1})
CuPc	303	4.785	13.66
	313	46.90	16.69
	323	18.24	16.13
TNCuPc	303	1.072	12.03
	313	9.943	14.94
	323	13.17	15.75

3.3.2.2 THERMODYNAMIC AND ACTIVATION PARAMETERS

The effect of temperature on the adsorption behaviour and activation energy parameters of the corrosion process can be evaluated using the Arrhenius equation written in the form of logarithms as follows [49, 50]:

$$\log C_R = \log A - \frac{E_a}{2.303RT}$$

(3.6)

where, C_R is the corrosion rate, E_a is the apparent activation energy, R is the molar gas constant (8.314 $JK^{-1}mol^{-1}$), T is the absolute temperature and A is the frequency factor. The plots of log (C_R) against 1/T for aluminium in 1 mol.L^{-1} HCl in the absence and presence of different concentrations of CuPc and TNCuPc are presented in Figure 3.5 (a) and (b), respectively. The values of the activation energy can be obtained from the slopes and the frequency factor can be obtained from the intercepts of the regression lines. Slope = $-E_a$/2.303R and c = logA where c is the intercept of the regression line. The process of adsorption between the metal surface and the inhibitor can sometimes be an exothermic process where the heat is given off, although in some cases, endothermic process is encountered. The results in Table 3.3 show that the E_a values in the presence of CuPc are generally higher than that of the blank acid at 40 and 80 ppm. The higher activation energy values indicate the physical adsorption mechanism while the lower activation energy values attribute for chemical adsorption mechanism [14, 50]. On the other hand, the values of E_a in the presence of TNCuPc are lower than that of the blank. The low E_a values are due to a slow rate of inhibitor adsorption with a resultant closer approach to equilibrium during the experiments at the higher temperature, or a shift of the net corrosion reaction from the region of the metal surface without adsorbed protective film to the covered region [14, 51, 52]. A more detailed discussion on various possibilities associated with lower values of *Ea* in the presence of inhibitors was also provided by Benali *et al.* [53].

Figure 3. 5 : Arrhenius plots for aluminium metal in 1M HCl in the absence and presence of different concentrations of CuPc (a) and TNCuPc (b); and Transition state plots at varying concentrations of CuPc (c) and TNCuPc (d).

The effect of temperature on the inhibition efficiency of the inhibitor on the Al metal surface can be used to calculate and determine the entropy ($\Delta S°$) and enthalpy of activation, $\Delta H_a°$ and the results are presented in Table 3.3. From these results, the values of $\Delta H_a°$ for both CuPc and TNCuPc inhibitors are positive indicating that the dissolution of Al metal and adsorption of these inhibitors are endothermic processes [51, 52]. Furthemore, the TNCuPc shows high values of $\Delta H_a°$ as compared to CuPc and blank. Ostovari *et al* [53] reported enthalpy values up to 41.86 kJ.mol^{-1} are related to physisorption mechanism, while those around 100 kJ.mol^{-1} or more are attributed to chemisorption mechanism. Our results are also in good agreement with the literature reported [53-57]. However, $\Delta H_a°$ values are lower for CuPc suggesting a chemisorption mechanism [14]. The negative values of $\Delta S°$ in both inhibitors indicate that the formation of the activated complex in the rate determining step is associative rather than dissociative [56].

The values of $\Delta S°$ and $\Delta H_a°$ can be calculated by using Equation (3.7) below:

$$\log(\frac{C_R}{T}) = \ln(\frac{k_B}{h}) + \frac{\Delta S^\circ}{R} - \frac{\Delta H^\circ}{RT}$$ (3.7)

where, k_B is the Boltzmann's constant, C_R is the corrosion rate and h is the Plank's constant.

Figure 3.5(c) and (d) show the plot of log(C_R/T) versus 1/T for CuPc and TNCuPc, respectively, giving straight lines with an intercept equal to ln(k_B/h) + ΔS°/R and the value of slope equal to -ΔH°/R. In these results, it can be seen that the blank shows a high C_R in comparison to CuPc and TNCuPc inhibitors. The lower values of C_R indicate that the dissolution of Al metal was minimised.

Table 3. 3: The obtained values of activation energy (E_a), entropy (ΔS°) and enthalpy of activation ($\Delta H^o{}_a$) are presented.

Inhibitor	Concentration (ppm)	E_a (kJ.mol^{-1})	$\Delta H^o{}_{ads}$ (kJ.mol^{-1})	ΔS° (JK^{-1}.mol^{-1})
CuPc	0	10.27	10.27	-258.98
	40	15.19	12.53	-258.76
	60	3.37	12.59	-259.35
	80	23.35	27.44	-211.58
TNCuPc	0	10.27	10.27	-258.98
	40	4.53	89.23	-286.77
	60	4.35	90.65	-288.19
	80	-0.14	106.31	-303.85

3.3.3. ELECTROCHEMICAL ANALYSIS

The effect of phthalocyanine inhibitor concentration in the polarisation curves for Al metal 1.0 mol. L^{-1} HCl at 298 K is shown in Figure 3.6, whereas the electrochemical parameters are given in Table 3.4, It can be seen that the Al metal sheet exhibits active-passive behaviour [58]. It was also seen that the addition of CuPc (Figure 3.6(a) and TNCuPc (Figure 3.6 (b)) inhibitor did not affect very much neither the E_{corr} nor the $i$corr values, however, they increased the passive current density and

passivation potential values, i_{pas} and E_{pas}, respectively. The polarisation curves in the presence of both CuPc and TNCuPc inhibitors shifted to more positive potentials (anodic region) compared to the blank, which suggests the formation of protective film of the inhibitors on the Al surface and reduction in the rate of anodic dissolution of the metal [14]. As a result, the E_{corr} value for the uninhibited solution was −535.6 mV, and with the addition of inhibitor this value was around −498.7 and -515.2 mV for 40 ppm CuPc and TNCuPc, respectively. The i_{corr} slightly decreased from 1.94 down to 0.091 and 0.26 mA.cm^{-2}, 40 ppm CuPc and TNCuPc, respectively, and the lowest value obtained was with the addition of 80 ppm in both inhibitors. The difference of greater than 85 mV between the corrosion potential values of the blank and the inhibited solutions suggest either an anodic or cathodic inhibitor type while that of less than 85 mV signify a mixed-type [59, 60]. The E_{corr} values are supported by the change in b_a and b_c values in blank, CuPc and TNCuPc inhibitors. Thus, the values of b_c are greater than the b_a values suggesting that cathodic is predominant [14].

On the other hand, as can be seen in Table 3.4, the passivation potential value, E_{pas}, for the blank solution was 465.4 mV, however, the value decreased with the addition of CuPc and TNCuPc inhibitor, obtaining the lowest value, -321.8 and -333.9 mV, respectively, with the addition of 80 ppm. Correspondingly, the passivation current density value, i_{pas}, of blank was 4.68 mA.cm^{-2}. Upon addition of CuPc and TNCuPc inhibitor, it decreased as the inhibitor concentration increased, obtaining the lowest value, 1.74 and 2.25 mA.cm^{-2} by adding 80 ppm of inhibitor, similar to the behaviour of the weight loss results shown in Figure 3.4. Accordingly, it could be concluded that the addition of phthalocyanine inhibitors decrease the corrosion rate of aluminium metal in acidic media by improving the passive film properties. The inhibition efficiencies (%IE$_{PDP}$) of CuPc and TNCuPc increase with an increase inhibitor concentration with CuPc generally showing higher values as compared to TNCuPc. Similar behaviour was observed in the case of gravimetric results (%IE).

In comparison, the difference in the values of %IE and %IE$_{PDP}$ from weight loss and electrochemical data is expected. This observation may be due to the fact that the C_R from weight loss analysis is chemically dependent, while independent of the

electrode potential, whereas PDP measurements depend on the operational potential [14, 53-57] and solubility of inhibitors [14].
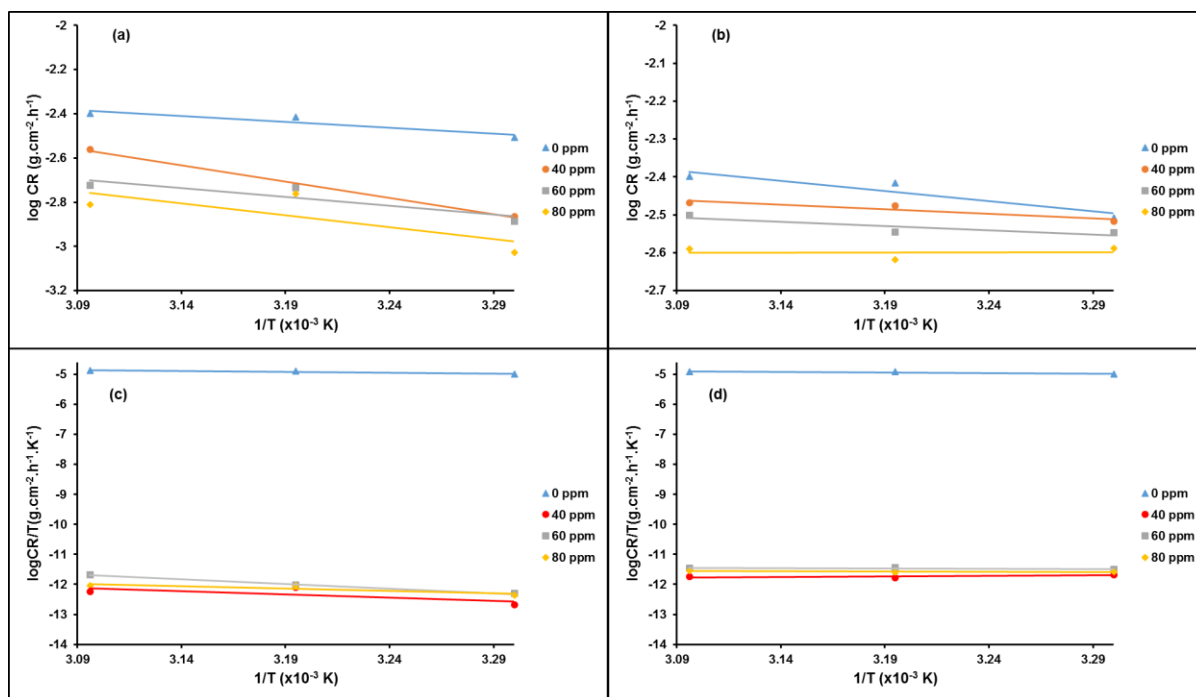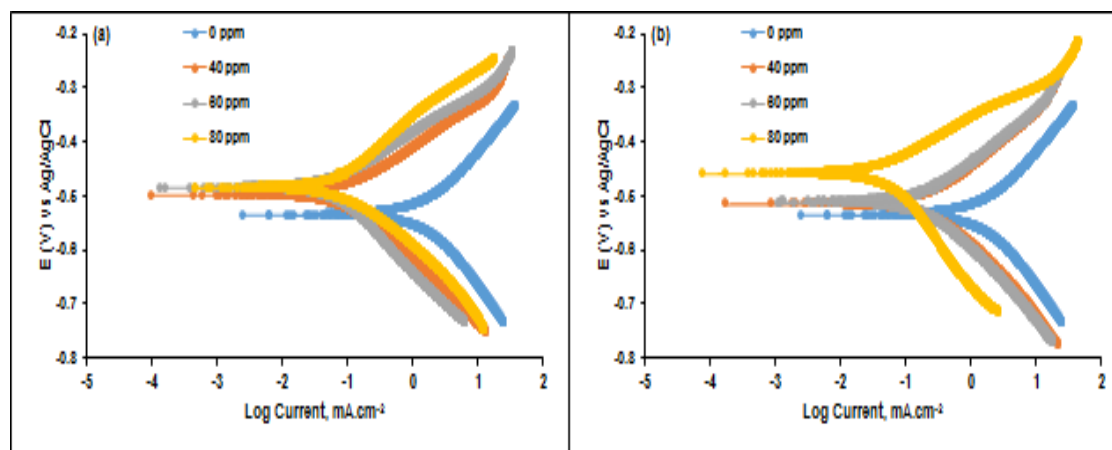

Figure 3. 6: Tafel plots for Al in 1 M HCl in the absence and presence of different concentrations of CuPc (a) and TNCuPc (b) inhibitor compounds.

Table 3. 4: Potentiodynamic polarisation (PDP) parameters such as corrosion potential (E_{corr}), corrosion current density (i_{corr}), anodic Tafel slope, b_a and cathodic Tafel slope, b_c, using different inhibitors.

Inhibitor	Conc (ppm)	$-E_{corr}$ (mV)	i_{corr} (mA.cm^{-2})	b_a (mV)	b_c (mV)	$-E_{pas}$ (mV)	I_{pas} (mA.cm^{-2})	%IE$_{PDP}$
Blank		535.6	1.94	155.3	179.6	465.4	4.677	-
CuPc	40	498.7	0.091	82.9	114.4	379.5	2.455	95.31
	60	484.9	0.061	78.9	127.9	330.8	1.905	96.86
	80	485.5	0.024	79.1	105.9	321	1.738	98.76
TNCuPc	40	515.2	0.26	108.9	124.9	413.7	2.188	86.60
	60	511.9	0.13	92.8	109.7	399.7	2.754	93.30
	80	459.1	0.04	68.0	143.9	333.9	2.249	97.94

3.3.4. ELECTROCHEMICAL IMPEDANCE SPECTROSCOPY (EIS)

The most essential information which is obtained from the electrochemical impedance spectroscopy is insights about the metal corrosion behaviour against time as well as the morphological properties of the metal and inhibitors. The Nyquist plots are characterized by the capacitive loop related to the charge transfer process

and double layer capacitance (C_{dl}) [61, 62]. From the Nyquist plots obtained from the EIS shown in Figure 3.7, the mechanism of the corrosion inhibition process can be determined. The semicircle of the uninhibited system has a lower diameter as compared to the inhibited system, and the least inhibitor concentration (40 ppm) shows the least diameter as compared to the highest inhibitor concentration (80 ppm). The semicircles are the results of the adsorption film formation on the metal surface and as well as charge transfer. At 80 ppm inhibitor concentration, the larger semicircle diameter size shows that the more inhibitor molecules present in the corrosive medium the more the rate of the formation of the adsorption film on aluminium thus higher inhibition efficiency value.
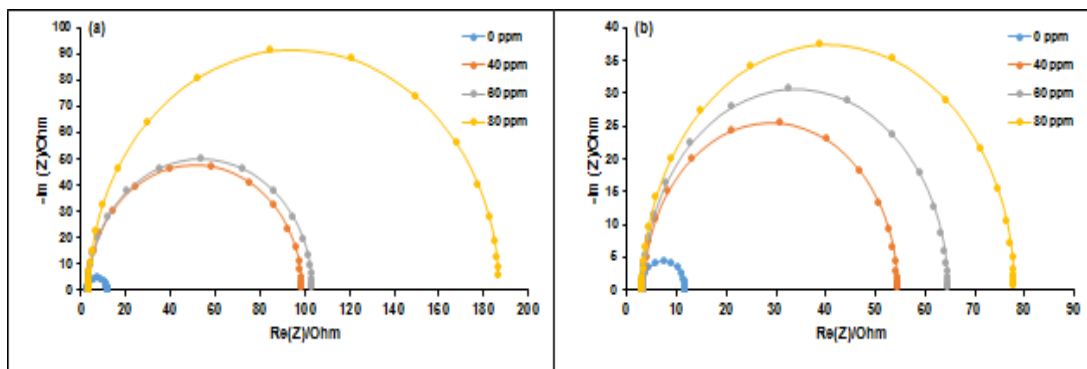
Figure 3. 7 Nyquist plot of aluminium in 1 M HCl in the absence and presence of various concentrations of (a) CuPc and (b) TNCuPc inhibitors.

Figure 3.8 shows the equivalent model circuit used to fit the impedance semicircles data resulting in the EIS kinetic parameters recorded in Table 3.5. According to the observations, as the inhibitor concentrations increases the R_{ct} values increases signifying that the surface coverage, Θ on Al by inhibitors increases due to the increased number of inhibitor molecules in the HCl medium. However, the C_{dl} values decrease as the TNCuPc concentration increases from 40ppm to 60ppm, this is due to the decrease in a local dielectric constant or an increase in the thickness of the electrical double layer [63]. From the data in Table 3.5 it is observed that the values of R_s which is the solution resistance between the working electrode (WE) and counter electrode (CE) are smaller as compared to the values of R_{ct} the charge transfer resistance.
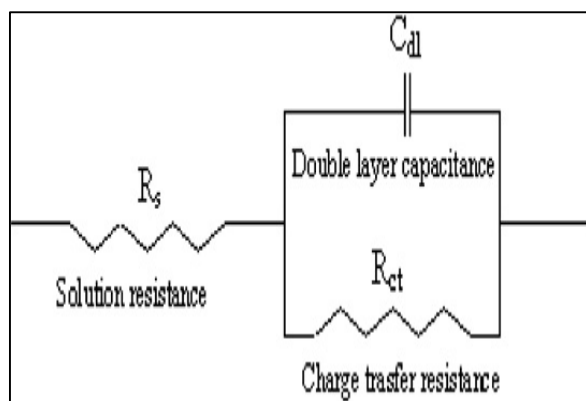
Figure 3. 8: The suggested equivalent circuit model for the studied system.

Table 3. 5: Impedance parameters for corrosion of Al in 1 M HCl containing different concentrations of CuPc and TNCuPc inhibitors.

Inhibitor	Concentration (ppm)	R_s (Ω)	R_{ct} (Ω)	C_{dl} ($\times 10^{-4}$ F)	$\%IE_{EIS}$
Blank		2.836	8.871	2.060	-
CuPc	40	3.245	95.50	1.210	90.71
	60	3.325	100.0	2.000	91.13
	80	3.619	183.3	2.720	95.16
TNCuPc	40	3.367	51.04	1.660	82.62
	60	3.216	61.33	1.560	85.54
	80	3.038	74.89	1.890	88.15

3.4. CONCLUSION

Copper (II) phthalocyanine (CuPc) and 4-tetranitro copper (II) phthalocyanine (TNCuPc) inhibitors were successfully synthesised and studied by XRD, FTIR, TGA and UV-vis spectroscopy. The XRD results exhibited that CuPc was more crystalline the TNCuPc. The TGA resulted showed that TNCuPc was most thermally stable than CuPc. From the weight loss analyses, the %IE values of the CuPc and TNCuPc were lower than in the the case of PDP results. Furthemore, the PDP results for both inhibitors exhibited a mixed-type inhibition mechanism. Additionally, inhibitor efficiencies decrease upon introduction of NO_2 group at peripheral of CuPc due to

steric hindrance. Electrochemical measurement showed that the properties of the passivation film formed on the Al metal surface was observed in both CuPc and TNCuPc by decrease in the passivation current density and passivation potential values. Nyquist data displayed a single capacitive, and depressed loop in both CuPc and TNCuPc inhibitors, indicating that the corrosion process is under charge transfer control. It is explored and proven in this contribution that CuPc and its counterpart carry tremendous potential for industrial usage as corrosion inhibitors.

3.5. REFERENCES

1. Y. F. Zheng, X. N. Gu, F. Witte, Biodegradable metals, *Materials Science and Engineering: R: Reports*. 77(2014) 1-34.

2. P. K. Bowen, J. Drelich, J. Goldman, Zinc exhibits ideal physiological corrosion behaviour for bioabsorbable stents, *Adv. Mater.* 25(2013) 2577-2582.

3. E. A. Starke, Aluminium alloys of the 70's: Scientific solutions to engineering problems. An invited review, *Adv. Mater. Sci. Eng.* 29(1997) 99-115.

4. J. T. Staley, Aluminum alloys and composites, *Encyclopedia of Physical Science*. (1992) 591.

5. P. Arellanes-Lozada, O. Olivares-Xometl, D. Guzmán-Lucero, N. V. Likhanova, M. A. Domínguez-Aguilar, I. V. Li janova, E. Arce-Estrada, the inhibition of aluminium corrosion in sulphuric acid by poly (1-vinyl-3-alkyl-imidazolium hexafluorophosphate), *Materials*. 7(2014) 5711-5734.

6. U. Trdan, J. Grum, Evaluation of corrosion resistance of AA6082-T651 aluminium alloy after laser shock peening by means of cyclic polarisation and EIS methods, *Corros. Sci*. 59(2012) 324-333.

7. M. T. Muniandy, A. A. Rahim, H. Osman, A. M. Shah, S. Yahya, P. B. Raja, Investigation of some schiff bases as corrosion inhibitors for aluminium alloy in 0.5 M hydrochloric acid solutions, *Surf. Rev. Lett.* 18(2011) 127-133.

8. M. Tourabi, K. Nohair, M. Traisnel, C. Jama, F. Bentiss, Electrochemical and XPS studies of the corrosion inhibition of carbon steel in hydrochloric acid pickling solutions by 3, 5-bis (2-thienylmethyl)-4-amino-1, 2, 4-triazole, *Corros. Sci.* 75(2013)123-133.

9. S. Şafak, B. Duran, A. Yurt, G. Türkoğlu, Schiff bases as corrosion inhibitor for aluminium in HCl solution*, Corros. Sci*. 54(2012) 251-259.

10. B. Sanyal, Organic compounds as corrosion inhibitors in different environments—a review, *Prog. Org. Coat.* 9(1981) 165-236.

11. A. Singh, Y. Lin, M. A. Quraishi, L. O. Olasunkanmi, O. E. Fayemi, Y. Sasikumar, B. Ramaganthan, I. Bahadur, I. B. Obot, I.B., Adekunle, M. M. Kabanda, Porphyrins as corrosion inhibitors for N80 Steel in 3.5% NaCl solution: Electrochemical, quantum chemical, QSAR and Monte Carlo simulations studies, *Molecules.* 20(2015) 15122-15146.

12. Z. Cao, Y. Tang, H. Cang, J. Xu, G. Lu, W. Jing, Novel benzimidazole derivatives as corrosion inhibitors of mild steel in the acidic media. Part II: Theoretical studies, *Corros. Sci.* 83(2014) 292-298.

13. L. O. Olasunkanmi, I. B. Obot, M. M. Kabanda, E. E. Ebenso, Some quinoxalin-6-yl derivatives as corrosion inhibitors for mild steel in hydrochloric acid: Experimental and theoretical studies, *J. Phys. Chem. C.* 119 (2015) 16004-16019.

14. M. Dibetsoe, L. O. Olasunkanmi, O. E. Fayemi, S. Yesudass, B. Ramaganthan, I. Bahadur, A. S. Adekunle, M. M. Kabanda, E. E. Ebenso, Some phthalocyanine and naphthalocyanine derivatives as corrosion inhibitors for aluminium in acidic medium: Experimental, quantum chemical calculations, QSAR studies and synergistic Effect of iodide ions, *Molecules.* 20(2015) 15701-15734.

15. C. Göl, M. Malkoç, S. Yeşilot, M. Durmuş, Novel zinc (II) phthalocyanine conjugates bearing different numbers of BODIPY and iodine groups as substituents on the periphery, *Dyes Pigm.* 111(2014) 81-90.

16. T. Peme, Absorption and Quantum Chemical studies on some DYES as Corrosion Inhibitors on Mild Steel in Acidic Medium (Doctoral dissertation) (2014).

17. O. K. Özdemir, A. Aytaç, D. Atilla, M. Durmuş, Corrosion inhibition of aluminum by novel phthalocyanines in hydrochloric acid solution, *J. Mater. Sci.* 46(2011) 752-758.

18. M. J. Bahrami, S. M. A. Hosseini, P. Pilvar, Experimental and theoretical investigation of organic compounds as inhibitors for mild steel corrosion in sulfuric acid medium, *Corros. Sci.* 52(2010) 2793-2803.

19. J. C. Valle-Quitana, G. F. Dominguez-Patiño, J. G. Gonzalez-Rodriguez, Corrosion Inhibition of Carbon Steel in 0.5 M H_2SO_4 by Phthalocyanine blue." *ISRN Corrosion* (2014).

20. P. Zhao, Q. Liang, Y. Li, Electrochemical, SEM/EDS and quantum chemical study of phthalocyanines as corrosion inhibitors for mild steel in 1mol/l HCl, *Appl. Surf. Sci.* 252(2005) 1596-1607.

21. Z. Bıyıklıoğlu, Synthesis, characterization and aggregation properties of water-soluble metal-free and metallophthalocyanines peripherally tetra-substituted with 2-[2-(dimethylamino) ethoxy] ethoxy moiety, *Synth. Met.*162 (2012) 26-34.

22. S. Zongo, M. S. Dhlamini, P. H. Neethling, A. Yao, M. Maaza, B. Sahraoui, Synthesis, characterization and femtosecond nonlinear saturable absorption behaviour of copper phthalocyanine nanocrystals doped-PMMA polymer thin fims. *Opt. Mater.* 50(2015) 138-143.

23. M. A. García-Sánchez, F. Rojas-González, E. C. Menchaca-Campos, S. R. Tello-Solís, R. Quiroz-Segoviano, L. A. Diaz-Alejo, E. Salas-Bañales, E. and Campero, rossed and linked histories of tetrapyrrolic macrocycles and their use for engineering pores within sol-gel matrices, *Molecules.* 18(2013) 588-653.

24. M. A. Ibrahim, M. Messali, Z. Moussa, A. Y. Alzahrani, S. N. Alamry, B. Hammouti, Corrosion inhibition of carbon steel by imidazolium and pyridinium cations ionic liquids in acidic environment, *Electrochim. Acta.* 29(2011) 375-389.

25. B. D. Mert, M. E. Mert, G. Kardaş, B. Yazıcı, Experimental and theoretical investigation of 3-amino-1, 2, 4-triazole-5-thiol as a corrosion inhibitor for carbon steel in HCl medium, *Corros. Sci.* 53(2011) 4265-4272.

26. F. Y. Chen, K. Z. Li, H. J. Li, Catalytic activity of tetranitro-copper phthalocyanine supported on carbon nanotubes towards oxygen reduction reaction, In Advanced Materials Research. 706(2013) 15-19.

27. C. Vergnat, V. Landais, J. F. Legrand, M. Brinkmann, Orienting semiconducting nanocrystals on nanostructured polycarbonate substrates: impact of substrate temperature on polymorphism and in-plane orientation, *Int. J. Biol. Macromol.* 44 (2011) 3817-3827.

28. A. Pick, M. Klues, A. Rinn, K. Harms, S. Chatterjee, G. Witte, Polymorph-Selective Preparation and Structural Characterization of Perylene Single Crystals, *Cryst. Growth Des.* 15(2015) 5495-5504.

29. S. Zongo, M.S. Dhlamini, P.H. Neethling, A. Yao, M. Maaza, B. Sahraoui, Synthesis, characterization and femtosecond nonlinear saturable absorption behavior of copper phthalocyanine nanocrystals doped-PMMA polymer thin films*, Opt. Mater.* (Amst).50(2015)138–143.

30. Y. Wan, S. Chen, G. Wang, Q. Liang, Z. Li, and S. Xu, Facile Synthesis and Characterization of Zinc Tetranitro Phthalocyanine-MWCNTs Nanocomposites with Efficient Visible-Light-Driven Photocatalytic Activity, *Acta Phys. Pol. A.* 130(2016) 785–790.

31. X. Zhou, X. Wang, B. Wang, Z. Chen, C. He, Y. Wu, preparation, characterization and NH 3-sensing properties of reduced graphene oxide/copper phthalocyanine hybrid material, *Sens. Actuators, B.* 193(2014) 340-348.

32. A. R. Koray, V. Ahsen, Ö. Bekâroğlu, Preparation of a novel, soluble copper phthalocyanine with crown ether moieties, *J. Chem. Soc., Chem. Commun.* 12(1986) 932-933.

33. M. Zhang, C. Shao, Z. Guo, Z. Zhang, J. Mu, P. Zhang, T. Cao, Y. Liu, Highly efficient decomposition of organic dye by aqueous-solid phase transfer and in situ photocatalysis using hierarchical copper phthalocyanine hollow spheres, *ACS Appl. Mater. Interfaces* 3(2011) 2573-2578.

34. P. Kumari, N. Sinha, P. Chauhan, S. MS Chauhan, Isolation, synthesis and biomimetic reactions of metalloporphyrinoids in ionic liquids, *Curr. Org. Chem.* 8(2011) 393-437.

35. F.D. Cong, B. Ning, H.F. Yu, X.J. Cui, B. Chen, S.G. Cao, and C.Y. Ma, The control of phthalocyanine properties through nitro-group electronic effect, *Spectrochim. Acta - Part A Mol. Biomol. Spectrosc.* 62 (2005)394–397.

36. T. H. Ibrahim, Y. Chehade, M. A. Zour, Corrosion inhibition of mild steel using potato peel extract in 2M HCL solution, *Int. J. Electrochem. Sci.* 6(2011) 6542-6556.

37. N. O. Obi-Egbedi, I. B. Obot, Inhibitive properties, thermodynamic and quantum chemical studies of alloxazine on mild steel corrosion in H_2SO_4, *Corros. Sci.* 53(2011) 263-275.

38. M. Gopiraman, N. Selvakumaran, D. Kesavan, I. S. Kim, R. Karvembu, Chemical and physical interactions of 1-benzoyl-3, 3-disubstituted thiourea derivatives on mild steel surface: corrosion inhibition in acidic media, *In. Eng. Chem. Res.* 51(2012) 7910-7922.

39. F. P. Schäfer, ed., 2013, *Dye lasers* (Vol. 1). *Springer Science & Business Media.*

40. T, Honda, T. Kojima, N. Kobayashi, S. Fukuzumi, Crystal Structures and Electronic Properties of Saddle-Distorted and Protonated Phthalocyanines. *Angew. Chem. Int. Ed*, 50(2011) 2725-2728.

41. R. Solmaz, E. Altunbaş, G. Kardaş, Adsorption and corrosion inhibition effect of 2-((5-mercapto-1, 3, 4-thiadiazol-2-ylimino) methyl) phenol Schiff base on mild steel*, Mater. Chem. Phys.* 125 (2011) 796-801.

42. Y. Wang, W. Ji, H. Sui, Y. Kitahama, W. Ruan, Y. Ozaki, B. Zhao, Exploring the Effect of Intermolecular H-Bonding: A Study on Charge-Transfer Contribution to Surface-Enhanced Raman Scattering of p-Mercaptobenzoic Acid, *J. Phys. Chem C*. 118(2014) 10191-10197.

43. Z. Zhang, W. Wang, L. Zhang, Large improvement of photo-response of CuPc sensitized Bi_2WO_6 with enhanced photocatalytic activity, *Dalton Trans*. 42(2013) 4579-4585.

44. T. Peme, L. O. Olasunkanmi, I. Bahadur, A. S. Adekunle, M. M. Kabanda, E. E. Ebenso, Adsorption and corrosion inhibition studies of some selected dyes as corrosion inhibitors for mild steel in acidic medium: gravimetric, electrochemical, quantum chemical studies and synergistic effect with iodide ions, *Molecules*. 20(2015) 16004-16029.

45. S. Kumar, D. Sharma, P. Yadav, M. Yadav, Experimental and quantum chemical studies on corrosion inhibition effect of synthesized organic compounds on N80 steel in hydrochloric acid, *In. Eng. Chem. Res.* 52(2013) 14019-14029.

46. V. Çakır, F. Demir, Z. Bıyıklıoğlu, A. Koca, H. Kantekin, Synthesis, characterization, electrochemical and spectroelectrochemical properties of metal-free and metallophthalocyanines bearing electropolymerizable dimethylamine groups, *Dyes Pigm*. 98(2013) 414-421.

47. L. C. Murulana, A. K. Singh, S. K. Shukla, M. M. Kabanda, E. E. Ebenso, Experimental and quantum chemical studies of some bis (trifluoromethyl-sulfonyl) imide imidazolium-based ionic liquids as corrosion inhibitors for mild steel in hydrochloric acid solution, *In. Eng. Chem. Res.* 51(2012) 13282-13299.

48. D. B. Hmamou, R. Salghi, A. Zarrouk, H. Zarrok, R. Touzani, B. Hammouti, A. El Assyry, Investigation of corrosion inhibition of carbon steel in 0.5 M H_2SO_4 by new bipyrazole derivative using experimental and theoretical approaches, *J. Environ. Chem. Eng*. 3(2015) 2031-2041.

49. A. Zarrouk, I. Warad, B. Hammouti, A. Dafali, S. S. Al-Deyab, N. Benchat, The effect of temperature on the corrosion of Cu/HNO3 in the presence of organic inhibitor: part-2, *Int. J. Electrochem. Sci*. 5(2010)1516-1526.

50. B. Hammouti, A. Zarrouk, S. S. Al-Deyab, I. Warad, Temperature Effect, Activation Energies and Thermodynamics of Adsorption of ethyl 2-(4-(2-ethoxy-2-oxoethyl)-2-p-Tolylquinoxalin-1 (4H)-yl) Acetate on Cu in HNO_3, *Orient. J. Chem.* 27(2011) 23-31.

51. M. A. Hegazy, A. M. Badawi, S. A. El Rehim, W. M. Kamel, Corrosion inhibition of carbon steel using novel N-(2-(2-mercaptoacetoxy) ethyl)-N, N-dimethyl dodecan-1-aminium bromide during acid pickling, *Corros. Sci.* 69(2013)110-122.

52. R. Solmaz, Investigation of adsorption and corrosion inhibition of mild steel in hydrochloric acid solution by 5-(4-Dimethylaminobenzylidene) rhodanine, *Corros. Sci.* 79(2014)169-176.

53. O. Benali, L. Larabi, M. Traisnel, L. Gengembre, Y. Harek, Electrochemical, theoretical and XPS studies of 2-mercapto-1-methylimidazole adsorption on carbon steel in 1M HClO 4, *Appl. Surf. Sci.* 253(2007) 6130-6139.

54. A. Zarrouk, H. Zarrok, R. Salghi, B. Hammouti, F. Bentiss, R. Touir, M. O. H. A. M. M. E. D. Bouachrine, Evaluation of N-containing organic compound as corrosion inhibitor for carbon steel in phosphoric acid, *J. Mater. Environ. Sci.* 4(2013) 177-192.

55. A. Anejjar, R. Salghi, A. Zarrouk, O. Benali, H. Zarrok, B. Hammouti, E. E. Ebenso, Inhibition of carbon steel corrosion in 1M HCl medium by potassium thiocyanate, *J. Assn. Arab. Univ. Basic. Appl. Sci.* 15(2014) 21-27.

56. M. Gopiraman, N. Selvakumaran, D. Kesavan, I. S. Kim, R. Karvembu, Chemical and physical interactions of 1-benzoyl-3, 3-disubstituted thiourea derivatives on mild steel surface: corrosion inhibition in acidic media, *In. Eng. Chem. Res.* 51(2012) 7910-7922.

57. A. Ostovari, S. M. Hoseinieh, M. Peikari, S. R. Shadizadeh, S. J. Hashemi, Corrosion inhibition of mild steel in 1M HCl solution by henna extract: A comparative study of the inhibition by henna and its constituents (Lawsone, Gallic acid, α-d-Glucose and Tannic acid), *Corros. Sci.* 51(2009) 1935-1949.

58. L. O. Olasunkanmi, M. M. Kabanda, E. E. Ebenso, Quinoxaline derivatives as corrosion inhibitors for mild steel in hydrochloric acid medium: Electrochemical and quantum chemical studies, *Physica E.* 76(2016) 109-126.

59. L. C. Murulana, M. M. Kabanda, E. E. Ebenso, Investigation of the adsorption characteristics of some selected sulphonamide derivatives as corrosion inhibitors

at mild steel/hydrochloric acid interface: Experimental, quantum chemical and QSAR studies, *J. Mol. Liq.* 215(2016) 763-779.

60. I. B. Obot, N. O. Obi-Egbedi, Anti-corrosive properties of xanthone on mild steel corrosion in sulphuric acid: Experimental and theoretical investigations, *Curr. Appl Phys.* 11(2011) 382-392.

61. H. H. Hassan, E. Abdelghani, M. A. Amin, Inhibition of mild steel corrosion in hydrochloric acid solution by triazole derivatives: Part I. Polarisation and EIS studies, *Electrochim. Acta. 52*(2007) 6359-6366.

62. X. Wu, H. Ma, S. Chen, Z. Xu, A. Sui, General equivalent circuits for faradaic electrode processes under electrochemical reaction control, *J. Electrochem. Soc.* 146(1999) 1847-1853.

63. M. A. Hegazy, H. M. Ahmed, A. S. El-Tabei, Investigation of the inhibitive effect of p-substituted 4-(N, N, N-dimethyldodecylammonium bromide) benzylidene-benzene-2-yl-amine on corrosion of carbon steel pipelines in acidic medium, *Corros. Sci.* 53(2011) 671-678.

CHAPTER FOUR

IMPROVEMENT OF CORROSION RESISTANCE OF ALUMINIUM METAL IN CORROSIVE ENVIRONMENT BY 4-TETRANITRO ZINC (II) PHTHALOCYANINE INHIBITOR USING ELECTROCHEMICAL AND GRAVIMETRIC STUDIES

This chapter will be submitted for publication

Thabo Pesha[1]*,* Gobeng R. Monama[1], Mpitloane J. Hato[1],*,* Mamookgo E. Makhatha[2], Kabelo E. Ramohlola[1], Kerileng M. Molapo[3], Kwena D. Modibane[1], **. Improvement of corrosion resistance of aluminium metal in corrosive environment by tetranitrozinc (II) phthalocyanine inhibitor as a corrosion inhibitor using electrochemical and gravimetric studies. Manuscript in preparation.

[1]Department of Chemistry, School of Physical and Mineral Sciences, Faculty of Science and Agriculture, University of Limpopo (Turfloop Campus), Polokwane, Sovenga 0727, South Africa

[2]Department of Metallurgy, School of Mining, Metallurgy and Chemical Engineering, Faculty of Engineering and Built Environment, University of Johannesburg (Doorfontein Campus), Johannesburg 2001, South Africa

[3]Department of Chemistry, Faculty of Natural Science, University of the Western Cape (Bellville Campus), Cape Town 7535, South Africa

*E-mails: kwena.modibane@ul.ac.za (KD Modibane); mpitloane.hato@ul.ac.za (MJ Hato)

ABSTRACT

Metallophthalocyanines such as zinc (II) phthalocyanine (ZnPc) and tetranitro zinc (II) phthalocyanine (TNZnPc) were studied as corrosion inhibitors for aluminium metal in 1 mol. L^{-1} hydrochloric acid solutions at 303-323 K. The structure and the successful synthesis of inhibitors were studied using XRD, FTIR and UV-vis spectroscopy. The gravimetric analysis, potentiodynamic polarisation (PDP) and electrochemical impedance spectroscopy (EIS) were used to study the corrosion inhibition properties, corrosion mechanism, corrosion inhibition efficiency and inhibitor-metal adsorption or desorption behaviour. Both ZnPc and TNZnPc inhibitors prevented corrosion of aluminium in 1.0 mol. L^{-1} HCl through adsorption of the inhibitor on the surface of Al metal sheet. The temperature effect from gravimetric analysis revealed that aluminium was mostly affected at lowest inhibition efficiencies at higher temperature. The results showed that adsorption process followed a Langmuir model. For electrochemical analyses, the introduction of the synthesised ZnPc and TNZnPc inhibitors altered the corrosion current densities obtained from PDP results, signifying that both the anodic dissolution of aluminium metal and the hydrogen evolution were inhibited. Both inhibitors exhibited a mixed-type inhibition mechanism. The EIS results showed that the inhibitor molecules protect the metal via adsorption at the metal/hydrochloric acid interface. The obtained electrochemical results showed that the inhibitors significantly increased the polarisation resistance of Al-metal by reducing corrosion current densities.

Keywords: Zinc (II) phthalocyanine, 4-tetranitro zinc (II) phthalocyanine, corrosion inhibitor, Al metal, gravimetric analysis, EIS and PDP.

4.1. INTRODUCTION

Metals and their resultant products are very essential in life and their significance in human lives cannot be emphasised more [1]. For instance, aluminium has an enormous benefit when compared to other metals. However, it is not continuously resistant to corrosion [1, 2]. Its shielding oxide layer can gradually become unstable when unprotected to extreme pH levels that results in a failure of the protective layer, and its spontaneous restoration may not be quick enough to inhibit corrosion [3]. To overcome these problems, studies have shown that there are various methods that could be used to prevent the metal corrosion behaviour, such as material upgrades, production fluid blending, the process control and chemical inhibition [4-6]. Among these methods, corrosion chemical inhibition is reported to be the paramount process in preventing the deterioration of metal surfaces in corrosive media due to economic and practical usage [7-9]. As a result, organic compounds are commonly used to reduce the corrosion attack on metal in acidic media [10-12]. It was demonstrated that these compounds adsorb on the metal surface, block the active sites on the surface, and thereby reduce the corrosion process [7-12].

Throughout the ages, phthalocyanines (Pcs) exhibit several interesting properties and applications due to their highly delocalised conjugated π electron system [13]. Pcs show to possess high inhibition action because of their strong chemical adsorption on the metal surface, which is determined by planarity and lone pairs of electrons in heteroatoms [14]. It was shown that the localised corrosion can be prevented by the action of adsorption and aggressive anions, or by the formation of a more resistant oxide film on the metal surface [7-12]. The effectiveness of some phthalocyanines as acid corrosion inhibitors have been studied [14, 15]. Consequently, Ozdemir *et al* [15] studied the corrosion inhibition of aluminium by novel phthalocyanines in hydrochloric acid solution using potentiodynamic polarisation and electrochemical impedance spectroscopy (EIS) techniques. It was seen that Langmuir adsorption isotherm fitted well with all their experimental data. Furthermore, the inhibition efficiency increased with increase in the phthalocyanine concentration, but decreased with an increase in temperature.

It is proven that the presence of central metal ion positively affects and improves the photo physical behaviour of metallophthalocyanines very strongly [13]. Especially, Zinc (II) phthalocyanine (ZnPc) inhibitors have been studied intensively by virtue of their photosensitising properties [15-17]. The addition of functional groups to peripheral position also affect the chemical properties of metallophthalocyanine complex [13], for example, the solubility, adsorption properties and the molecular weight of the inhibitor compound.

It is reported that inhibitors which are completely soluble in the medium of interest exhibit higher inhibition efficiency [14]. To our knowledge, the use of ZnPc and tetranitrozinc (II) phthalocyanine (TNZnPc, Figure 4.1) as corrosion inhibitors for aluminium metal sheet in HCl environment was not reported to date. In the present paper, ZnPc and TNZnPc as simple phthalocyanines that could be obtained easily were selected as the object to be examined. Furthermore, TNZnPc has nitro group at the peripheral to enhance adsorption of the inhibitor on the aluminium metal. The corrosion inhibition behaviour of these inhibitors was investigated by gravimetric and electrochemical analyses as part of our contribution to the quest for a substance which does not only possess good inhibitive effect but also eco-friendly. The mechanism of their corrosion inhibition on the metal surface is well explained by the formation of a physically or chemically adsorbed film [14, 17, 18].
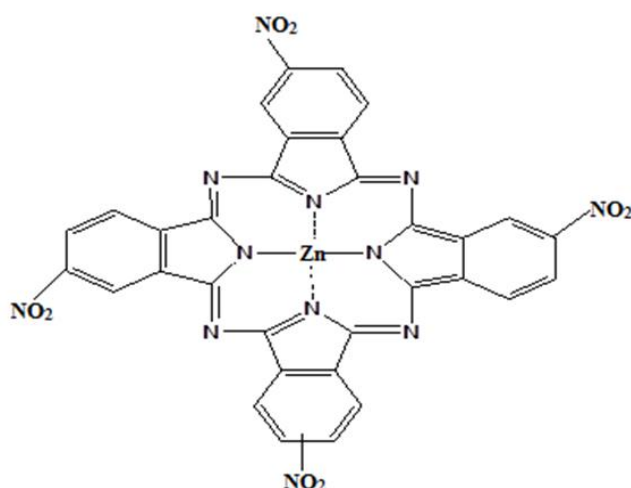
Figure 4. 1: Molecular structure of tetranitro zinc (ll) phthalocyanine [17].

4.2. EXPERIMENTAL

4.2.1. MATERIALS

Zinc acetate Zn $(O_2CCH_3)_2$ was purchased from Sigma Aldrich, South Africa. Phthalimide, 32% hydrochloric acid (HCl), methanol, nitrobenzene, ethanol, sulphuric acid (H_2SO_4) and 55% nitric acid (HNO_3) were purchased from Rochelle chemicals. Ammonium molybdate $(NH_4)_2MoO_4$, and urea CH_4N_2O were purchased from uniLAB.

4.2.2. SYNTHESIS OF ZINC (II) PHTHALOCYANINES

Zinc (II) phthalocyanine (ZnPc) used as corrosion inhibitor was synthesised by modifying the procedure described in the literature [17]. Under a blanket of nitrogen, a mixture of phthalimide (3.00 g, 0.0204 mol) in the presence of excess urea (3.00 g, 0.0500 mol), ammonium molybdate (0.0800g, 0.0600 mol) and zinc acetate (1.29 g, 0.0058 mol) in nitrobenzene (15.00 mL) was refluxed at 180°C for 5 hours with constant stirring. The product was finely ground and washed with ethanol three times for purification. Uv-vis (H_2SO_4): λ_{max} (log ε); 785nm (5.74), 688nm (5.06), 412 (4.09). FTIR: v_{max} (cm^{-1}); 3000 (Ar-H), 1608 (C=C), 1483 (C=C); 890, 783, 781, 730, 693 (Pc skeletal).

Synthesis and purification of tetranitro zinc (II) phthalocyanine (TNZnPc) was as outlined for ZnPc. The amount of the reagents employed was as follows: 4-nitrophthalimide [19]. UV-vis (H_2SO_4): λ_{max} (log ε); 765nm (5.42), 683nm (4.74), 413nm (4.40). FTIR: v_{max} (cm^{-1}); 3307 (Ar-H), 1516 (C=C), 1514 (N-O), 1326 (N-O); 920, 843, 724, 479 (Pc skeletal).

Corrosion tests were performed on 98% Al sheets with freshly prepared surface. The surface of the Al specimens were grounded using silicon carbide papers of various grades (600–1000), washed with distilled water, degreased in acetone, wiped with a clean towel paper and finally air-dried. Aggressive solution of 1.0 mol.L^{-1} HCl was prepared by diluting 32% analytical grade using distilled water. ZnPc and TNZnPc were first dissolved in minimum amount (10 mL equivalent to 4% by vol.) of H_2SO_4

and later diluted to various concentrations (40, 60, and 80 ppm) in 250 mL volumetric flask.

4.2.3. CHARACTERISATION

Optical absorption spectra were recorded at room temperature in the wavelength region 200 – 900 nm using a Varian Cary 300 UV-vis-NIR spectrophotometer. The structure of ZnPc and TNZnPc was analysed using X-ray diffraction (XRD Phillips PW 1830, CuK$_\alpha$ radiation, λ = 1.5406 A). The successful synthesis of inhibitors was confirmed by Fourier transform infrared (FTIR) spectrometer (Perkin-Elmer Spectrum II). The spectra were obtained at room temperature in the wave number range between 500 and 4500 cm^{-1}. A minimum of 32 scans were collected at a resolution of 4cm^{-1}. The thermal stability of inhibitors was investigated by a simultaneous thermal analyser (STA Perkin-Elmer 6000). Samples ranging between 1 to 4 mg were heated from 30-500 °C at a heating rate of 20 °C/min under N$_2$ environment.

4.2.4. GRAVIMETRIC METHOD

Gravimetric measurements were achieved using 3 cm × 4 cm dimensions in corrosive solution of 1mol.L^{-1} hydrochloric acid. MPcs were dissolved in minute amount of H$_2$SO$_4$ and diluted to several concentrations of 0, 40, 60 and 80 ppm in 250ml analytical reaction vessel. The Al were weighed and freely suspended in a 100 ml reaction vessel containing the corrosive solution for the first corrosion test. The specimens were removed from the test after 15 hrs immersion time, brushed and used distil water for washing, applied acetone and finally left to dry then re-weighed. Three crucial parameters such as the rate of corrosion, inhibition efficiency percentage and the surface coverage were determined using Equations (Eq. 4.1, 4.2, 4.3.) [20, 21]:

$$C_R = \frac{\Delta W}{St} \tag{4.1}$$

$$\% IE = \left(1 - \frac{\rho_1}{\rho_2}\right) \times 100\% \tag{4.2}$$

$$\theta = \frac{K_{ads}C_{inh}}{1 + K_{ads}C_{inh}}$$
(4.3)

4.2.5. ELECTROCHEMICAL ANALYSIS

Electrochemical measurements were achieved using Bio-Logic SP150 potentiostat. The data was collected using a conventional three electrode setup with Ag/AgCl as a refence electrode, Pt wire as a counter electrode and Al metal as a working electrode. The working electrode was prepared using Al metal in the presence and absence of both ZnPc and TNZnPc inhibitors as concentrations. The repetitive scanning of solution ZnPc and TNZnPc (1.0 M HCl) was measured from -0.250 to +0.250 mV at 1mV/s. In addition, EIS measurements were done using 100 kHz to 10 MHz frequency range with 10 mV peak to peak amplitude. From EIS measurements [22] values of the double layer capacitance and the charge transfer resistance were obtained. Furthermore, the Tafel slopes (cathodic and anodic) with inclusion of the corrosion current density were determined from the extrapolations of the cathodic and anodic Tafel plots. Moreover, the values of the inhibition efficiency were calculated with the help of the Equation 2.18 [23, 24]:

4.3. RESULTS AND DISCUSSION

4.3.1. STRUCTURAL PROPERTIES

Figure 4.2 (a) shows the XRD patterns of ZnPc and TNZnPc inhibitors. It is noticeable that both inhibitors show higher crystalline diffraction with a well pronounced sharp peaks appearing at $2q$ = 6.8 and 4.5 °C for ZnPc and TNZnPc, respectively. These peaks are in good agreement with the work reported by Schünemann $et\ al.$ [26]. In most metallophthalocyanine the films are mainly of $\beta-$ form [25] with preferential orientation of the plane (100) in structural studies using X-ray diffractometry and IR spectral analysis. The diffraction line at around $2q = 6.8$ °C is attributed to ZnPc which corresponds to 1.29 nm spacing this indicates the preferred orientation of (101) plane [26, 27]. The complexes display a mild crystallographic pattern, although in literature it has been reported that ZnPc exhibits the high crystalline character [28, 29]. The patterns at around $2\theta = 6.4$ °C and $2\theta =$

8.3 °C reflect the crystalline nature of ZnPc [28]. The observed patterns of TNZnPc are broad and shifted to lower $2q$ as compared to ZnPc due to the NO_2 orientated at the periphery of the ZnPc. These functional groups hinder the effective stacking of metallophthalocyanine.
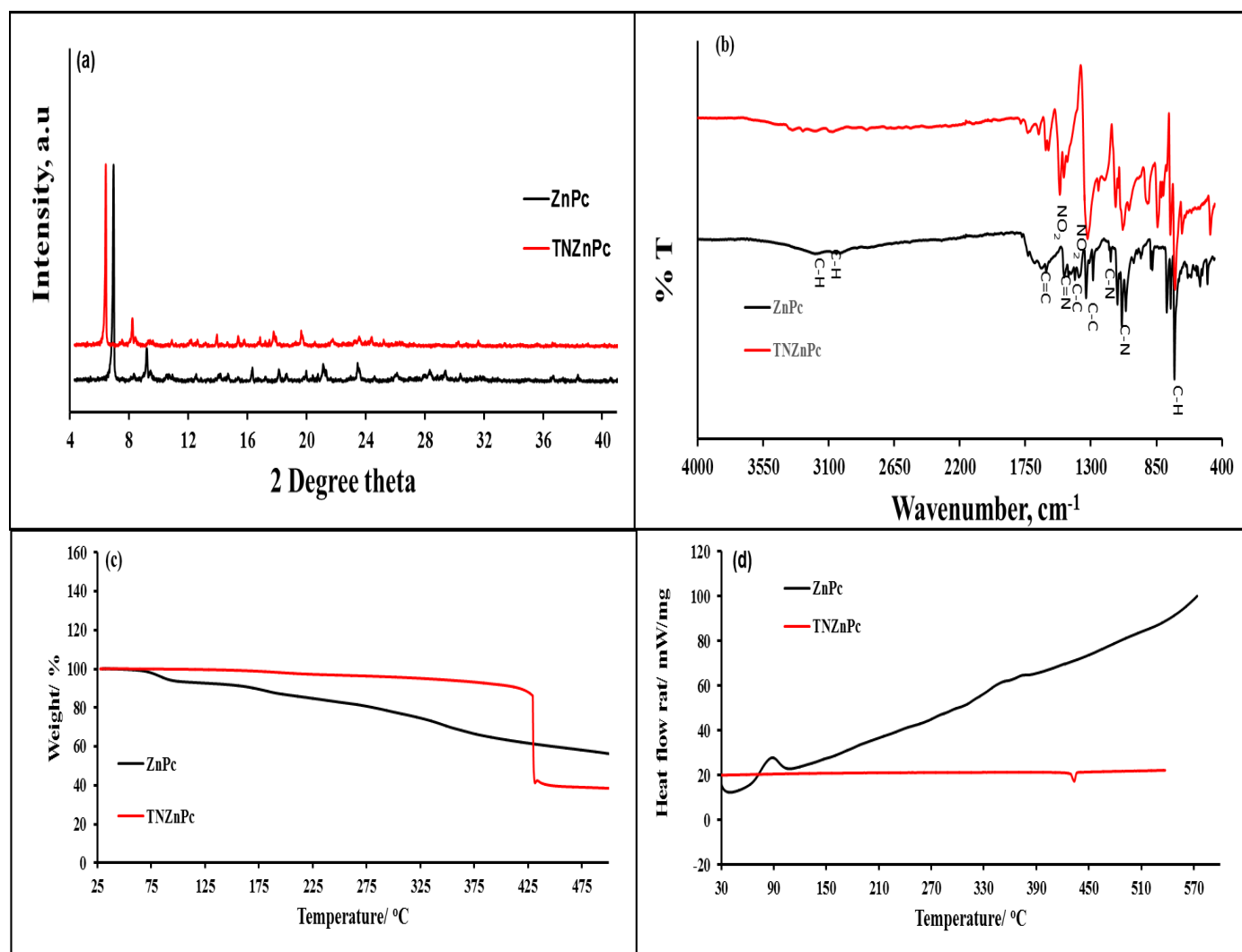
Figure 4. 2: (a) XRD, (b) FTIR, (c) TGA, and (d) DSC of ZnPc and TNZnPc

Figure 4.2 (b) presents the FTIR spectra of both inhibitors investigated. FTIR was used as a tool to confirm the synthesis of both ZnPc and TNZnPc. It can be seen that both inhibitors exhibit some bands at 3000 and 3307 cm^{-1}, which are attributable to C-H stretching bands. For the peaks at 1732 and 1724 cm^{-1} correspond to anhydride, C=O bonds, whereas the one at 1639 and 1618 cm^{-1} show C=C macrocyclic ring deformation of ZnPc and TNZnPc respectively. The peaks at 1609 and 1587 cm^{-1}, are due to bending of the N-H groups of ZnPc and TNZnPc

respectively, and the characteristic peaks of nitro groups are seen at 1514 and 1326 cm^{-1}. The peaks at 1337 and 1327 cm^{-1} were due to the C-C stretching in isoindole of ZnPc and TNZnPc, respectively. The peaks at 890, 783, 781, 730, 693 cm^{-1} and at 920, 843, 724, 479 cm^{-1} are vibrations for the skeletal phthalocyanine ring of ZnPc and TNZnPc, respectively. The results in Figure 4.2 (c) represent the TGA curcves with their DSC profiles shown in Figure 4.2 (d) for ZnPc and TNZnPc.The TGA profile of ZnPc shows two degradation steps at around 75 and 330 °C [30]. It is noticeable that TNZnPc depicts a single degradation at about 443 °C and their corresponding weight percentages is 69.81%. The high thermal stability may be due to the stabilising effect of nitro groups introduced on the periphery of the ZnPc [31].

The UV-vis results of ZnPc and TNZnPc inhibitors are given in Figure 4.3 (a) and both the inhibitors show absorption at three different bands with the B-band appearing between 300-400 nm. The characteristic absorption of phthalocyanine molecules is seen at around 412 and 413 nm for ZnPc and TNZnPc, respectively [32]. Furthermore, in the Q-band region it appears around 785 and 765 nm respectively, and these bands arise from $\pi - \pi^*$ transitions and this can be inferred from the four frontier orbitals (HOMO and LUMO orbitals) [33]. Furthermore, the Q-band of TNZnPc is slightly blue shifted as compared to the one for ZnPc due to the presence of an electron withdrawing group NO_2 on the periphery of ZnPc [34]. Moreover, Beer-Lambert's law was obeyed for the compound ranging from 2 to 8 ppm in Figure 4.3 (b).
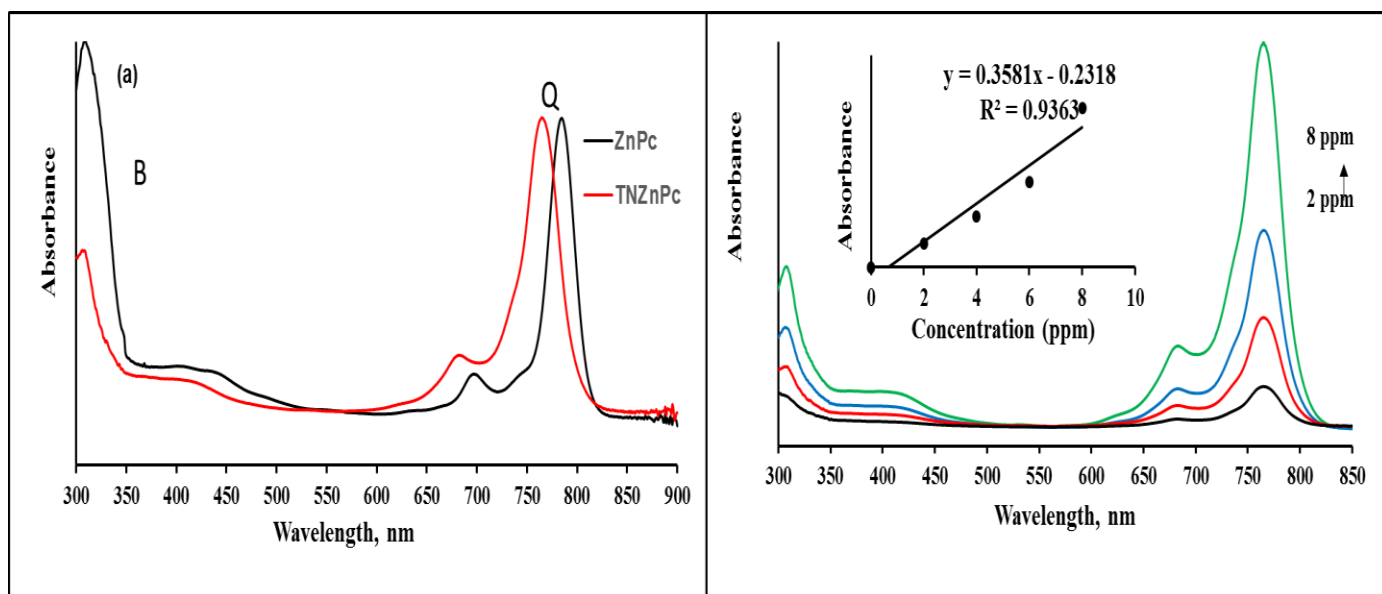
Figure 4. 3: (a) UV-vis spectra of ZnPc and TNZnPc in H_2SO_4 (~10 ppm), and (b) UV-vis spectra of ZnPc at different concentration 0 to 8 ppm. Inset: concentration dependence of TNZnPc.

4.3.2. GRAVIMETRIC MEASUREMENTS

4.3.2.1. EFFECT OF INHIBITOR CONCENTRATION AND TEMPERATURE

Figure 4.4 (a) and (b) show the plots of inhibition efficiency versus concentration for each inhibitor at different temperatures for ZnPc and TNZnPc. From the results, it is clearly shown that the percentage inhibition efficiency (%IE) increases as the concentration of the inhibitor increases for TNZnPc and increase from 40 to 60 ppm for ZnPc, while the %IE decreases with an increase in temperature from 40 to 60 ppm and at 40 ppm for ZnPc and TNZnPc respectively as shown in Fig. 4.4(a) and (b). This is observed because at higher temperatures the corrosive medium becomes more aggressive, however there is a discrepancy concerning the above trend at 80 ppm and 60 to 80 ppm for ZnPc and TNZnPc respectively. The non-uniform of %IE values for both ZnPc and TNZnPc may be due to the inhibitor's varying aggregative interactions [35]. According to what is mostly reported is that substituted molecules possess a higher solubility [36] hence higher inhibition efficiency. However, in this study, ZnPc showed more pronounced %IE values than TNZnPc and this may be associated with the fact that phthalocyanine in nature are

95

insoluble in most solvents [37]. However, ZnPc and TNZnPc showed pronounced %IE at the inhibitor concentration of 60 ppm (82.29%) for ZnPc and at 80 ppm (69.77%) for TNZnPc with a reduced rate of corrosion (0.550 g.cm^{-2}.h^{-1} and 1.760g.cm^{-2}.h^{-1}) compared to the blank, respectively at 303K as shown in Table 4.1.
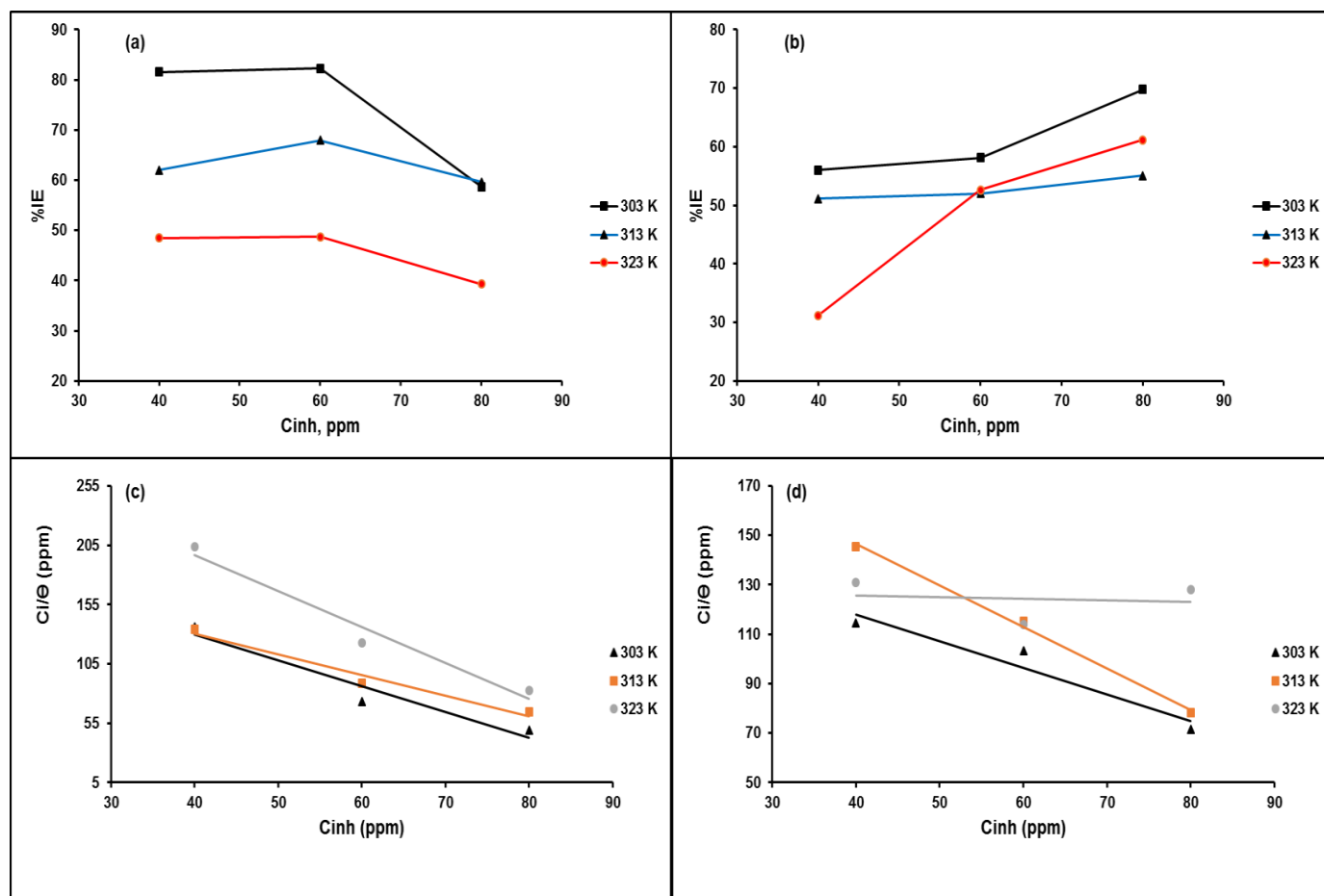
Figure 4. 4: Plots of inhibition efficiency (%IE) against inhibitor concentration (ppm) (a) ZnPc and (b) TNZnPc; and Langmuir adsorption isotherm plots for the adsorption of (c) ZnPc and (d) TNZnPc on Al metal sheet at different temperature.

It was shown that the temperature effect on the inhibited acid-metal reaction is highly complex due to many changes occurring on the metal surface such as rapid etching, inhibitor desorption, and decomposition or rearrangement undergone by the inhibitor [38]. Consequently, the adsorption coverage of the inhibitor on aluminium surface increases with inhibitor concentration from 40 to 60 ppm for ZnPc and from 40 to 80

ppm for TNZnPc and this is inferred from Figure 4.4 (c) and (d) complimented by Table 4.1.

Table 4. 1: The values of corrosion rate (C_R), percentage inhibition efficiency (%IE) and surface coverage (θ) of ZnPc and TNZnPc at 303, 313 and 323 K for aluminium metal sheet.

Sample	Temp. (K)	Conc. (ppm)	Δw (g)	C_R (X10^{-3} g.cm^{-2}.hr^{-1})	%IE	ϴ	C/ϴ (ppm)
ZnPc	303	0	0.559	3.106	_	_	_
		40	0.103	0.572	81.58	0.8158	49.033
		60	0.099	0.550	82.29	0.8229	72.911
		80	0.231	1.283	58.68	0.5868	136.328
	313	0	0.692	3.844	_	_	_
		40	0.263	1.460	61.99	0.6199	64.527
		60	0.222	1.230	67.92	0.6792	88.345
		80	0.279	1.550	59.68	0.5968	134.054
	323	0	0.718	3.989	_	_	_
		40	0.37	3.844	48.47	0.4847	82.526
		60	0.368	2.060	48.75	0.4875	123.082
		80	0.436	2.040	39.28	0.3928	203.679
TNZnPc	303	0	0.559	3.106	_	_	_
		40	0.299	1.660	56.00	0.56	71.430
		60	0.205	1.114	58.55	0.5815	103.189
		80	0.318	1.760	69.77	0.6977	114.660
	313	0	0.692	3.844	_	_	_
		40	0.381	2.120	51.15	0.5115	78.201
		60	0.367	2.040	52.02	0.5202	115.346
		80	0.443	2.460	55.05	0.5505	145.316
	323	0	0.718	3.989	_	_	_
		40	0.433	2.406	31.20	0.3120	128.206
		60	0.373	2.072	52.65	0.5265	113.965
		80	0.459	2.550	61.14	0.6114	130.841

In order to gain more insight as how the inhibitor compound adsorb on a metal surface, several adsorption isotherms such as Langmuir, Frumkin, Freundlich and

Temkin isotherm. The surface coverage, θ, values at 30 °C for different inhibitor concentrations have been used to better explain the isotherm determining the adsorption process. The value of θ relates to the equilibrium adsorption constant, K_{ads} and the inhibitor concentration according to Langmuir adsorption isotherm (Equations 4.3) and the results are given in Table 4.2. From these results, it can bee seen that data fitted the Langmuir isotherm adsorption very well for both ZnPc and TNZnPc inhibitors [39].

Table 4. 2: Adsorption parameters derived from the Langmuir adsorption isotherm for ZnPc and TNZnPc for aluminium.

Inhibitor	T (K)	K_{ads} (x 10^3 L.mol^{-1})	$-\Delta G^o_{ads}$ (kJ.mol^{-1})
ZnPc	303	2.66	29.99
	313	2.89	31.20
	323	1.82	30.94
TNZnPc	303	4.70	31.42
	313	3.55	31.73
	323	5.91	34.11

The free energy of adsorption (ΔG^o_{ads}) was calculated using the Equation 3.3.

The literature reports that the energy values of -20 kJmol^{-1} or less negative are associated with physisorption adsorption mechanism, which is an electrostatic interaction between charged molecules and charged metal surface [39]. In contrast, if the ΔG^o_{ads} values are -40 kJmol^{-1} or more negative indicates a chemisorption mechanism which is sharing or transfer of charge from the inhibitor molecules to the metal surface forming a coordinate covalent bond [40]. Based on Table 4.2, it is observed that both ZnPc and TNZnPc inhibitors result into a mixed-type adsorption mechanism. In addition, the adsorption process of both inhibitors on a metal surface was spontaneous [41].

4.3.2.2. THERMODYNAMIC AND ACTIVATION PARAMETERS

The corrosion rate dependence on temperature can be expressed by Arrhenius equation and transition state equations presented in Equation 4.4 and 4.5 [39, 40].

$$\frac{C_{inh}}{\theta} = \frac{1}{K_{ads}} + C_{inh} \tag{4.4}$$

$$\Delta G^o = -2.303RT \log(55.5 K_{ads}) \tag{4.5}$$
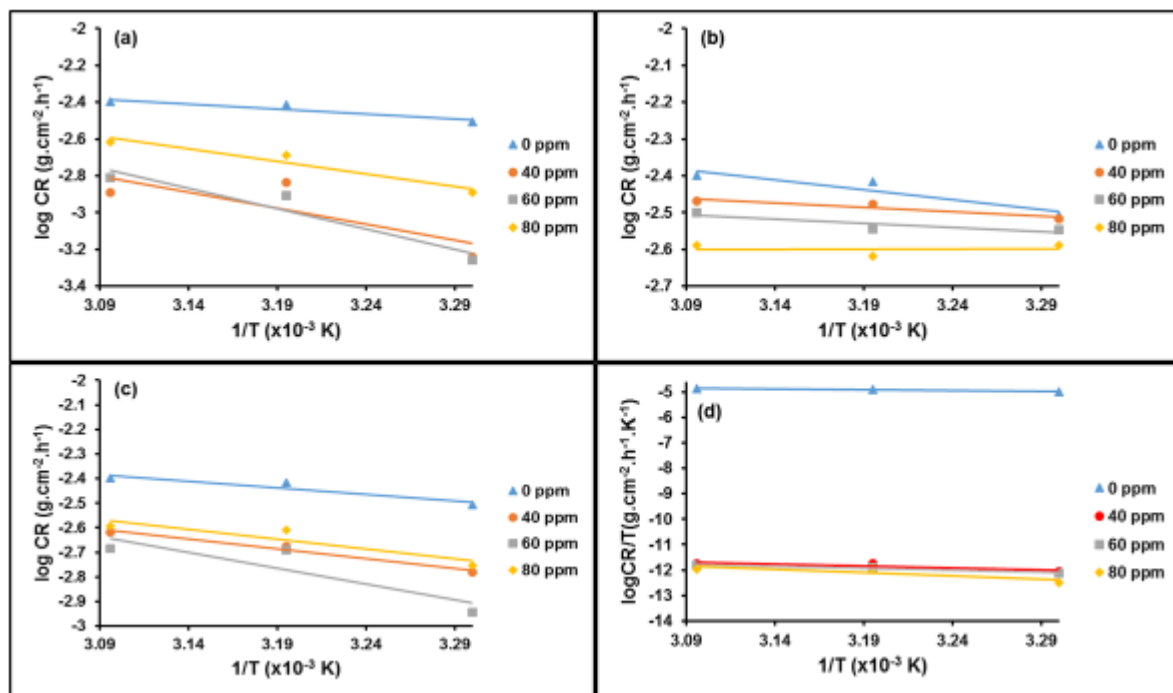
Figure 4. 5: Arrhenius plots for Al metal in 1M HCl in the absence and presence of various concentrations of ZnPc (a) and TNZnPc (b); and Transition state plots at different concentrations of ZnPc (c) and TNZnPc (d) respectively.

The activation energy, entropy and enthalpy at different concentrations of ZnPc and TNZnPc were calculated from the Arrhenius Equation (4.4) and its transition state Equation (4.5). From the Arrhenius plots given in parts (a) and (b) of Figure 4.5, activation energy values were calculated, which are the plots between log (C_R) and reciprocal temperature (1/T). In this study, values of ΔS^o and ΔH^o were obtained using the transition state equation (4.5) [42].

Part (c) and (d) of Figure 4.5 show the transition state plots for ZnPc and TNZnPc at different temperatures. For a chemical reaction to take place, activation energy

which is expressed in terms of joules per reactants mole is required. Higher activation energy values (at 40 and 60 ppm for ZnPc and TNZnPc respectively) are a sign for a good inhibition action by the metallophthalocyanine compounds; this is done by increasing energy barrier for corrosion activity. Higher E_a values are related with increasing a double layer thickness that improves the activation energy of the corrosion process. Positive ΔH^o values indicate an endothermic [42] process upon the dissolution of aluminium in the inhibitor solution while negative values reveal that the adsorption of the inhibitor molecules is an exothermic process, Furthermore, TNZnPc exhibited endothermic reaction while ZnPc exhibited exothermic reaction at 40 and 60 ppm [43]. The negative value of ΔS^o in all cases indicates that the formation of the activated complex in the rate determining step is associative rather than dissociative and can be interpreted to decrease in disorderliness as the reaction proceeds from reactants to activated complex.This can be observed in the blank values, it is shown that both ZnPc and TNZnPc exhibited a great disorder of -267.55 $JK^{-1}.mol^{-1}$ as compared to the inhibited corrosive solution. Table 4.3 presents different parameters from the Arrhenius and transition state plots.

Table 4. 3: Activation energy (E_a), entropy (ΔS^o) and enthalpy of activation (ΔH^o_a) values for aluminium metal at different inhibitor concentrations of inhibitors in corrosive environment.

Inhibitor	Concentration (ppm)	E_a (kJ.mol^{-1})	ΔH^o_{ads} (kJ.mol^{-1})	ΔS^o (JK^{-1}.mol^{-1})
ZnPc	0	10.27	70.00	-267.55
	40	32,56	-55.30	-252.84
	60	2,25	-20.93	-218.47
	80	6,62	32.38	-229.92
TNZnPc	0	10.27	70.00	-267.55
	40	15.14	25.78	-214.922
	60	24.62	12.75	-257.80
	80	15.07	18.08	-242.41

4.3.3. ELECTROCHEMICAL ANALYSIS

The polarisation behaviour of aluminium in 1.0 M HCl in the absence and presence of different concentrations (from 40ppm to 80ppm) of ZnPc and TNZnPc inhibitors is shown in Figure 4.6. It is observed that both anodic and cathodic reactions of Al electrode corrosion retarded with increasing concentration of the prepared inhibitors, that is, the anodic dissolution of the metal was minimised even the hydrogen evolution was reduced. From Tafel plots, the electrochemical parameters such as corrosion potential (E_{corr}), corrosion current density (i_{corr}), anodic and cathodic Tafel slopes (b_a and b_c) were calculated and tabulated in Table 4.4. The polarisation curves in the presence of both ZnPc and TNZnPc inhibitors shifted to more positive potentials (anodic region) compared to the blank, suggesting the formation of passivation film of the inhibitors on the Al surface and reduction in the rate of anodic dissolution of the metal [9]. As a result, the E_{corr} value for the uninhibited solution was −535.6 mV, and with the addition of inhibitor this value was around 529.6 and 500.9 mV for 40 ppm ZnPc and TNZnPc, respectively. The i_{corr} slightly decreased from 1.94 down to 1.77 and 0.096 mA.cm^{-2}, 40 ppm ZnPc and TNZnPc, respectively, and the lowest value obtained was with the addition of 80 ppm in both inhibitors. The difference of greater than 85 mV between the corrosion potential values of the blank and the inhibited solutions suggest either an anodic or cathodic inhibitor type while that of less than 85mV signify a mixed-type, in this regard, both ZnPc and TNZnPc showed a mixed-type inhibition meachanism.

For i_{corr} values, the maximum reduction was observed for TNZnPc inhibitor. This maybe due to an increase in the electron cloud by NO_2 which in turn enhances the adsorption of TNZnPc on the metal surface, thus inhibiting the corrosion current density [10-12]. The E_{corr} values of the as-synthesised inhibitor compounds shifted toward both anodic and cathodic directions slightly. This may suggest a mixed-type adsoprtion mechanism of both ZnPc ad TNZnPc on the Al metal. Moreover, the values of b_a and b_c were changed upon the introduction of the inhibitors, signifying that the inhibitors affect the anodic and cathodic reaction mechanism without the Al metal reaction sites being blocked.

Figure 4. 6: Tafel plots for Al in 1 M HCl in the absence and presence of different concentrations of ZnPc (a) and TNZnPc (b) inhibitor compounds.

The change in the relative magnitude of the Tafel slope values anodic, b_a, and cathodic, b_c, before and after the addition of ZnPc and TNZnPc inhibitors has been used in addition to the displacement in E_{corr} to further classify the mode of inhibition as predominantly anodic or cathodic [9]. As shown in Table 4.4, the change in b_a values of the blank, ZnPc and TNZnPc inhibitors are lower than that of b_c. This indicates that the inhibitors predominantly inhibit cathodic dissolution of Al, even though anodic reaction is also inhibited. On the other hand, as seen in Table 4.4, the passivation potential value, E_{pas}, for the blank solution was 465.4 mV. However, this value decreased upon addition of ZnPc and TNZnPc inhibitors with the lowest values of -412.2 and -352.5mV, respectively at 80 ppm. Correspondingly, the passivation current density value, i_{pas}, of blank was 4.68 mA.cm^{-2}. Upon addition of ZnPc and TNZnPc inhibitors, i_{pas}, decreased with an increase in the inhibitor concentration resulting to the lowest values of 3.45 and 1.12 mA.cm^{-2} by adding 80 ppm of inhibitor, similar to the behaviour of the weight loss results shown in Figure 4.4. Accordingly, it could be concluded that the addition of phthalocyanine inhibitors decrease the corrosion rate of aluminium metal in acidic media by improving the passive film properties. Table 4.4 reveals that as the inhibitor concentration increases the inhibition efficiency (EI) increases also with the TNZnPc showing high values of EI as compared to ZnPc.

Table 4. 4: Potentiodynamic polarisation (PDP) parameters such as corrosion potential (E_{corr}), corrosion current density (i_{corr}), anodic Tafel slope, b_a and cathodic Tafel slope, b_c, using different inhibitors.

Inhibitor	Conc (ppm)	$-E_{corr}$ (mV)	i_{corr} (mA.cm^{-2})	b_a (mV)	b_c (mV)	E_{pas} (mV)	i_{pas} (mA.cm^{-2})	%IE$_{PDP}$
Blank		535.6	1.94	155.3	179.6	465.4	4.68	-
ZnPc	40	529.6	1.77	165.1	206.1	453.7	4.51	8.76
	60	521.6	1.58	137.7	187.4	456.7	4.16	18.56
	80	520.8	0.35	105.5	124.2	412.2	3.45	81.96
TNZnPc	40	500.9	0.096	99.0	132.4	385.1	1.56	95.05
	60	490.8	0.042	113.7	160.3	321.4	1.25	97.84
	80	459.1	0.040	68.0	143.9	352.5	1.12	97.94

4.3.4. ELECTROCHEMICAL IMPEDANCE SPECTROSCOPY (EIS)

Aluminium corrosion behaviour in 1M HCl in the uninhibited and inhibited system was also studied by the electrochemical impedance spectroscopy. Nyquist plots of aluminium absence and presence of synthesized inhibitors with different concentrations showed the semicircles as shown in Figure 4.7.
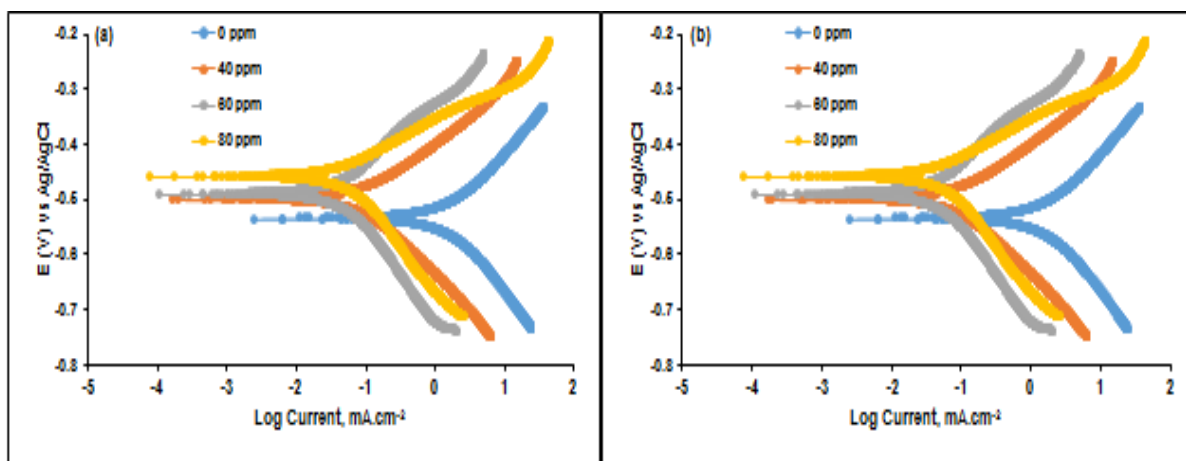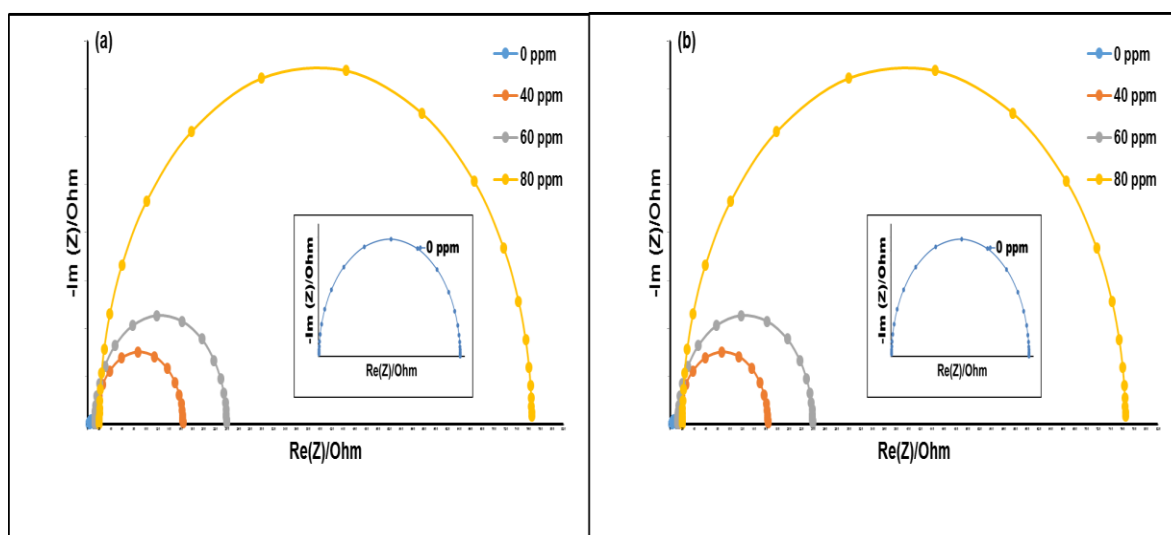

Figure 4. 7: Nyquist plots of Al in 1 M HCl in the absence and presence of different concentrations of ZnPc (a) and TNZnPc (b) inhibitor compounds.

The impedance response was changed by the introduction of inhibitors as indicated by the plots. The impedance parameters obtained from these plots are listed in Table 4.5. The inhibition efficiency was calculated by charge transfer resistance in the case of EIS according Equation 2.19 [47]. As seen in the table, the values of R_s which is the solution resistance between the working electrode (WE) and counter electrode (CE) are smaller in comparison to the R_{ct} values which is the charge transfer resistance. The inhibitor concentrations increased with the increasing R_{ct} values signifying that the surface coverage on aluminium by the inhibitors increases due to the increased number of inhibitor molecules in the corrosive medium and as a result the inhibition efficiency values increased. It is observed that values of the double layer capacitance (C_{dl}) decreased as the concentration of both the inhibitors increased from 40-80pmm, this could be the reason of a decrease in local dielectric constant or the increasing thickness of the C_{dl}. This implies that the prepared inhibitors function through adsorption at the solution metal interface [48].

Table 4. 5: Impedance parameters for corrosion of aluminium in 1M HCl containing different concentrations of inhibitors.

Inhibitor	Inhibitor Conc (ppm)	R_s (Ω)	R_{ct} (Ω)	C_{dl} (x10^{-4} F)	%IE$_{EIS}$
Blank		2.836	8.871	2.060	-
ZnPc	40	10.511	153.448	0.835	94.22
	60	13.618	170.323	0.771	94.79
	80	21.196	1826.121	0.153	99.51
TNZnPc	40	13.619	150.553	0.929	94.11
	60	12.276	226.985	0.427	96.09
	80	20.117	745.251	0.235	98.81

The analyses of EIS spectra were done using an equivalent circuit displayed in Figure 4.8. A single charge transfer reaction was shown by this figure. The capacitive loop diameter was found to increases upon the introduction of the inhibitors which signifies that the process of corrosion was inhibited.
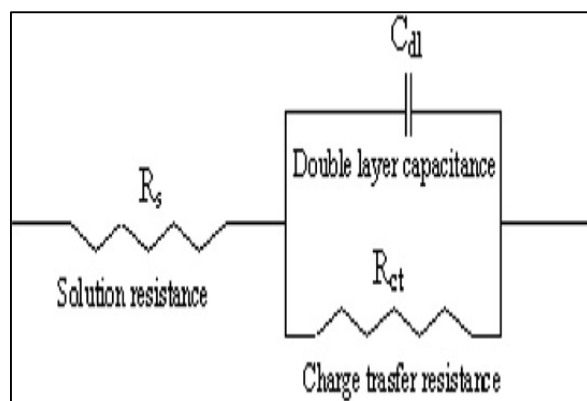
Figure 4. 8: The suggested equivalent circuit model for the studied system.

4.4 CONCLUSION

Zinc (II) phthalocyanine and 4-tetranitro zinc (II) phthalocyanine were successfully synthesised and confirmed by UV-vis, XRD, FTIR, and STA. ZnPc and TNZnPc exhibited an intense absorption peak at the Q-band region of the spectra which is complemented by the literature. The two inhibitor inhibitors proved to be thermally stable (TGA) and (DSC) and can be used at elevated temperatures. The XRD was used for phase identification and ZnPc was reported to be more crystalline than TNZnPc due to the presence of NO_2. FTIR spectra were in agreement with Uv-vis. A study of the use of ZnPc and TNZnPc inhibitors as corrosion inhibitors for aluminium metal in 1 mol.L^{-1} HCl has been carried out. It has been found from gravimetric measurement that ZnPc acts as a good corrosion inhibitor with its efficiency reaching its highest value by adding 60 ppm due to the formation of an adherent, compact, protective film. Additionally, inhibitor efficiency decreases with introduction of NO_2 group at peripheral due to steric hindrance. Electrochemical measurement, the improved the properties of the passive film formed on the Al surface was observed in both ZnPc and TNZnPc by decrease in the passivation current density and passivation potential values. Nyquist data displayed a single capacitive, and depressed loop in both ZnPc and TNZnPc inhibitors, indicating that the corrosion process is under charge transfer control. It is explored and proven in this contribution that zinc phthalocyanine and its tetra zinc counterpart carry tremendous potential for industrial usage as corrosion inhibitors. The results obtained from potentiodynamic polarisation showed that the prepared inhibitors represent a mixed-type of inhibitors

106

and the proposed adsorption mechanism is a mixed-type. In determining the corrosion inhibition efficiency, gravimetric analysis, potentiodynamic polarisation, and electrochemical impedance spectroscopy, gave similar trends.

4.5. REFERENCES

1. Z. Ahmad, Principles of corrosion engineering and corrosion control, Butterworth Heinemann, Oxford, UK, (2006) 1-8.
2. S. Edrah, S. K. Hasan, Studies on thiourea derivatives as corrosion inhibitor for aluminium in sodium hydroxide Solution, *J Appl Sci Res.* 6(2010) 1045-1049.
3. F. Jaspard-Mécuson, T. Czerwiec, G. Henrion, T. Belmonte, L. Dujardin, A. Viola, J. Beauvir, Tailored aluminium oxide layers by bipolar current adjustment in the Plasma Electrolytic Oxidation (PEO) process, *Surf. Coat. Technol.* 201(2007) 8677-8682.

4. C. Soriano, A. Alfantazi, Corrosion behavior of galvanized steel due to typical soil organics, *Constr. Build. Mater.* 102(2016) 904-912.
5. P. Arellanes-Lozada, O. Olivares-Xometl, D. Guzmán-Lucero, N. V. Likhanova, M. A. Domínguez-Aguilar, I. V. Li janova, E. Arce-Estrada, the inhibition of aluminium corrosion in sulphuric acid by poly (1-vinyl-3-alkyl-imidazolium hexafluorophosphate), *Materials.* 7(2014) 5711-5734.
6. U. Trdan, J. Grum, Evaluation of corrosion resistance of AA6082-T651 aluminium alloy after laser shock peening by means of cyclic polarisation and EIS methods, *Corros. Sci.* 59(2012) 324-333.
7. S. Zheng, C. Li, Y. Qi, L. Chen, C. Chen, Mechanism of (Mg, Al, Ca)-oxide inclusion-induced pitting corrosion in 316L stainless steel exposed to sulphur environments containing chloride ion, *Corros. Sci.* 67(2013) 20-31.
8. M. T. Muniandy, A. A. Rahim, H. Osman, A. M. Shah, S. Yahya, P. B. Raja, Investigation of some schiff bases as corrosion inhibitors for aluminium alloy in 0.5 M hydrochloric acid solutions, *Surf. Rev. Lett.* 18(2011) 127-133.
9. M. Dibetsoe, L. O. Olasunkanmi, O. E. Fayemi, S. Yesudass, B. Ramaganthan, I. Bahadur, A. S. Adekunle, M. M. Kabanda, E. E. Ebenso, Some phthalocyanine and naphthalocyanine derivatives as corrosion inhibitors for aluminium in acidic

medium: Experimental, quantum chemical calculations, QSAR studies and synergistic Effect of iodide ions, *Molecules.* 20(2015) 15701-15734.

10. S. Şafak, B. Duran, A. Yurt, G. Türkoğlu, Schiff bases as corrosion inhibitor for aluminium in HCl solution*, Corros. Sci.* 54(2012) 251-259.

11. Z. Cao, Y. Tang, H. Cang, J. Xu, G. Lu, W. Jing, Novel benzimidazole derivatives as corrosion inhibitors of mild steel in the acidic media. Part II: Theoretical studies, *Corros. Sci.* 83(2014) 292-298.

12. S. H. Zaferani, M. Sharifi, D. Zaarei, M. R. Shishesaz, Application of eco-friendly products as corrosion inhibitors for metals in acid pickling processes–A review, J*. Environ. Chem. Eng.* 1(2013) 652-657.

13. K. D. Modibane, T. Nyokong, Synthesis, photophysical and photochemical properties of octa-substituted antimony phthalocyanines, *Polyhedron.* 28(2009**)** 479–484.

14. E. Stupnišek-Lisac, S. Podbršcˇek, T. Soricˊ, Non-toxic organic zinc corrosion inhibitors in hydrochloric acid, *J. Appl. Electrochem.* 24(1994) 779–784.

15. O. K. Özdemir, A. Aytaç, D. Atilla, M. Durmuş, Corrosion inhibition of aluminum by novel phthalocyanines in hydrochloric acid solution, *J. Mater. Sci.* 46(2011) 752-758.

16. X. F. Zhang, H.-J. Xu, Influence of halogenation and aggregation on photosensitizing properties of zinc phthalocyanine (ZnPC), *J. Chem. Soc., Faraday Trans.* 89(1993) 3347-3351.

17. P. C. Martin, M. Gouterman, B. V. Pepich, G. E. Rezoni, D. C. Schindele, Effects of ligands, solvent, and variable sulfonation on dimer formation of aluminum and zinc phthalocyaninesulfonates, *Inorg. Chem.* 30(1991) 3305-3309.

18. L. Tang, X. Li, L. Li, G. Mu, G. Liu, Interfacial behavior of 4-(2-pyridylazo) resorcin between steel and hydrochloric acid, *Surf. Coat. Technol.* 201 (2006) 384–388.

19. M. Arıcı, D. Arıcan, A. L. Uğur, A. Erdoğmuş, A. Koca, Electrochemical and spectroelectrochemical characterization of newly synthesized manganese, cobalt, iron and copper phthalocyanines, *Electrochim. Acta.* 87(2013) 554-566.

20. K. M. Manamela, L. C. Murulana, M. M. Kabanda, E. E. Ebenso, Adsorptive and DFT studies of some imidazolium based ionic liquids as corrosion inhibitors for zinc in acidic medium, *Int. J. Electrochem.Sci.* 9 (2014) 3029-3046.

21. M. A. Ibrahim, M. Messali, Z. Moussa, A. Y. Alzahrani, S. N. Alamry, B. Hammouti, Corrosion inhibition of carbon steel by imidazolium and pyridinium cations ionic liquids in acidic environment, *Electrochim. Acta.* 29(2011) 375-389.

22. M. Tourabi, K. Nohair, M. Traisnel, C. Jama, F. Bentiss, Electrochemical and XPS studies of the corrosion inhibition of carbon steel in hydrochloric acid pickling solutions by 3, 5-bis (2-thienylmethyl)-4-amino-1, 2, 4-triazole, *Corros. Sci.* 75(2013)123-133.

23. U. M. Eduok, S. A. Umoren, A. P. Udoh, Synergistic inhibition effects between leaves and stem extracts of Sida acuta and iodide ion for mild steel corrosion in 1M H 2 SO 4 solutions, *Arabian J. Chem.* 5(2012) 325-337.

24. B. D. Mert, M. E. Mert, G. Kardaş, B. Yazıcı, Experimental and theoretical investigation of 3-amino-1, 2, 4-triazole-5-thiol as a corrosion inhibitor for carbon steel in HCl medium, *Corros. Sci.* 53(2011) 4265-4272.

25. M. Serri, W. Wu, L. R. Fleet, N. M. Harrison, C. F. Hirjibehedin, C. W. Kay, A. J. Fisher, G. Aeppli, S. Heutz, High-temperature antiferromagnetism in molecular semiconductor thin films and nanostructures, *Nat. Commun.* 5(2014) 3079.

26. C. Schünemann, Elschner, A. A. Levin, M. Levichkova, K. Leo, M. Riede, Zinc phthalocyanine—Influence of substrate temperature, film thickness, and kind of substrate on the morphology*, Int. J. Thin Solid Films.* 519(2011) 3939-3945.

27. A. C Cruickshank, C. J. Dotzler, S. Din, S. Heutz, M. F. Toney, M. P. Ryan, The crystalline structure of copper phthalocyanine films on ZnO (1100*), J. Am. Chem. Soc.* 35(2012) 14302-14305.

28. S. Senthilarasu, Y. B. Hahn, S. H. Lee, Structural analysis of zinc phthalocyanine (ZnPc) thin films: X-ray diffraction study, *J. Appl. Phys.* 102(2007) 043512.

29. S. Senthilarasu, S. Velumani, R. Sathyamoorthy, A. Subbarayan, A., Ascencio, G. Canizal, P. J. Sebastian, J. A. Chavez, R. Perez, Characterization of zinc phthalocyanine (ZnPc) for photovoltaic applications, *Mater. Sci. Process.* 77(2003) 383-389.

30. A. Y. Tolbin, A. V. Dzuban, V. I. Shestov, Y. I. Gudkova, V. K. Brel, L. G. Tomilova, N. S. Zefirov, Peripheral functionalisation of a stable phthalocyanine J-type dimer to control the aggregation behaviour and NLO properties: UV-Vis, fluorescence, DFT, TDHF and thermal study, *RSC Adv.* 5(2015) 8239-8247.

31. N. Karousis, J. Ortiz, K. Ohkubo, T. Hasobe, S. Fukuzumi, A. Sastre-Santos, N. Tagmatarchis, Zinc phthalocyanine–graphene hybrid material for energy

conversion: synthesis, characterization, photophysics, and photoelectrochemical cell preparation, *J. Phys. Chem C.* 116(2012) 20564-20573.

32. M. Arıcı, D. Arıcan, A.L. Uğur, A. Erdoğmuş and A. Koca, *Electrochemic. Acta.* 87(2013) 554.

33. X. Zhou, X. Wang, B. Wang, Z. Chen, C. He, Y. Wu, Preparation, characterization and NH 3-sensing properties of reduced graphene oxide/copper phthalocyanine hybrid material, *Sens. Actuators, B.* 193(2014) 340-348.

34. T. M. Kumar, B. N. Achar, Synthesis and characterization of lead phthalocyanine and its derivatives, *J. Organomet. Chem.* 691(2006) 331-336.

35. M. Dibetsoe, L. O. Olasunkanmi, O. E. Fayemi, S. Yesudass, B. Ramaganthan, I. Bahadur, A. S. Adekunle, M. M. Kabanda, E. E. Ebenso, Some phthalocyanine and naphthalocyanine derivatives as corrosion inhibitors for aluminium in acidic medium: Experimental, quantum chemical calculations, QSAR studies and synergistic Effect of iodide ions, *Molecules.* 20(2015) 15701-15734.

36. N. Karousis, J. Ortiz, K. Ohkubo, T. Hasobe, S. Fukuzumi, A. Sastre-Santos, N. Tagmatarchis, Zinc phthalocyanine–graphene hybrid material for energy conversion: synthesis, characterization, photophysics, and photoelectrochemical cell preparation, *J. Phys. Chem C.* 116(2012) 20564-20573.

37. O. Taratula, C. Schumann, M. A. Naleway, A. J. Pang, K. J. Chon, O. Taratula, A multifunctional theranostic platform based on phthalocyanine-loaded dendrimer for image-guided drug delivery and photodynamic therapy, *Mol. Pharmaceutics.* 10(2013) 3946-3958.

38. N. I. Kairi, J. Kassim, The effect of temperature on the corrosion inhibition of mild steel in 1 M HCl solution by curcuma longa extract, *Int J Electrochem Sci.* 8(2013) 7138-7155.

39. A. Zarrouk, I. Warad, B. Hammouti, A. Dafali, S. S. Al-Deyab, N. Benchat, The effect of temperature on the corrosion of Cu/HNO$_3$ in the presence of organic inhibitor: part-2, *Int. J. Electrochem. Sci.* 5(2010)1516-1526.

40. B. Hammouti, A. Zarrouk, S. S. Al-Deyab, I. Warad, Temperature Effect, Activation Energies and Thermodynamics of Adsorption of ethyl 2-(4-(2-ethoxy-2-oxoethyl)-2-p-Tolylquinoxalin-1 (4H)-yl) Acetate on Cu in HNO$_3$, *Orient. J. Chem.* 27(2011) 23.

41. D. Daoud, T. Douadi, S. Issaadi, S. Chafaa, Adsorption and corrosion inhibition of new synthesized thiophene Schiff base on mild steel X52 in HCl and H_2SO_4 solutions, *Corros. Sci.* 79(2014) 50-58.

42. I. Naqvi, A. R. Saleemi, S. Naveed, Cefixime: a drug as efficient corrosion inhibitor for mild steel in acidic media. Electrochemical and thermodynamic studies, *Int. J. Electrochem. Sci.* 6(2011) 146-161.

43. Z. A. Hadi, A. M. Aljeboree, A. F. Alkaim, Adsorption of a cationic dye from aqueous solutions by using waste glass materials: isotherm and thermodynamic studies, *Int. J. Sci.* 12(2014) 1273-1288.

44. R. Solmaz, E. Altunbaş, G. Kardaş, Adsorption and corrosion inhibition effect of 2-((5-mercapto-1,3,4-thiadiazol-2-ylimino) methyl) phenol Schiff base on mild steel, *Mater. Chem. Phys.* 125(2011) 796-801.

45. H. Elmsellem, N. Basbas, A. Chetouani, A. Aouniti, S. Radi, M. Messali, B. Hammouti, Quantum chemical studies and corrosion inhibitive properties of mild steel by some pyridine derivatives in 1 N HCl solution, *Electrochim. Acta.* 32(2014) 77-108.

46. D. Li, F. Wang, X. Yu, J. Wang, Q. Liu, P. Yang, Y. He, Y. Wang, M. Zhang, Anticorrosion organic coating with layered double hydroxide loaded with corrosion inhibitor of tungstate, *Prog. Org. Coat.* 71(2011) 302-309.

47. A. M. Atta, O. E. El-Azabawy, H. S. Ismail, M. A. Hegazy, Novel dispersed magnetite core-shell nanogel polyneers as corrosion inhibitors for carbon steel in acidic medium, *Corros. Sci.* 53(2011) 1680-1689.

48. M. A. Hegazy, H. M. Ahmed, A. S. El-Tabei, Investigation of the inhibitive effect of p-substituted 4-(N, N, N-dimethyldodecylammonium bromide) benzylidene-benzene-2-yl-amine on corrosion of carbon steel pipelines in acidic medium, *Corros. Sci.* 53(2011) 671-678.

CHAPTER FIVE

PROTECTION OF CORROSION RATE ON ALUMINIUM METAL IN ACIDIC MEDIA BY UNSUBSTITUTED AND 4-TETRANITRO SUBSTITUTED NICKEL (II) PHTHALOCYANINE INHIBITORS VIA ELECTROCHEMICAL AND GRAVIMETRIC STUDIES FOR HYDROGEN FUEL CELL

Thabo Pesha[1], *Gobeng R. Monama*[1], *Mpitloane J. Hato*[1],*, *Mamookgo E. Makhatha*[2], *Kabelo E. Ramohlola*[1], *Kerileng M. Molapo*[3], *Kwena D. Modibane*[1], ** Protection of corrosion rate on aluminium metal in acidic media by unsubstituted and 4-tetranitro substituted nickel (ii) phthalocyanine inhibitors via electrochemical and gravimetric studies for hydrogen fuel cell. Results in Physics.

[1]Department of Chemistry, School of Physical and Mineral Sciences, Faculty of Science and Agriculture, University of Limpopo (Turfloop Campus), Polokwane, Sovenga 0727, South Africa

[2]Department of Metallurgy, School of Mining, Metallurgy and Chemical Engineering, Faculty of Engineering and Built Environment, University of Johannesburg (Doorfontein Campus), Johannesburg 2001, South Africa

[3]Department of Chemistry, Faculty of Natural Science, University of the Western Cape (Bellville Campus), Cape Town 7535, South Africa

*E-mails: kwena.modibane@ul.ac.za (KD Modibane); mpitloane.hato@ul.ac.za (MJ Hato)

ABSTRACT

One of the ways to protect corrosion process of aluminium metal in polymer electrolyte membrane (PEM) hydrogen fuel cell is through the use of chemical inhibition method. In this work, we present unsubstituted (NiPc) and tetra substituted nickel phthalocyanines (TNNiPc) as corrosion inhibitors for aluminium (Al) metal in 1 mol.L^{-1} hydrochloric acid (HCl) solution. The synthesised inhibitors were characterised using ultraviolet visible (Uv-vis), Fourier transform infrared spectroscopy (FTIR), X-ray diffraction (XRD) and simultaneous thermal analysis (STA). The XRD patterns demonstrated that NiPc was more crystalline as compared to TNNiPc because of the presence of the nitro group at peripheral position. FTIR spectra for all the inhibitors showed similar vibration band at around 730 cm^{-1}, which was due to C-H deformations with appearance of asymmetric and symmetric NO_2 observed in TNNiPc inhibitor. The Uv-vis spectrum of NiPc showed an intense Q-band at around 774 nm in 1 mol.L^{-1} H_2SO_4, whereas TNNiPc resulted in a blue shift of the Q-band due to electron withdrawal properties of NO_2 group. This was supported by the differential scanning calorimeter (DSC) with endothermic melting transition at around 450 ^{o}C for decomposition of NO_2 group. Even though, thermogravimetric analysis (TGA) demonstrated similar thermal stability of both inhibitors. In gravimetric corrosion analysis, NiPc and TNNiPc effectively inhibited the corrosion inhibition process by becoming adsorbed on the Al metal surface following the Langmuir adsorption isotherm model and involve both physisorption and chemisorption mechanisms. The electrochemical studies showed that inhibitors prevent Al metal sheet corrosion by adsorbing on Al surface to form pseudo-capacitive interface. The inhibitive effect of NiPc and TNNiPc inhibitors increase with increasing concentration and decrease with increasing temperature. Furthermore, potentiodynamic polarisation measurements revealed that the inhibitors are mixed-type corrosion inhibitors.

Keywords: Phthalocyanines inhibitor; Aluminium metal; Corrosion rate; Gravimetric and Electrochemical analyses

5.1. INTRODUCTION

Aluminium and its alloys have an amount of valuable mechanical, electrical, and thermal properties. They are extensively used in numerous fields, such as transportation, building, electrical engineering, as well as packaging [1, 2]. Based on its high energy density of 29 MJ/kg, there has been a cumulative concern on the use of aluminium-based materials as an energy storage in previous years [3]. In addition, the tri-valence of aluminium together with its light weight nature gives a high electrochemical equivalence of 2.98 Ah/g [4]. The above-mentioned factors make aluminium a convenient anode material for a large number of years [3, 4]. Furthermore, aluminium is considered as a metal with characteristics such as higher corrosion resistance, cost effectiveness and excellent manufacturability in polymer electrolyte membrane [PEM] hydrogen fuel cell design [5]. However, the major disadvantage of aluminium is the lack of ability to resist corrosion in harsh acidic and humid environment inside the PEM fuel cell without oxidants, passive layers and metal ions forming resulting in a considerable power degradation [6].

Attempts have been made in mitigating aluminium corrosion behaviour such as the use of materials upgrade, blending of production fluids, process control and chemical inhibition [7-9]. Amongst these methods, the corrosion chemical inhibition has been reported as suitable method to prevent destruction or degradation of metal surfaces in corrosive media due to economic and practical usage [10-12]. It has been discovered that the use of organometallic compounds such as corrosion inhibitors is one of the most practical ways for providing protection of metals [13-15]. This is due to their possession of $\pi-$electron systems presence of highly electronegative atoms such as O, N, S and P [16, 17].

In this investigation, we focused on metallophthalocyanines (MPcs) as organometallic complexes contain eight nitrogen atoms in a phthalocyanine ring and have 18 conjugated electron systems [9]. The dependability of their inhibition effect is mainly on physicochemical properties of the inhibitor c due to its functional groups, steric effect, electronic density of the donor atoms, and orbital character of donating electrons [10, 11]. The mechanism of inhibition is mainly explained by adsorption film studies where the inhibitor compound adsorbs on the metal surface either physically

or chemically [12, 13]. Furthermore, the aim of this work is to evaluate the corrosion inhibitory properties of Pc inhibitors for Al metal in acidic environment, organic inhibitors with good solubility in H_2SO_4, whose chemical structures are given in Figure 5.1 and possesses NO_2 and Ni metal. In the previous decade, NiPc has been used in several fields such as molecular electronics, optoelectronics, and photonics because it has high electron transfer abilities [14, 15]. The functions of NiPc are based on electron transfer reactions almost universally because of the 18-electron conjugated ring system found in its molecular structure. The presence of NO_2 groups was to enhance adsorption of Pc on the Al metal.
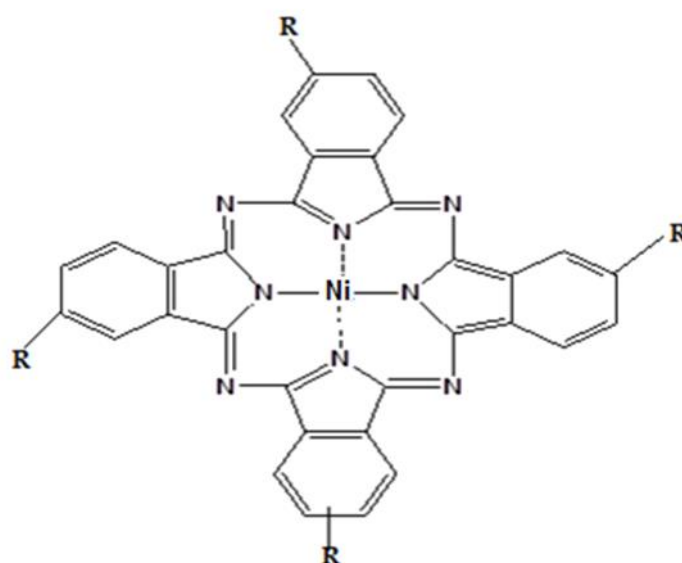
Figure 5. 1: Molecular structure of tetranitro nickel (II) phthalocyanine.

5.2. EXPERIMENTAL

5.2.1. MATERIALS AND AGGRESSIVE SOLUTION

Nickel sulphate ($NiSO_4$) was purchased from Sigma Aldrich, South Africa. Phthalimide, 32% hydrochloric acid (HCl), methanol, nitrobenzene, ethanol, sulphuric acid (H_2SO_4) and 55% nitric acid (HNO_3) were purchased from Rochelle chemicals. Ammonium molybdate ($(NH_4)_2MoO_4$), and urea CH_4N_2O were purchased from uniLAB.

5.2.2. SYNTHESIS OF NICKEL (II) PHTHALOCYANINES

Nickel phthalocyanine (NiPc) used as corrosion inhibitor was synthesised by modifying the procedure described in the literature [18]. Under a blanket of nitrogen, a mixture of phthalimide (3.00 g, 0.0200 mol) in the presence of excess urea (3.00 g, 0.0500 mol), ammonium molybdate (0.0800 g, 0.0600 mol) and nickel sulphate (1.69 g, 0.0058 mol) in nitrobenzene (15.00 mL) was refluxed at 180 OC for 5 hours with constant stirring. The product was finely ground and washed with ethanol three times for purification. Synthesis and purification of tetranitro nickel phthalocyanine (TNNiPc) was as outlined for NiPc [18]. 4-nitrophthalamide was used instead of phthalimide according to the reported method for preparation of phthalocyanine inhibitor [19]. Uv-vis (H_2SO_4): λ_{max} (log ε); 757 nm (5.82), 675 nm (5.53), 409 nm (5.05). FTIR: $v_{max}.cm^{-1}$; 3084 (Ar-H), 1607 (C=C), 1525 (N-O), 1336 (N-O); 913, 810, 729 (Pc skeletal).

Corrosion tests were performed on 98% Al sheets with freshly prepared surface. The surface of the Al specimens were ground using silicon carbide papers of various grades (600–1000), washed with distilled water, degreased in acetone, wiped with a clean towel paper and finally air-dried. Aggressive solution of 1 mol. L^{-1} HCl was prepared by diluting 32% analytical grade using distilled water. Metallophthalocyanines were first dissolved in minimum amount (10 mL equivalent to 4% by vol.) of H_2SO_4 and later diluted to various concentrations (40, 60, and 80 ppm) in 250 mL volumetric flask.

5.2.3. CHARACTERISATION

Optical absorption spectra were recorded at room temperature in the wavelength region 200 – 900 nm using a Varian Cary 300 Uv-vis-NIR spectrophotometer. The structure of MPcs was analysed using X-ray diffraction (XRD Phillips PW 1830, CuKα radiation, λ = 1.5406 A). The formation of the composite was confirmed by Cary 600 series Fourier transform infrared (FTIR) spectrometer (Agilent Technologies). The spectra were obtained at room temperature in the wave number range between 500 and 4500 cm^{-1}. A minimum of 32 scans were collected at a resolution of 4 cm^{-1}. The thermal stability of the samples was investigated using simultaneous thermal

analyser (STA) (Perkin-Elmer 6000). The weight of the samples ranging between 1 and 4 mg were heated from 30-500 °C at a heating rate of 20 °C/min under N_2 environment.

5.2.4. GRAVIMETRIC ANALYSIS

Gravimetric measurements were achieved using 3 cm × 4 cm dimensions in corrosive solution of $1mol.L^{-1}$ hydrochloric acid. MPcs were dissolved in minute amount of H_2SO_4 and diluted to several concentrations of 0, 40, 60 and 80 ppm in 250ml analytical reaction vessel. The Al were weighed and freely suspended in a 100 ml reaction vessel containing the corrosive solution for the first corrosion test. The specimens were removed from the test after 15 hrs immersion time, brushed and used distil water for washing, applied acetone and finally left to dry then re-weighed. Three crucial parameters such as the rate of corrosion, inhibition efficiency percentage and the surface coverage were determined using Equations (Eq. 5.1, 5.2, 5.3) [20, 21].

$$C_R = \frac{\Delta W}{St} \tag{5.1}$$

$$\%IE = \left(1 - \frac{\rho_1}{\rho_2}\right) \times 100\% \tag{5.2}$$

$$\theta = \frac{K_{ads}C_{inh}}{1 + K_{ads}C_{inh}} \tag{5.3}$$

5.2.5. ELECTROCHEMICAL MEASUREMENT

Electrochemical measurement were achieved using Bio-Logic SP150 potentiostat in three electrode cell of Ag/AgCl and platinum as the reference and counter electrode, respectively. The working electrode was prepared using aluminium metal in the presence and absence of corrosion inhibitor concentrations. The scanning range was from -0.250 to +0.250 mV at 1mV/s constant sweep rate on the open circuit. In addition, EIS measurements were done using 100 kHz to 10 MHz frequency range with 10 mV peak to peak amplitude. From EIS measurements [22] values of the double layer capacitance and the charge transfer resistance were obtained.

Furthermore, the Tafel slopes (cathodic and anodic) with inclusion of the corrosion current density were determined from the extrapolations of the cathodic and anodic Tafel plots. Moreover, the values of the inhibition efficiency were calculated with the help of the Equation 2.18 [23, 24].

5.3. RESULTS AND DISCUSSION

5.3.1. STRUCTURAL PROPERTIES

The crystal forms of NiPc and TNNiPc were characterised by XRD analysis presented in Figure 5.2(a) and showing α crystal structure [25]. In NiPc, the most preferred orientation was observed in NiPc at (001) plane corresponding to a diffraction line at $2\Theta = 6.9°$ [26]. However, the diffraction peaks of TNNiPc possessed reduction and broadening patterns as an indicative of poor crystallinity degree with amorphous character. FTIR spectra (Figure 5.2(b)) demonstrated peaks at around 733, 917, 1124, and 1615 cm−1 in NiPc whereas in TNNiPc were observed at 731, 947, 1145, and 1619 cm−1 bands [18]. These bands were accredited to the phthalocyanine ring characteristic vibration peaks [18]. There are two strong N=O stretch peaks for a nitro group present in TNNiPc, with symmetric stretch appearing at 1336 cm^{-1} and asymmetric stretch appearing at 1525 cm^{-1}. The TGA profiles in Figure 5.2(c) demonstrated two stage decomposition of TNNiPc at 371.69-394.24°C (1.69% weight loss) and at 436.33-454.76°C (1.82%), however, NiPc remained stable. The decomposition was due to the loss of peripheral positions of NiPc. This was supported by DSC profile whereby TNNiPc (Figure 5.2(d)) exhibited the corresponding crystallisation transitions which conveyed the exothermic curves relating to the TNNiPc. It was reported that the decomposition products might be the nitro groups, ammonia and metal oxide contained in the samples upon metallophthalocyanines synthesis [27].
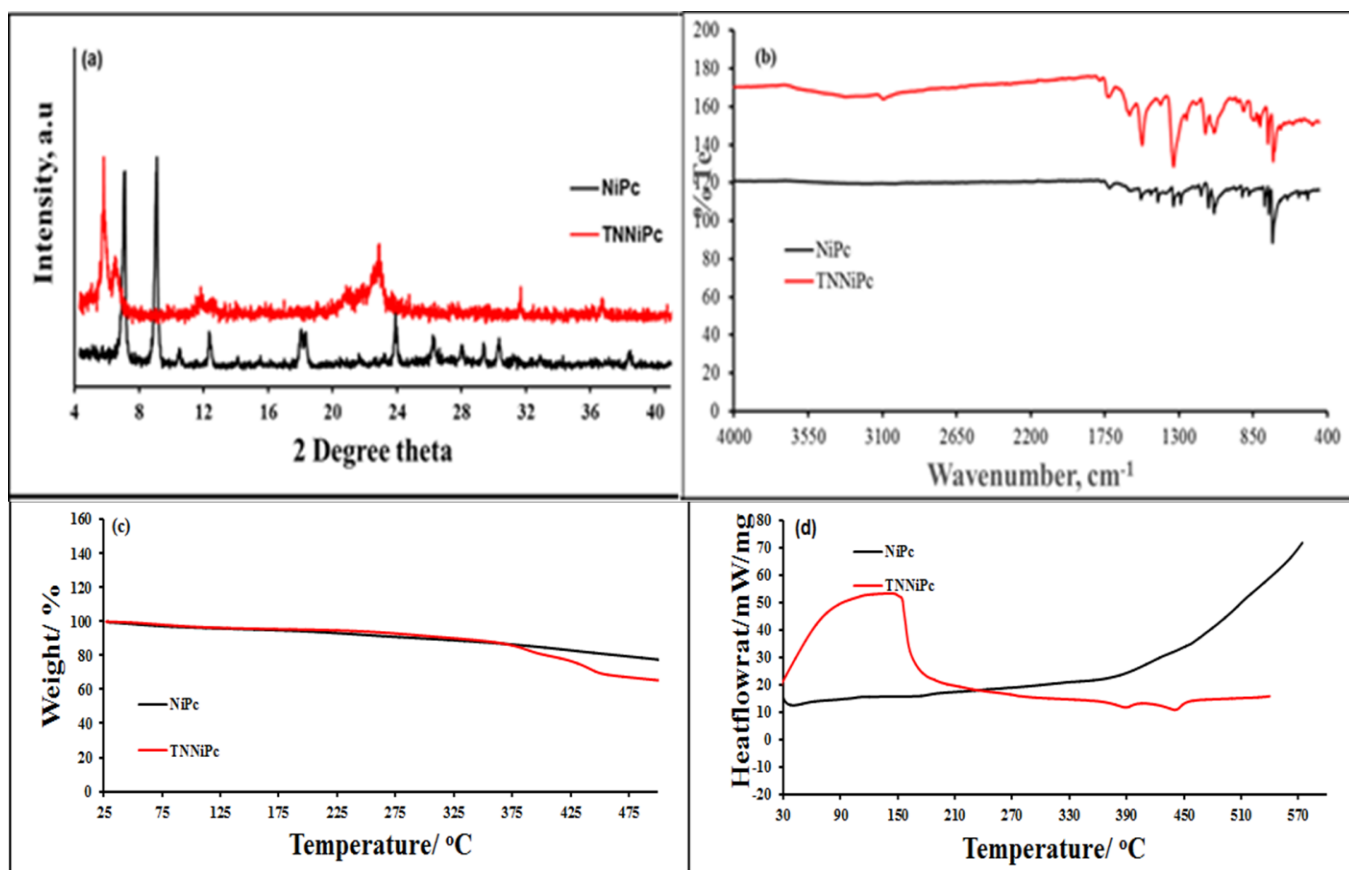
Figure 5. 2: (a) XRD, (b) FTIR, (c) TGA, and (d) DSC of NiPc and TNNiPc.

The UV-vis spectra of NiPc and TNNiPc are shown in Figure 5.3(a). As displayed, the Q and B band at 774 and 350 nm, respectively, were of the phthalocyanine conjugated system characteristic electronic absorption [18, 26, 27]. The Q band of NiPc and TNNiPc was observed to be wide and sharp with a bulged shape as compared to the reported TNH2Pc [28] due to transitions [29]. Furthermore, this attributed to the system of 18 electron and they were nearly insoluble in common organic solvents [30]. In comparison, the Q-band of TNNiPc was observed to be slightly blue shifted as compared to the one for NiPc due to the presence of an electron withdrawing group NO_2 on the NiPc peripheral position [31]. It has been reported that metallophthalocyanine possess low solubility in numerous organic solvents and as a result they aggregate [30]. It is dependent on the concentration, nature of the solvent, nature of the substituents, complexed metal ions and temperature [32].

119

The aggregation behaviour of TNNiPc was investigated at different concentrations in H_2SO_4 as showed in Figure 5.3(b).The intensity of the Q- and B-bands was observed to be increased with increase in concentration and there were no new bands observed due to aggregated species [32]. In this work, the solubility is increased by introducing NO_2 groups into the peripheral positions of the phthalocyanine framework [32]. Furthermore, Beer-Lambert's law was obeyed for the compound ranging from 0 to 8 ppm in H_2SO_4 (Figure 5.3(b). The absorptivity coefficient of NiPc from Beer-Lamberts increase in concentration and there were no new bands observed due to aggregation of Pc compound [18]. On the other hand, the absorptivity coefficient of TNNiPc was found to be logε of 5.82 at 757 nm. These log ε values also show that there are lot of molecules interacting with light which will enhance the inhibition efficiency of the inhibitor on Al metal [33].
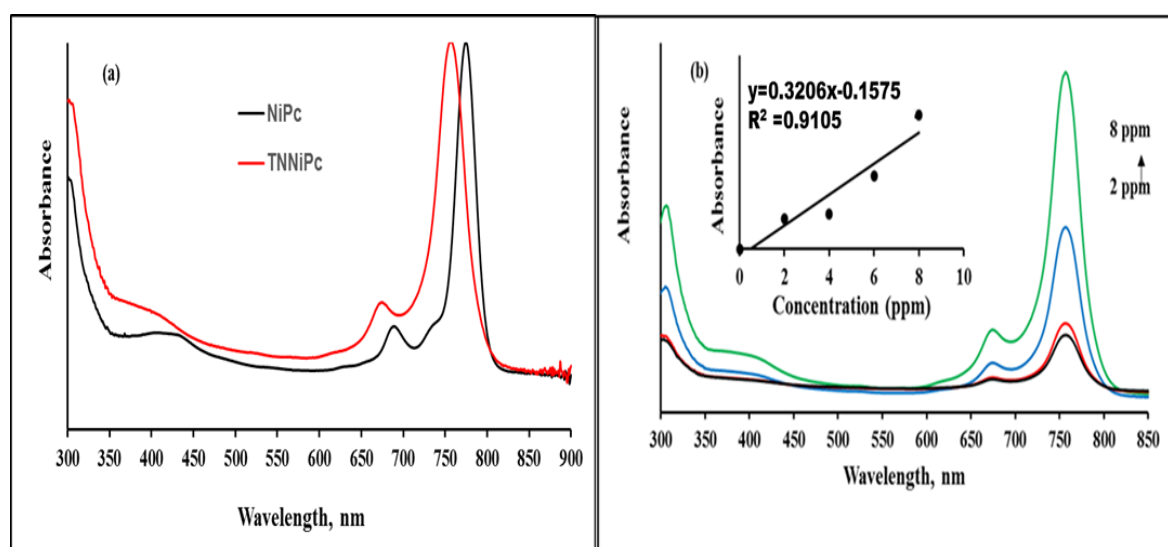
Figure 5. 3: (a) UV-vis spectra of NiPc and TNNiPc in H_2SO_4 (~10 ppm), and (b) UV-vis spectra of NiPc at different concentration 0 to 8 ppm. Inset: concentration dependence of TNNiPc.

5.3.2. GRAVIMETRIC MEASUREMENTS

5.3.2.1. EFFECT OF INHIBITOR CONCENTRATION AND TEMPERATURE

The gravimetric tests of these NiPc and TNNiPc inhibitors were represented by the plots of percentage inhibition efficiencies (%IE) against inhibitor concentration at

303-323 K as given in Figure 5.4(a) and (b), respectively, complimented by Table 5.1. As the inhibitor concentration increases from 40 to 60ppm, the %IE is observed to increase at 313 and 323 K for NiPc and at 303 and 323 K for TNNiPc respectively. As the temperature is increased, the inhibition efficiency of NiPc is observed to decrease due to the increase in the rate of corrosion which increases with temperature. The temperature effect can be shown by the inhibition efficiency values at 40 ppm for NiPc. For NiPc at 303 K, 96.42% while at 313 and 323 K, 41.61% and 37.05% were obtained respectively. The increase in temperature increases the density of corrosion rate severely. Tetranitro phthalocyanine (TNNiPc) exhibits similar trend. At 303 K, 62.26% inhibition efficiency was obtained and at 313 and 323 K, 52.16% and 47.49 % were obtained respectively.

The metal dissolution rate is opposed by increasing the inhibitor concentration as shown from studies [34, 35]. The similar behaviour was observed with the aluminium metal sheet whereby the rate of corrosion decreased as the concentration of the inhibitor increased. The corrosion rate was found to be 3.106, 3.844 and 3.989×10^{-3} $g.cm^{-2}.h^{-1}$ in the absence of inhibitor at 303, 313 and 323 K, respectively. However, upon the introduction of the inhibitor in the solution, corrosion rate decreased according to observations. The similar behaviour was observed by Li et al. [36] and Hong et al. [37] using fungicides and 4-amino-antipyrine on the corrosion of copper in NaCl solution, respectively. At 303 K, corrosion rate was obtained to be 0.111 $g.cm^{-2}.h^{-1}$ at 40 ppm for NiPc and 1.172×10^{-3} $g.cm^{-2}.h^{-1}$ at 40 ppm for TNNiPc. Upon increased temperature, corrosion rate at 40 ppm concentration increased to 2.200, and 2.511×10^{-3} $g.cm^{-2}.h^{-1}$ (NiPc) and 1.839 and 2.094×10^{-3} $g.cm^{-2}.h^{-1}$ (TNNiPc). However, the metal dissolution was found to decrease to a value of 0.400×10 $g.cm^{-2}.h^{-1}$ in NiPc and 2.361×10^{-3} $g.cm^{-2}.h^{-1}$ in TNNiPc at 80 ppm inhibitor concentration. It was very clear that increasing the concentrations of NiPc and TNNiPc reduces the corrosion rate, this is due to the decreased weight loss of the metal by the adsorption of the inhibitor.
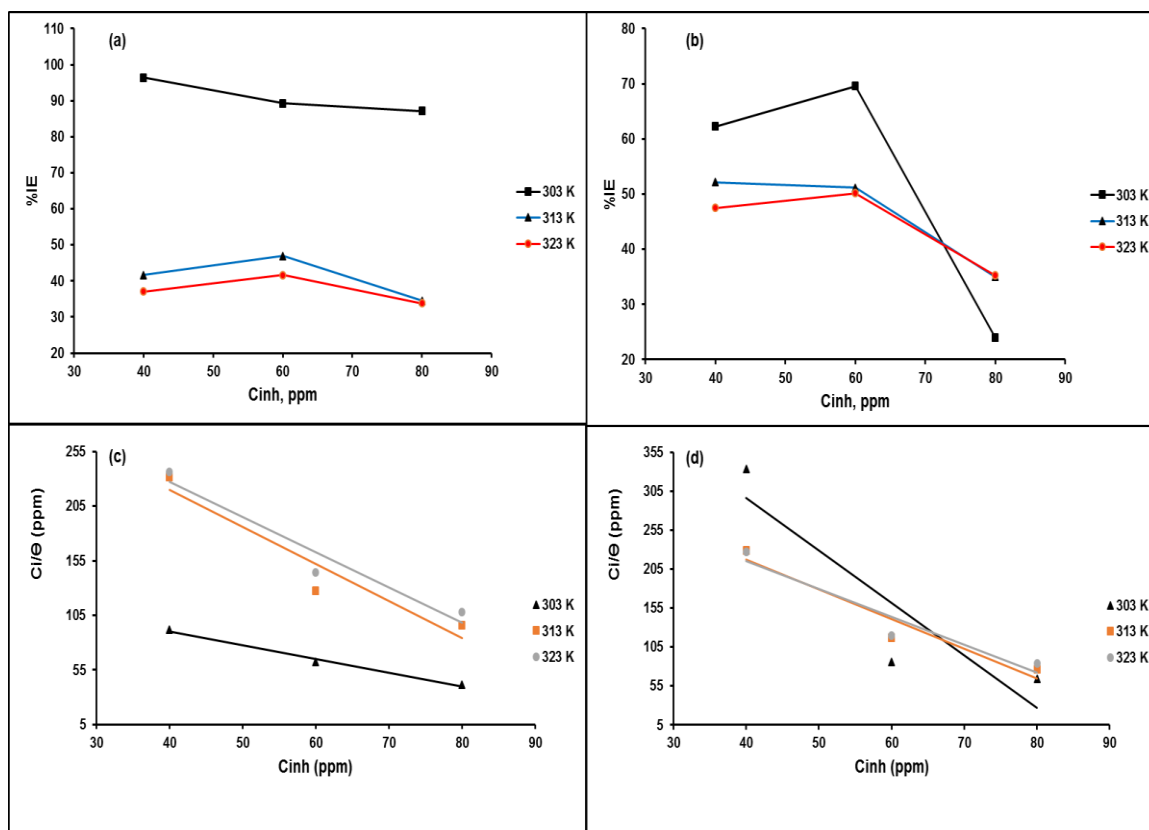
Figure 5. 4: Plot of inhibition efficiency (%IE) against inhibitor concentration (ppm) (a) NiPc and (b) TNNiPc; and Langmuir adsorption isotherms using (c) NiPc and (d) TNNiPc respectively on aluminium metal sheet at 303, 313 and 323 K.

Moreover, in order to determine the mechanism type followed during the process of adsorption between the inhibitor and metal, a crucial way have been investigated by fitting different adsorption isotherms with the best regression line R^2 value. The surface coverage and the inhibitor concentrations of NiPc and TNNiPc relationship adhered to Langmuir and Freundlich adsorption isotherm were expressed by Equation 5.3.

Figure 5.4 (c) and (d) are the Langmuir and Freundlich adsorption isotherm plots with R^2 values between 0.8-0.99 [33] with a slight inconsistency at 313 K regression line for TNNiPc. The Langmuir plots confidence is supported by R^2 values close to unity. The values of adsorption equilibrium constant and the standard free energy of

adsorption are noted in Table 5.2. The values obtained from the slopes of regression lines were indication of the number of inhibitor layers adsorbed on the metal surface. The free energy of adsorption (ΔG^o_{ads}) was calculated using the Equation 5.4.

$$\Delta G^o = -2.303RT \log(55.5K_{ads})$$

(5.4)

The standard free energy of adsorption gives information about the inhibition process spontaneity and adsorption stability [38, 39]. According to literature, negative values of free energy of adsorption signify a spontaneous process [39]. Free energy of adsorption of -20 kJmol^{-1} and below imply physisorption while those of -40 kJmol^{-1} and above represent chemisorption adsorption mechanism. It was observed that both NiPc and TNNiPc gave a mixed-type adsorption mechanism as observed from Table 5.2, for Gibbs free energy values are between -20 kJmol^{-1} and -40 kJmol^{-1}.

Table 5. 1: The values of corrosion rate (C$_R$), percentage inhibition efficiency (%IE) and surface coverage (θ) of NiPc and TNNiPc at 303, 313 and 323 K for aluminium metal sheet.

Sample	Temp. (K)	Conc. (ppm)	Δw (g)	C$_R$ (X10^{-3} g.cm^{-2}.hr^{-1})	%IE	θ	C/θ (ppm)
NiPc	303	0	0.559	3.106	_	_	_
		40	0.103	0.111	96.42	0.9642	41.48
		60	0.099	0.333	89.27	0.8927	62.213
		80	0.231	0.400	87.12	0.8712	91.826
	313	0	0.692	3.844	_	_	_
		40	0.263	2.200	41.61	0.4161	96.127
		60	0.222	2.000	46.96	0.4696	127.770
		80	0.279	2.500	34.53	0.3453	231.683
	323	0	0.718	3.989	_	_	_
		40	0.37	2.511	37.05	0.3705	107.965
		60	0.368	2.328	41.65	0.4165	144.075
		80	0.436	2.639	33.85	0.3385	236.365
TNNiPc	303	0	0.559	3.106	_	_	_
		40	0.299	1.172	62.26	0.6226	64.247
		60	0.205	0.944	69.59	0.6959	86.216
		80	0.318	2.361	23.98	0.2398	333.579
	313	0	0.692	3.844	_	_	_
		40	0.381	1.839	52.16	0.5216	76.684
		60	0.367	1.878	51.15	0.5115	117.301
		80	0.443	2.500	34.96	0.3496	228.881
	323	0	0.718	3.989	_	_	_
		40	0.433	2.094	47.49	0.4749	84.220
		60	0.373	1.989	50.14	0.5014	119.663
		80	0.459	2.583	35.24	0.3524	227.024

Table 5. 2: Adsorption parameters obtained from the Langmuir adsorption isotherms for NiPc and TNNiPc for aluminium.

Inhibitor	T (K)	Kads (x 10^3 L.mol^{-1})	$-\Delta G^\circ_{ads}$ (kJ.mol^{-1})
NiPc	303	4.060	31.05
	313	1.608	29.67
	323	1.607	30.62
TNNiPc	303	1.328	28.24
	313	2.035	30.28
	323	2.099	31.33

5.3.2.2 THERMODYNAMIC AND ACTIVATION PARAMETERS

Temperature is known to increase the metal dissolution effectively, and as an outcome, there is a lower activation barrier [40, 41]. By means of Arrhenius equations and plots, the temperature effect on the adsorption of MPcs onto the aluminium surface is evaluated. The corrosion rate dependence on temperature can be expressed by Arrhenius equation and transition state equations presented in Equation 5.5 and 5.6, respectively [42, 43]:

$$\log C_R = \log A - \frac{E_a}{2.303RT} \tag{5.5}$$

$$\log(\frac{C_R}{T}) = \ln(\frac{k_B}{h}) + \frac{\Delta S^\circ}{R} - \frac{\Delta H^\circ}{RT} \tag{5.6}$$

The $\log C_R$ against 1/T as shown in Figure 5.5(a) and (b) for NiPc and TNNiPc, respectively. The plots helped in calculating the activation energy values for the corrosion process. Calculated parameters of activation are recorded in Table 5.3. The activation values in the absence of inhibitor concentration were less than those obtained in the presence of the inhibitor concentration for both NiPc and TNNiPc. However, TNNiPc in 80 ppm inhibitor concentration showed a slow adsorption process of the inhibitor compounds on a metal surface, this behaviour might be due to the large insoluble amount of the TNNiPc since the solubility enhances inhibitor adsorption on the metal. Higher activation values in the presence of the inhibitor

compounds advocated to a prolong corrosion rate due to the formation of metallophthalocyanines aluminium complex [19].
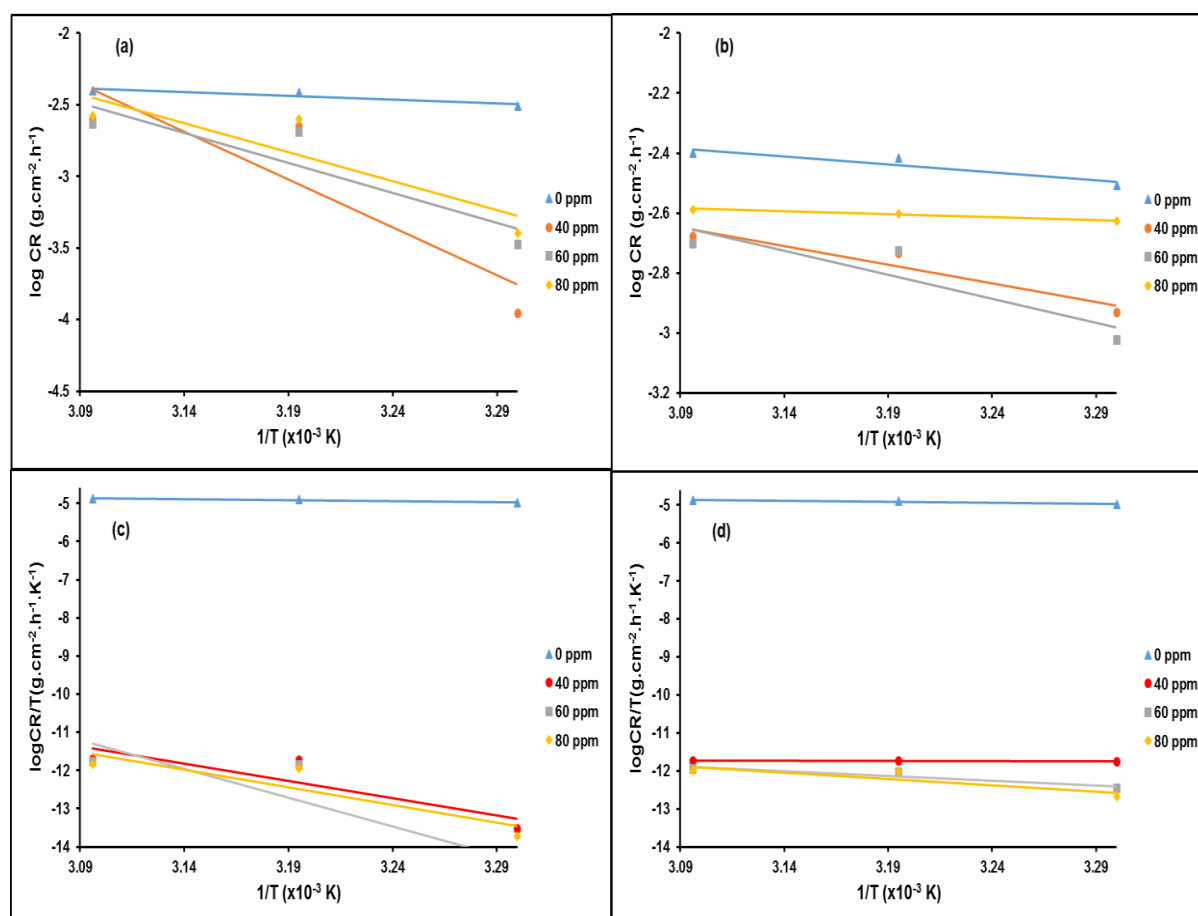
Figure 5.5: Arrhenius plot for Al metal in 1mol.L^{-1} HCl in the absence and presence of different concentrations of NiPc (a) and TNNiPc (b); and Transition state plots at different concentrations of NiPc (c) and TNNiPc (d) respectively.

Furthermore, inhibition efficiency investigation on aluminium metal surface can be represented by entropy and enthalpy of activation. It has been seen that negative entropy values show a lowering of the destruction on the metal surface, whereas positive entropy values indicate an increase in the disordering of the system [44, 45]. Depending on the sign of the value, values of enthalpy can present both the endothermic or exothermic reaction. Endothermic processes are associated with chemical adsorption while the exothermic processes are associated to chemical or physical adsorption [46, 47]. However, chemical adsorption is most preferred than physical adsorption when dealing with obtaining prolonged results. This is due to

chemical adsorption which refers to the sharing of charges from the inhibitor to the metal surface on the other hand, physical adsorption deals with electrostatic interactions between charged inhibitor molecules and charged metal surface. The transition plots are derived from Equation 8 and presented in Figure 5.5(c) for NiPc and Figure 5.5(d) for TNNiPc. Also the kinetic and thermodynamic parameters were obtained from the transition state plots recorded in Table 5.3. It has been shown that enthalpy values up to 41.86 kJmol^{-1} are associated with physical adsorption while those at 100 kJ.mol^{-1} or more are associated with chemical adsorption [19, 48]. In this work, the obtained enthalpy energy is slightly lower than that of activation energy as shown in Table 5.3.

Table 5. 3: Activation energy (E_a), enthalpy (ΔH^o_a) and entropy (ΔS^o) values for aluminium metal at different inhibitor concentrations in 1 M HCl.

Inhibitor	Concentration (ppm)	E_a (kJ.mol^{-1})	ΔH^o_{ads} (kJ.mol^{-1})	ΔS^o (JK^{-1}.mol^{-1})
NiPc	0	10.27	4.46	-224.2
	40	128.22	125.58	97.46
	60	79.87	77.25	-54.00
	80	77.60	74.98	-60.32
TNNiPc	0	10.27	4.46	-224.2
	40	23.78	21.17	-230.9
	60	30.60	27.99	-209.8
	80	3.67	1.07	-291.8

Furthermore, in comparison with the inhibited process, enthalpy for the uninhibited is much lower. The enthalpy values of TNNiPc are all less than 41.86 kJmol^{-1} signifying a physisorption adsorption mechanism [19]. However, those for NiPc in 60 and 80 ppm were between 41.86 and 100 kJ.mol^{-1} and above 100 kJ.mol^{-1} for 40 ppm NiPc which might signify a mixed-type adsorption mechanism [10].

5.3.3. ELECTROCHEMICAL ANALYSIS

Figure 5.6 (a) and (b) display the anodic and cathodic polarisation plots of aluminium in 1M HCl in the absence and presence of three different concentrations of NiPc and TNNNiPc as corrosion inhibitors. The polarisation curves reveal both in the absence and presence of the inhibitor with similar trend. This showed that both NiPc and TNNiPc act as adsorptive inhibitors and the inhibition role of these compounds was not through the interference the metal dissolution and proton reduction. The presence of the inhibitors in the corrosive medium minimised the anodic aluminium dissolution and cathodic reduction of hydrogen ions [49]. Electrochemical parameters such as corrosion potential (E_{corr}), anodic (b_a) and cathodic (b_c) Tafel slopes and corrosion current density (i_{corr}) were obtained by the extrapolation of Tafel plots and data is shown in Table 5.4.

.
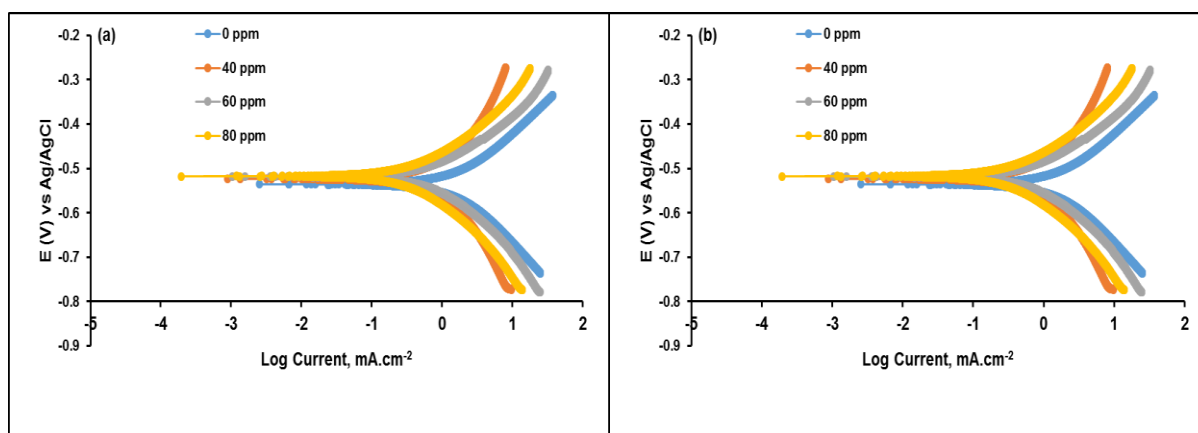
Figure 5. 6: Tafel plots for aluminium in 1 M HCl in the absence and presence of different concentrations of NiPc (a) and TNNiPc (b) inhibitor compounds.

It can be seen in Table 5.4 that the corrosion current density values in the uninhibited system is lower than those in the inhibited system. At 40 ppm and 60 ppm NiPc shows an efficient inhibition potential since it has lower corrosion current density values. Furthermore, it was seen in Table 5.4 that the passivation potential value, E_{pas}, for the blank solution was -465.4 mV, however, the value decreased with the addition of NiPc and TNNiPc inhibitor, obtaining the lowest value, -261.2 and -439.1mV respectively, with the addition of 80 ppm. Correspondingly, the passivation current density value, i_{pas}, of blank was 4.68 mA.cm^{-2}. Upon addition of NiPc and

TNNiPc inhibitor, it decreased as the inhibitor concentration increased, obtaining the lowest value, 1.31 and 1.79 mA.cm^{-2} at 80ppm, respectively. Accordingly, it could be concluded that the addition of phthalocyanine inhibitors decrease the corrosion rate of aluminium metal in acidic media by improving the passive film properties. The differences in the %IE and %IE$_P$ values from weight loss and electrochemical experiments respectively could be due to the fact that weight loss measurement determines the rate of corrosion chemically, without the electrode potential, whereas potentiodynamic polarisation measurements rely on the operational potential [10, 48, 49] and solubility has an important role in in this regard [10].

Table 5. 4: Potentiodynamic polarisation (PDP) parameters such as corrosion potential (E_{corr}), corrosion current density (i_{corr}), anodic Tafel slope, b_a and cathodic Tafel slope, b_c, using different inhibitors.

Inhibitor	Conc (ppm)	-E_{corr} (mV)	i_{corr} (mA.cm^{-2})	b_a (mV)	b_c (mV)	-Epas (mV)	ipas (mA/cm^2)	%IE$_{PDP}$
Blank		535.6	1.94	155.3	179.6	465.4	4.68	-
NiPc	40	511.5	0.12	85.1	102.6	402.3	1.99	93.81
	60	498.7	0.076	81.5	142.9	401.3	1.43	96.08
	80	482.5	0.087	170.0	212.1	261.2	1.31	95.52
TNNiPc	40	523.4	1.70	333.7	344.1	425.3	2.51	12.37
	60	521.4	1.0	141.7	169.1	463.4	1.83	53.61
	80	517.5	0.47	136.2	162.0	439.1	1.79	75.77

5.3.4. ELECTROCHEMICAL IMPEDANCE SPECTROSCOPY (EIS)

The inhibitor concentration effect on the impedance behaviour of aluminium in 1M HCl is presented in Figure 5.7. The Nyquist plots possess a depressed semicircle with the center below the real X-axis, which magnitude increases upon increasing the inhibitor concentration, signifying that the corrosion is a charge transfer process [50]. It should be taken into consideration that the introduction of inhibitor molecules didn't change the style of the impedance curves, suggesting the same inhibition mechanism is involved [50].
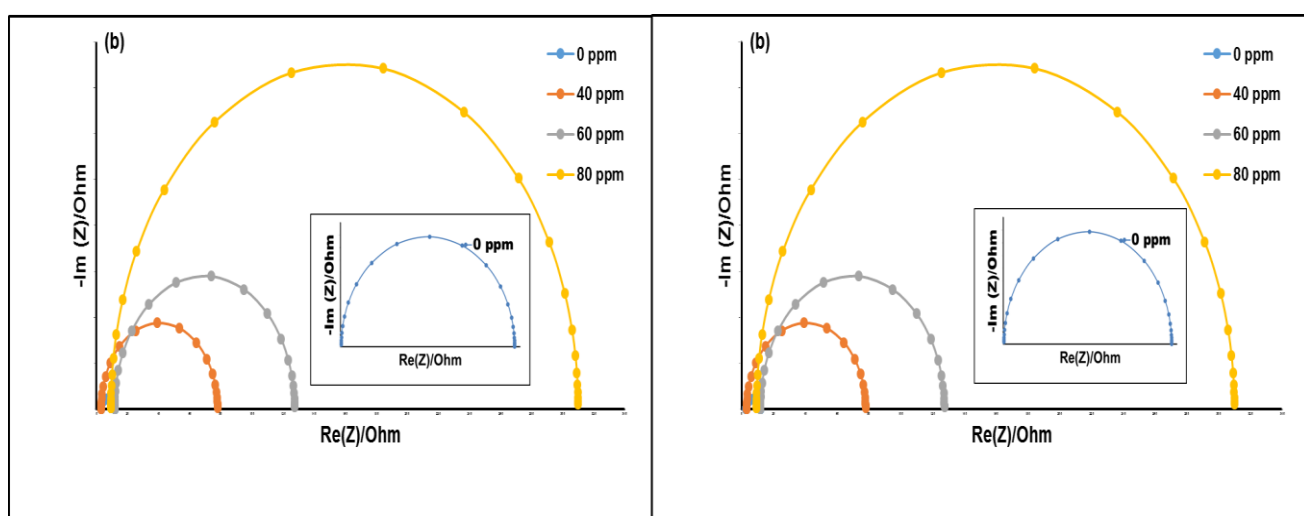

Figure 5. 7: Nyquist plots of Al in 1 M HCl in the absence and presence of different concentrations of NiPc (a) and TNNiPc (b) inhibitor compounds.

Data in Table 5.5 represent the impedance parameters derived from the Nyquist plots. The inhibition efficiency values are calculated using Equation 2.19.

Table 5. 5: Impedance parameters for corrosion of aluminium in 1M HCl containing different concentrations of inhibitors.

Inhibitor	Inhibitor Conc(ppm)	R_s (Ω)	R_{ct} (Ω)	C_{dl} ($\times 10^{-4}$F)	%IE$_{EIS}$
Blank		2.836	8.871	2.060	-
NiPc	40	20.417	205.051	0.690	95.67
	60	14.576	558.110	0.270	98.41
	80	10.935	886.601	0.190	99.0
TNNiPc	40	18.529	74.886	1.890	82.62
	60	11.651	115.842	1.090	85.54
	80	9.213	300.807	0.382	88.15

As observed from Table 5.5, the R_{ct} values increases as the inhibitor concentration increases, whereas, the C_{dl} values decreased with increase in inhibitor concentration which is due to the decrease in local dielectric constant or increase in the electrical double layer thickness suggesting that NiPc and TNNiPc protects the metal via adsorption at the metal/solution interface [50, 51]. The decrease of C_{dl} could be to the replacement of water molecules by adsorbing inhibitor molecule on the electrode surface, which minimises the metal dissolution extent [51]. The percentage inhibition efficiency values revealed the same trend obtained from the weight loss measurements and potentiodynamic polarisation plots. The equivalent circuit used to fit the EIS data is given in Figure 5.8 where R_s is the solution resistance between the working electrode (Al metal) and the counter electrode (platinum), R_{ct} is the charge transfer resistance which decreases with the increasing inhibitor concentration and C_{dl} is the double layer capacitance formed at the metal solution interface, as the inhibitor concentration increases, the C_{dl} thickness decreases which hinders the mobility of charges thus a higher inhibition efficiency.
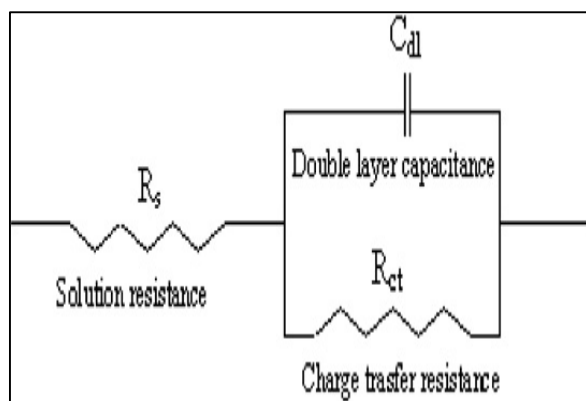
Figure 5. 8: The suggested equivalent circuit model for the studied system.

5.4. CONCLUSION

Nickel phthalocyanine and tetra nickel phthalocyanine were successfully synthesized following the method reported in the literature and where confirmed to be successfully synthesized by XRD, FTIR, TGA, DSC and UV-vis. NiPc and TNNiPc exhibited an intense absorption peak at the Q-band region of the spectra which is complemented by the literature. The two inhibitors proved to be thermally stable as supported by TGA at elevated temperatures. The XRD was used for phase identification, both NiPc and TNNiPc were reported to be poorly crystalline and exhibited an amorphous nature. FTIR spectra agreed with Uv-vis. A study of the use of NiPc and TNNiPc inhibitors as corrosion inhibitors for aluminium metal in 1 mol. L^{-1} HCl has been carried out. It has been found from gravimetric measurement that NiPc acts as a good corrosion inhibitor with its efficiency reaching its highest value by adding 40 ppm due to the formation of an adherent, compact, protective film. Additionally, inhibitor efficiency decreases with introduction of NO_2 group at peripheral due to steric hindrance. Electrochemical measurements showed the properties of the passive film formed on the Al surface was observed in both NiPc and TNNiPc by a reduction in the passivation current density and passivation potential values. Nyquist data displayed a single capacitive, and depressed loop in both NiPc and TNNiPc inhibitors, indicating that the corrosion process is under charge transfer control. It is explored and proven in this contribution that nickel phthalocyanine and its tetra nickel counterpart carry tremendous potential for industrial usage as corrosion inhibitors. The results obtained from potentiodynamic

polarisation showed that the prepared inhibitors represent a mixed-type of inhibitors and the proposed adsorption mechanism is a mixed-type. In determining the corrosion inhibition efficiency, gravimetric analysis, PDP, and EIS gave similar trends.

5.5. REFERENCES

1. J. Li, B. Hurley, R. Buchheit, Effect of temperature on the localized corrosion of aa2024-t3 and the electrochemistry of intermetallic compounds during exposure to a dilute NaCl solution, *Corros.* 72(2016) 1281-1291.
2. R. van Berkel, Eco-efficiency in primary metals production: Context, perspectives and methods, *Resour. Conserv. Recycl.* 51(2011) 511-540.
3. S. Yang, H. Knickle, Design and analysis of aluminium/air battery system for electric vehicles, *J. Power Sources.* 112(2002) 162-173.
4. Q. Li, N. J. Bjerrum, Aluminum as anode for energy storage and conversion: a review, *J. Power Sources.* 110(2002) 1-10.
5. M. Whelan, K. Barton, J. Cassidy, J. Colreavy, B. Duffy, Corrosion inhibitors for anodised aluminium, *Surf. Coat. Technol.* 227(2013) 75-83.

6. S. I. Durowaye, G. I. Lawal, I. A. Raheem, V. O. Durowaye, Corrosion Response of Cast Aluminium Alloy for Extension Clamp Fabrication, *American J. Mater. Sci.* 4(2014) 159-164.
7. M. Salahshoor, Y. Guo, iodegradable orthopedic magnesium-calcium (MgCa) alloys, processing, and corrosion performance, *Materials.* 5(2012) 135-155.

8. N. O. Eddy, S. R. Stoyanov, E. E. Ebenso, Fluoroquinolones as corrosion inhibitors for Mild steel in acidic medium; experimental and theoretical studies, *Int. J. Electrochem. Sci.* 5(2010) 1127-1150.
9. O. K. Özdemir, A. Aytaç, D. Atilla, M. Durmuş, Corrosion inhibition of aluminum by novel phthalocyanines in hydrochloric acid solution, *J. Mater. Sci.* 46(2011) 752-758.
10. M. Dibetsoe, L. O. Olasunkanmi, O. E. Fayemi, S. Yesudass, B. Ramaganthan, I. Bahadur, A. S. Adekunle, M. M. Kabanda, E. E. Ebenso, ome phthalocyanine and naphthalocyanine derivatives as corrosion inhibitors for aluminium in acidic

medium: Experimental, quantum chemical calculations, QSAR studies and synergistic Effect of iodide ions, *Molecules*. 20(2015) 15701-15734.

11. P. Zhao, Q. Liang, Y. Li, Electrochemical, SEM/EDS and quantum chemical study of phthalocyanines as corrosion inhibitors for mild steel in 1mol/l HCl, *Appl. Surf. Sci*. 252(2005) 1596-1607.

12. F. Touhami, A. Aouniti, Y. Abed, B. Hammouti, S. Kertit, A. Ramdani, K. Elkacemi, Corrosion inhibition of armco iron in 1 M HCl media by new bipyrazolic derivatives, *Corros. Sci*. 42(2000) 929–940.

13. L. Tang, X. Li, L. Li, G. Mu, G. Liu, Interfacial behavior of 4-(2-pyridylazo) resorcin between steel and hydrochloric acid, *Surf. Coat. Technol*. 201(2006) 384–388.

14. K. Sakamoto, E. Ohno-Okumura, Syntheses and functional properties of phthalocyanines, *Materials*. 2(2009) 1127-1179.

15. G. De La Torre, P. Vázquez, F. Agullo-Lopez, T. Torres, Role of structural factors in the nonlinear optical properties of phthalocyanines and related compounds, *Chem. Rev*. 104(2004) 3723-3750.

16. M. A. García-Sánchez, F. Rojas-González, E. C. Menchaca-Campos, S. R. Tello-Solís, R. Quiroz-Segoviano, L. A. Diaz-Alejo, E. Salas-Bañales, E. and Campero, rossed and linked histories of tetrapyrrolic macrocycles and their use for engineering pores within sol-gel matrices, *Molecules*. 18(2013) 588-653.

17. L. O. Olasunkanmi, I. B. Obot, M. M. Kabanda, E. E. Ebenso, Some quinoxalin-6-yl derivatives as corrosion inhibitors for mild steel in hydrochloric acid: Experimental and theoretical studies, *J. Phys. Chem C*. 119(2015) 16004-16019.

18. M. Arıcı, D. Arıcan, A. L. Uğur, A. Erdoğmuş, A. Koca, Electrochemical and spectroelectrochemical characterization of newly synthesized manganese, cobalt, iron and copper phthalocyanines, *Electrochim. Acta.* 87(2013) 554-566.

19. K. M. Manamela, L. C. Murulana, M. M. Kabanda, E. E. Ebenso, Adsorptive and DFT studies of some imidazolium based ionic liquids as corrosion inhibitors for zinc in acidic medium, *Int. J. Electrochem.Sci*. 9(2014) 3029-3046.

20. A. R. Hoseizadeh, I. Danaee, M. H. Maddahy, Thermodynamic and adsorption behaviour of vitamin B1 as a corrosion inhibitor for AISI 4130 steel alloy in HCl solution, *Z. Phys. Chem.* 227(2013) 403-418.

21. M. A. Ibrahim, M. Messali, Z. Moussa, A. Y. Alzahrani, S. N. Alamry, B. Hammouti, Corrosion inhibition of carbon steel by imidazolium and pyridinium cations ionic liquids in acidic environment, *Electrochim. Acta.* 29 (2011) 375-389.

22. M. Tourabi, K. Nohair, M. Traisnel, C. Jama, F. Bentiss, Electrochemical and XPS studies of the corrosion inhibition of carbon steel in hydrochloric acid pickling solutions by 3, 5-bis (2-thienylmethyl)-4-amino-1, 2, 4-triazole, *Corros. Sci.* 75(2013)123-133.

23. U. M. Eduok, S. A. Umoren, A. P. Udoh, Synergistic inhibition effects between leaves and stem extracts of Sida acuta and iodide ion for mild steel corrosion in 1M H 2 SO 4 solutions, *Arabian J. Chem.* 5(2012) 325-337.

24. B. D. Mert, M. E. Mert, G. Kardaş, B. Yazıcı, Experimental and theoretical investigation of 3-amino-1, 2, 4-triazole-5-thiol as a corrosion inhibitor for carbon steel in HCl medium, *Corros. Sci.* 53(2011) 4265-4272.

25. D. Atilla, A. G. Gürek, T. V. Basova, V. G. Kiselev, A. Hassan, L. A. Sheludyakova, V. Ahsen, synthesis and characterization of novel mesomorphic octa-and tetra-alkylthio-substituted lead phthalocyanines and their films, *Dyes Pigm.* 88(2011) 280-289.

26. S. A. Mahmoud, A. Shereen, A. T. Mou'ad, Structural and optical dispersion characterisation of sprayed nickel oxide thin films, *Int. J. Mod. Phys.* 2(2011) 1178.

27. R. Veerapur, H. Shamsipour, C. Mason, P. Budd, M. C. Ferrari, S. Brandani, Mixed Gas Permeation Measurements on Novel Modified PIMs Materials for Postcombustion Carbon Capture, *Procedia Eng.* (2012) 491-492.

28. J. M. Ramosa, M. C. Maurıcio, C. C. Anilton Jr, V. Otavio, A. T. S. Claudio, Fourier transform infrared spectrum: Vibrational assignments using density functional theory and natural bond orbital analysis of the bis (guanidoacetate) nickel (II) complex, *ScienceAsia.* 37(2011) 247-255.

29. X. Zhou, X. Wang, B. Wang, Z. Chen, C. He, Y. Wu, Preparation, characterization and NH 3-sensing properties of reduced graphene oxide/copper phthalocyanine hybrid material, *Sens. Actuators, B.* 193(2014) 340-348.

30. S. Tuncel, F. Dumoulin, J. Gailer, M. Sooriyaarachchi, D. Atilla, M. Durmuş, D. Bouchu, H. Savoie, R. W. Boyle, V. Ahsen, A set of highly water-soluble tetraethyleneglycol-substituted Zn (II) phthalocyanines: synthesis, photochemical and photophysical properties, interaction with plasma proteins and in vitro phototoxicity, *Dalton Trans.* 40(2011) 4067-4079.

31. T. M. Kumar, B. N. Achar, Synthesis and characterization of lead phthalocyanine and its derivatives, J*. Organomet. Chem.* 691(2006) 331-336.

32. A. Beck, K. M. Mangold, M. Hanack, Lösliche (Tetraethylphthalocyaninato) eisen (II)-und-cobalt (II)-Verbindungen, *European Journal of Inorg. Chem.* 124(1991) 2315-2321.

33. T. H. Ibrahim, Y. Chehade, M. A. Zour, Corrosion inhibition of mild steel using potato peel extract in 2M HCL solution, *Int. J. Electrochem. Sci.* 6(2011) 6542-6556.

34. A. Hamdy, N. S. El-Gendy, Thermodynamic, adsorption and electrochemical studies for corrosion inhibition of carbon steel by henna extract in acid medium, *Egypt. J. Pet.* 22(2013) 17-25.

35. R. Yıldız, A. Döner, T. Doğan, I. Dehri, Experimental studies of 2-pyridinecarbonitrile as corrosion inhibitor for mild steel in hydrochloric acid solution,*Corros. Sci.*82(2014) 125-132.

36. W. Li, L. Hu, S. Zhang, B. Hou, Effects of two fungicides on the corrosion resistance of copper in 3.5% NaCl solution under various conditions, *Corros. Sci.* 53(2011) 735-745.

37. S. Hong, W. Chen, H. Q. Luo, N. B. Li, Inhibition effect of 4-amino-antipyrine on the corrosion of copper in 3wt. % NaCl solution, *Corros. Sci.* 57(2012) 270-278.

38. B. Hammouti, A. Zarrouk, S. S. Al-Deyab, I. Warad, Temperature Effect, Activation Energies and Thermodynamics of Adsorption of ethyl 2-(4-(2-ethoxy-2-oxoethyl)-2-p-Tolylquinoxalin-1 (4H)-yl) Acetate on Cu in HNO3, *Orient. J. Chem.* 27(2011) 23-31.

39. X. Xu, Y. Wang, Z. Zhang, Potential and concentration dependent electrochemical dealloying of Al2Au in sodium chloride solutions, *J. Phys. Chem C.* 116(2012) 5689-5699.

40. X. Zheng, S. Zhang, W. Li, M. Gong, L. Yin, Experimental and theoretical studies of two imidazolium-based ionic liquids as inhibitors for mild steel in sulfuric acid solution, *Corros. Sci.* 95(2015) 168-179.

41. Y. Chen,Y. Zhu, Z. Wang, Y. Li, L. Wang, L. Ding, X. Gao,Y. Ma, Y. Guo, Application studies of activated carbon derived from rice husks produced by chemical-thermal process—A review, *Adv. Colloid Interface Sci.* 163(2011) 39-52.

42. B. S. Sanatkumar, J. Nayak, A. N. Shetty, Influence of 2-(4-chlorophenyl)-2-oxoethyl benzoate on the hydrogen evolution and corrosion inhibition of 18 Ni

250 grade weld aged maraging steel in 1.0 M sulfuric acid medium, *Int. J. Hydrogen Energy.* 37(2012) 9431-9442.

43. Z. I. N. A. B. U. Wolde, W. A. S. S. I. E. Haile, Phosphorus sorption isotherms and external phosphorus requirements of some soils of southern Ethiopia, *J. Trop Crop. Sci.* 23(2015) 89-99.

44. A. K. Singh, S. K. Shukla, M. Singh, M. A. Quraishi, Inhibitive effect of ceftazidime on corrosion of mild steel in hydrochloric acid solution, *Mater. Chem. Phys.* 129(2011) 68-76.

45. H. Elmsellem, N. Basbas, A. Chetouani, A. Aouniti, S. Radi, M. Messali, B. Hammouti, Quantum chemical studies and corrosion inhibitive properties of mild steel by some pyridine derivatives in 1 N HCl solution, *Electrochim. Acta. 32*(2014) 77-108.

46. R. Sivakumar and B. L. Mordike, High temperature coatings for gas turbine blades: a review, *Surf. Coat. Technol.* 37(1989), 139-160.

47. A. R. Troiano, The role of hydrogen and other interstitials in the mechanical behavior of metals, *Met. Micro. Ana.* 5(2016) 557-569.

48. A. Zarrouk, I. Warad, B. Hammouti, A. Dafali, S. S. Al-Deyab, N. Benchat, The effect of temperature on the corrosion of Cu/HNO3 in the presence of organic inhibitor: part-2, *Int. J. Electrochem. Sci.* 5(2010)1516-1526.

49. P. Singh, Priyanka, E. E. Ebenso, L. O. Olasunkanmi, I. B. Obot, M. A. Quraishi, Electrochemical, theoretical, and surface morphological studies of corrosion inhibition effect of green naphthyridine derivatives on mild steel in hydrochloric acid, *J. Phys. Chem C.* 120(2016), 3408-3419.

50. X. Wang, H. Yang, F. Wang, An investigation of benzimidazole derivative as corrosion inhibitor for mild steel in different concentration HCl solutions, *Corros. Sci.* 53(2011) 113-121.

51. B. D. Mert, M. E. Mert, G. Kardas, B. Yazici, Experimental and theoretical investigation of 3-amino-1, 2, 4-triazole-5-thiol as a corrosion inhibitor for carbon steel in HCl medium, *Corros. Sci.* 53(2011) 4265-4272.

CHAPTER SIX
GENERAL DISCUSSION, CONCLUSIONS AND RECOMMENDATIONS

6.1. GENERAL DISCUSSION AND CONCLUSIONS

In this study, inhibition efficiency towards corrosion protection of Al in 1M HCl by using blue-green pigments inhibitors namely CuPc, ZnPc and NiPc together with their nitro substituted compounds (TNCuPc, TNZnPc and TNNiPc) was investigated by gravimetric analysis and electrochemical methods. For CuPc and TNCuPc as corrosion inhibitors, it was found that the studied inhibitors exhibited good inhibitive properties for aluminium metal in 1 M HCl solution. The acquired inhibition efficiency of these inhibitors from EIS, polarisation curves and weight loss shows that the inhibition efficiency increases with increasing inhibitor concentration. In addition, Inhibition efficiencies are associated to temperature and chemical structure of the inhibitors. Upon the temperature increase, the inhibition efficiency of TNCuPc decrease significantly, while the inhibition efficieny of CuPc decreased slightly. Polarisation curves showed that the observed inhibitors behave as mixed-type inhibitor. From EIS results, it is indicated that the double layer capacitances decrease as compared to the blank solution when these inhibitors are introduced. This information can be explained based on the adsorption of these inhibitors on Al metal surface. Their adsorption on the Al metal obeyed the Langmuir adsorption isotherm. Moreover, the negative values of free Gibbs energy exhibits adsorption spontaneity.

Chapter 4 dealt with the synthesis and characterisation of ZnPc and TNZnPc as corrosion inhibitors for Al metal in 1M HCl, ZnPc proved to be a better inhibitor as compared to TNZnPc by having inhibition efficiency of 82.29% in 40 ppm at 303 K. ZnPc and TNZnPc are adsorptive inhibitors and their adsorption obeyed the Langmuir isotherm. Furthermore, it is observed that corrosion current density is increased when the temperature increases, however, its rate of increase is lower upon the introduction of the inhibitors under this chapter. Parameters such as G^{o}_{ads}, H^{o}_{ads} and S^{o}_{ads}, indicate that the inhibitors are adsorbed by a spontaneous endothermic process and a physisorption process can be proposed ZnPc and TNZnPc.

Furthermore, the study focused on NiPc and TNNiPc as corrosion inhibitors for Al metal in 1 M HCl medium. It was found that the inhibitors acted as suitable inhibitors for the corrosion of Al metal. Polarisation measurements show that the inhibitors acted as mixed-type. The inhibitor adsorption on the surface of Al metal followed Langmuir adsorption isotherm for NiPc, while TNNiPc predominantly followed Langmuir adsorption isotherm and a slight Freundlich isotherm. NiPc revealed a higher percentage inhibition efficiency of 96.42% as compared to TNNiPc. The inhibition activity of NiPc and TNNiPc against the corrosion of Al metal is due to the adsorption process.

In Chapter 5, NiPc and TNNiPc were used as potential corrosion inhibitors for Al metal corrosion protection in 1 mol. L^{-1} HCl solution at 303-323 K. The study was carried out making use of gravimetric analysis (weight loss), PDP, electrochemical impedance spectroscopy (EIS) and characterisations were carried out using UV-vis, FTIR, XRD and thermal analysis. XRD results showed that NiPc exhibited a more crystalline characteristics as compared to TNiPc. Furthermore, FTIR spectra for the NiPc and TNNiPc showed similar vibration band approximately around 730 cm^{-1} which is due to C-H deformations which serves as a good indicator for phthalocyanine crystalline phases, furthermore, the asymmetric and symmetric NO_2 were observed in TNNiPc at the fingerprint showing tentative complex assignments. From the Uv-vis results, it was observed that TNNiPc displayed a blue-shift instead of a red-shift, this is due to the NO_2 electron withdrawing group thus deactivating the inhibitor.

TGA results showed that NiPc is most thermally stable and the decomposition of TNNiPc took place at higher temperatures as compared to NiPc. NiPc and TNNiPc inhibited aluminium corrosion behaviour through adsorption of the inhibitor molecules on Al surface. The comparison on the effect of temperature on Al corrosion showed that the metal was affected the most with the lowest inhibition efficiencies at the highest temperature of 323 K. Furthermore, NiPc resulted in lower metal weight loss with a higher inhibition potential of 96.42% at 40 ppm under gravimetric analysis and 99.0% at 80 ppm under EIS results. The imperfect semicircles on the Nyquist plots showed competent inhibition of Al metal by NiPc and TNNiPc. The electrochemical impedance spectroscopy curves exhibited a passive region, this is because Al forms oxide films. Potentiodynamic polarisation results indicated that both NiPc and

TNNiPc protect Al metal surfaces through a mixed type (chemisorption and physisorption) adsorption at the Al/ HCl interface. Furthermore, PDP results indicated that the corrosion current densities for both anodic and cathodic half reactions were altered. This signifying that the anodic Al metal dissolution and the hydrogen evolution were minimised therefore enhancing the inhibition efficiencies as the inhibitor concentration increased.

6.2. RECOMMENDATIONS FOR FUTURE WORK

Further improvement of metallophthalocyanine inhibitors will aid towards an increase of their inhibition efficiency on the corrosion of the Al metal. An important milestone in the work was to synthesise substituted MPcs to enhance their solubility, thus high inhibition efficiency. MPcs in most organic solvents showed to be insoluble and it was clear from the work. The introduction of functional group may improve MPc solubility and result in increase of corrosion efficiency. However, the solubility of MPcs in this work were predominant as compared to their substituted compounds due to steric hindrance and aggregation caused by NO_2 groups. Hence, it will of a good idea to introduce the functional group which will improve aggregation behavior of the MPc in solution.

The low inhibition efficiencies of the substituted MPcs have also been attributed to the presence of NO_2 which is an electron withdrawing group, a different substituent can potentially be explored in the future to improve the MPcs inhibition potentials. First is to consider an electron donating group as the alternative substituent for MPcs. The second strategy is to investigate the suitable solvent for the solubility of the inhibitors. This is because MPcs were dissolved in a heterogeneous mixture of H_2SO_4 and deionised water. Moreover, the unsubstituted MPcs predominantly exhibited a high equilibrium adsorption constant, however quantification of the amount of the inhibitor will be important since larger molecular weight compounds ensures an optimum adsorption. This can be achieved by introducing more electron donating functional groups on the inhibitor. Furthermore, it will be noteworthy to consider other metals for corrosion testing since aluminium is a very corrosion

resistant metal, in this way the optimum performance of the inhibitor compounds will be clearly revealed.

It is of a very paramount importance for the film formed on the surface of the metal to be studied in order to examine how well the inhibitor does adsorb on the metal, and also morphological studies are essential for studying the adsorption process that occurs at the metal surface. In addition, FTIR, SEM and EDS are the convenient techniques for the above mentioned endeavors.

Fwd: Manuscript Submission
7 messages

Modibane, Kwena <kwena.modibane@ul.ac.za>   Thu, Jan 4, 2018 at 4:07 PM
To: Thabo Pesha <thabopesha@yahoo.co.uk>, Mpitloane Hato <mpitloane.hato@ul.ac.za>, kerileng mildred molapo <g.molapo947@gmail.com>, Kabelo Ramohlola <kabelo.ramohlola@ul.ac.za>, "Monama, Release" <Release.Monama@ul.ac.za>

---------- Forwarded message ----------
From: **Milan Antonijevic** <milan.antonijevic@esgpublisher.com>
Date: Thursday, January 4, 2018
Subject: Manuscript Submission
To: "Modibane, Kwena" <kwena.modibane@ul.ac.za>

Dear Dr Modibane,

I have received your manuscript. The paper will be sent to review soon. When I receive the referee's report I will inform you about status of your paper.

Thank you for your interest for our journal.

Best regards

M. Antonijevic
Editor
International Journal of Electrochemical Science
www.electrochemsci.org

Your co-authored submission
1 message

Results in Physics <EviseSupport@elsevier.com>   Fri, Feb 16, 2018 at 1:50 AM
Reply-To: system@evise.com
To: mpitloane.hato@ul.ac.za

Dear Dr. Hato,

You have been listed as a Co-Author of the following submission:

Journal: Results in Physics

Title: Protection of corrosion rate on aluminium metal in acidic media by unsubstituted and 4-tetranitro substituted nickel (II) phthalocyanine dyes via electrochemical and gravimetric studies for hydrogen fuel cell

Corresponding Author: Kwena Modibane

Co-Authors: Thabo Pesha, Phuti Ramaripa, Kabelo Ramohlola, Gobeng Monama, Mpitloane Hato, Mamookho Makhatha, Kerileng Molapo, Thabang Tsoeunyane

Kwena Modibane submitted this manuscript via Elsevier's online submission system, EVISE®. If you are not already registered in EVISE®, please take a moment to set up an author account by navigating to http://www.evise.com/evise/faces/pages/navigation/NavController.jspx?JRNL_ACR=RINP

If you already have an ORCID, we invite you to link it to this submission. If the submission is accepted, your ORCID will be transferred to ScienceDirect and CrossRef and published with the manuscript.

To link an existing ORCID to this submission, or sign up for an ORCID if you do not already have one, please click the following link: Link ORCID

What is ORCID?

ORCID is an open, non-profit, community-based effort to create and maintain a registry of unique researcher identifiers and a transparent method of linking research activities and outputs to these identifiers.

More information on ORCID can be found on the ORCID website, http://www.ORCID.org, or on our ORCID help page:
http://help.elsevier.com/app/answers/detail/a_id/2210/p/7923

If you did not co-author this submission, please contact the Corresponding Author directly at kwena.modibane@ul.ac.za.

Thank you,
Results in Physics

This message was sent automatically. Please do not reply